Average composition and genesis of the lower continental crust

Peter B Kelemen[a], Mark D Behn[b], and Bradley R Hacker[c], [a]Columbia University, New York, NY, United States; [b]Boston College, Chestnut Hill, MA, United States; [c]UCSB, Santa Barbara, CA, United States

This chapter has been reviewed by the section editor Matthew Kohn.

Abstract

We constrain the average composition of lower and middle continental crust using observed seismic wave speeds, and the physical properties of thermodynamically-constrained, equilibrium mineral assemblages in granulites and amphibolites. Focusing on old, stable crust with steady state geotherms, we find that average lower continental crust has an intermediate composition with 55.7–57.7 wt% SiO_2 (with a preferred range of 56.9–57.6 wt%), a density of 3000 tons/m^3, radioactive heat production of 0.53–0.65 μW/m^3, seismic P-wave speed, Vp, of 6.9 km/s at an average pressure of 0.92 GPa and 410–510 °C. Similarly, we derive a middle continental crust composition with 61–62 wt% SiO_2, a density of 2800 tons/m^3, radioactive heat production of 0.68–0.65 μW/m^3, and Vp of 6.6–6.7 km/s at 280–300 °C and 0.54 GPa. Combining layer thicknesses modified from CRUST1.0 with the well-constrained composition of the upper crust yields a bulk continental crust composition with 62 wt% SiO_2. Given heat flow of 11–18 mW/m^2 from the mantle into the crust, this yields a surface heat flow of 47–55 mW/m^2, consistent with observed heat flow from stable continental regions.

Our results indicate that average lower crust is intermediate in composition, not mafic as is commonly stated. It is similar in its major and trace element composition to the upper crust, the bulk crust, and intermediate arc lavas and plutons. Though the lower crust may record partial melting and melt extraction, complementary to a melt component in the upper crust, it does not have the composition of a cumulate or residue produced by crystal fractionation from a primitive, mantle-derived melt composition. Average lower continental crust is significantly more enriched in incompatible trace elements than lower arc crust, even at depths at which lower arc crust is buoyant with respect to the underlying mantle. Although continental genesis has certainly involved a variety of processes, it is likely that the average composition is primarily the result of density sorting of subducting, arc-derived material, either via thrusting of volcanoclastic sediments and forearc crust beneath lower arc crust, combined with density sorting at the arc Moho, or via ascent of buoyant, viscous, eclogite-facies lithologies in diapirs or a subduction channel.

Keywords

Lower crust; Continental crust; Arc crust; Delamination; Foundering; Relamination; Underplating

Introduction

In this paper we derive new average compositions for middle and lower continental crust, focusing on regions of stable continental crust more than 200 million years old that have steady state geotherms. Our new compositions are then combined with well-established estimates for the composition of continental upper crust to produce new estimates for the composition of bulk continental crust. We then review potentially successful models for the genesis of lower continental crust and present a new model of density sorting of underplated material at the base of arc crust.

The literature on the composition of continental crust been reviewed many times, perhaps most authoritatively by Rudnick and Fountain (1995) and Rudnick and Gao (2003, 2014), with older reviews cited in those papers and also in more recent reviews by Hacker et al. (2015) and Sammon et al. (2022). However, to provide context for what follows, we offer the following summary.

The composition and physical properties of continental crust are distinctly different from those of oceanic crust. The oceanic crust has a mafic composition with 48–52 wt% SiO_2, and probably has a bulk Mg# (molar Mg/(Mg + Fe)) ~0.7, equivalent to that of a primitive magma derived by partial melting of mantle peridotite with a residual Mg# ~0.91. Trace element data support formation of oceanic crust via crystallization of a mantle-derived magma formed by polybaric, near-fractional decompression melting, at an average pressure of ~1.5 GPa.

In contrast, all published estimates of the composition of bulk continental crust are distinctly different from oceanic crust, with 56–66 wt% SiO_2 and an Mg# between 0.6 and 0.4 (Fig. 1). Indeed, there are no known mid-ocean ridge magmatic rocks with these compositional characteristics. These major element differences yield distinctive physical properties, most notably lower density and more compositional buoyancy for continental crust (and continental lithospheric mantle, as discussed elsewhere, e.g., Griffin et al., 1999 and references cited therein, Griffin et al., 1998, Jordan, 1978, Jordan, 1988, Kelly et al., 2003, O'Reilly et al., 2001) compared to denser oceanic crust and oceanic mantle lithosphere. In turn, this difference in buoyancy causes the first order, strongly bimodal topography of the planet, in which continental crust has an average elevation of several hundred meters above sea level, whereas oceanic crust has an average elevation more than 3000 m below sea level (Fig. 2). Yet, despite the importance of these features, there is no consensus on the composition and origin of the continental crust, mainly due to uncertainty about the nature of the lower continental crust.

In addition to the major elements, trace elements in primitive mid-ocean ridge basalts (MORB), bulk oceanic crust, and the mantle source of MORB ("depleted MORB mantle," DMM), when normalized to estimated primitive mantle (McDonough and Sun, 1995), have a light rare-earth element (REE) depleted, relatively smooth, extended trace element pattern (Hofmann, 1988). The depletion in light REE and other highly incompatible elements (which partition strongly into melt during mantle anatexis) in the MORB source is commonly attributed to prior extraction of continental crust from the "primitive mantle" aka "bulk silicate earth," with the complementary formation of DMM (e.g., Hofmann, 1988; Hofmann et al., 2022). In contrast to oceanic crust, continental crust is enriched in light REE, K, Ba, Th and U, depleted in heavy REE and Y, and has distinctively low Nb and Ta concentrations relative to U, Th and K, with high Pb/Ce and Sr/Nd. It is crucial to recognize that *these trace element characteristics are shared by all estimates for the composition of upper, middle and lower continental crust*, and thus are common to all estimated continental bulk compositions (Fig. 3).

However, unlike the trace elements, as emphasized by Hacker et al. (2015), consensus on the major element composition of the lower crust has been elusive. In the past few years, renewed efforts have been made to characterize the lower crust, on regional and global scales (e.g., Cui et al., 2023; Emo et al., 2021; Pease et al., 2023; Sammon and McDonough, 2021; Sammon et al., 2022; Sui et al., 2022). These newer studies agree with Rudnick et al., that average lower continental crust has a mafic[1] composition, with less than 55 wt% SiO_2. In contrast, Hacker et al. (2011, 2015) questioned these results, suggesting that constraints from the composition of samples whose mineral assemblages indicate equilibration at lower crustal pressures (granulites, Section "Rock samples from of the middle and lower crust"), seismic wave speeds and heat flow could be met by a broader range of compositions, extending up to 62 wt% SiO_2. Similarly, in this paper we conclude that average lower crust in stable continental regions contains about 57 wt% SiO_2.

Published estimates of the major and trace element composition of lower continental crust are illustrated in Figs. 1 and 3 and reported in Table 1. These estimates can be viewed through different lenses. By the standards of igneous and metamorphic petrology, the major element estimates show significant variability — for example, published, average SiO_2 contents in granulite xenoliths and granulite terrain samples range from 49 to 66 wt%. As discussed by Hacker et al. (2015), based on geophysical data, much of this range (49–62 wt% SiO_2) could correspond to regional variation in the composition of lower continental crust. In turn, this variation suggests that there could have been substantial variation in the processes that formed the crust in different regions.

Despite this variability, there is considerable utility in estimating a global average composition for lower continental crust, for example to characterize global geochemical reservoirs, and to constrain which processes *predominated* during formation of the lower

[1]The terms mafic, intermediate and felsic are used to refer to compositions with <55 wt% SiO_2, 55 < wt% SiO_2 < 65 wt%, and > 65 wt%, respectively.

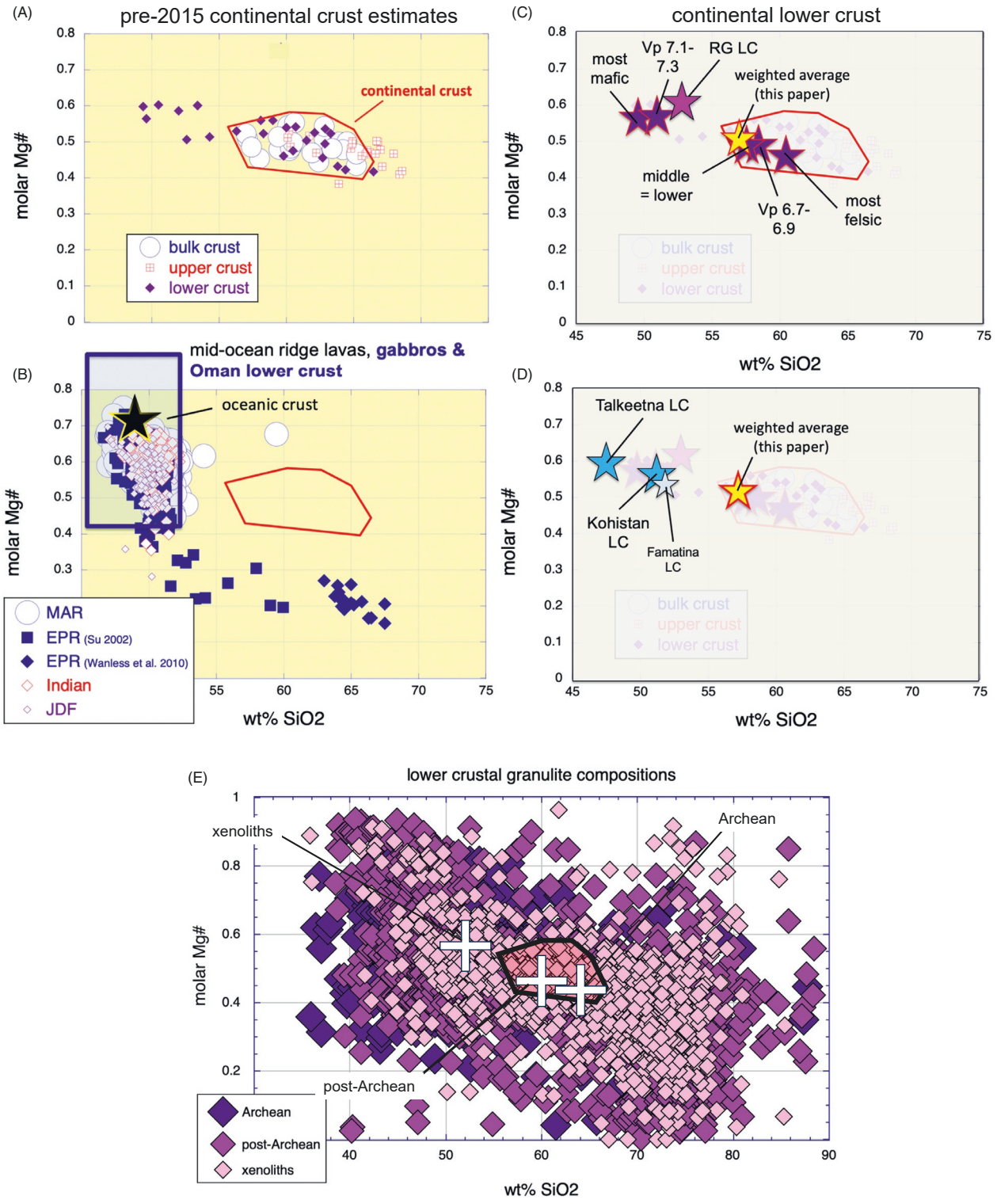

Fig. 1 Plots of wt% SiO_2 versus molar Mg/(Mg + Fe), or Mg#, for continental and oceanic crustal compositions, modified from our prior work (Kelemen, 1995; Kelemen and Behn, 2016; Kelemen et al., 2003a, 2014, 2003c). The red polygon in panels A-D, and the black polygon in panel E, encloses all published estimates of bulk continental crust. References are given in the caption of Supplementary Fig. 1 of Kelemen and Behn (2016) unless otherwise given here. (A) Compiled, proposed compositions of lower, upper and bulk continental crust prior to 2015. (B) Compositions of mid-ocean ridge lavas (MORB) and gabbros. Points are compositions of MORB glasses from PetDB (https://www.earthchem.org/resources/support/petdb-documentation/) downloaded in 2003, plus dacites from Wanless et al. (2010). Blue rectangle encloses the compositions of gabbros recovered via ocean drilling (Dick et al., 2002; Godard et al., 2009; Kelemen et al., 2007; Natland and Dick, 1996) and studies of the Wadi Tayin massif of the Samail ophiolite in Oman (Garbe-Schönberg et al., 2022; VanTongeren et al., 2021). The black star indicates the approximate composition of average, bulk oceanic crust, based on the highest Mg# glass compositions, corresponding to a mantle-derived basaltic magma. The compositions of minor granitic veins in lower oceanic crust are omitted for clarity, but see Hart et al. (1999) for data on strip samples including these veins and Kelemen et al. (2007) for major element plots and a discussion of vein formation. (C) Five proposed lower continental crust compositions from Hacker et al. (2015, purple stars), together with a magenta star for the lower crust composition of Rudnick and Gao (2003, 2014) and a yellow star for the preferred lower crust composition from this paper, overlain on panel (A). (D) Average compositions of lower arc crust derived from the Talkeetna (Kelemen et al., 2003a, 2014), Kohistan (Jagoutz and Schmidt, 2012) and Famatina (Ducea et al., 2015; Otamendi et al., 2012; Otamendi et al., 2010; Walker Jr et al., 2015) exposed arc sections, overlain on panel (B). (E) Compiled compositions of granulite facies metamorphic rocks recording lower crustal compositions (Supplementary Table 2 in the online version at https://doi.org/10.1016/B978-0-323-99762-1.00121-2). White crosses indicate average compositions for Archean granulite terrains, post-Archean granulite terrains, and granulite xenoliths. Archean and post-Archean compilations are from Hacker et al. (2015), building upon prior compilations from Huang et al. (2013).Compilation of xenoliths (and amphibolites used in other figures and calculations) from Huang et al. (2013). Note expanded axis limits in panel (E), compared to panels (A–D).

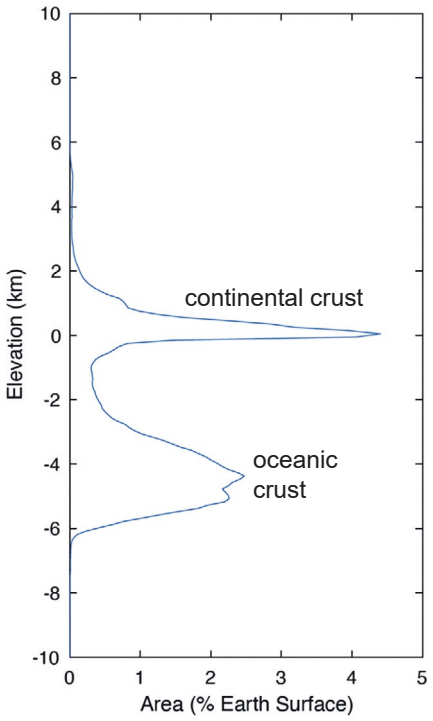

Fig. 2 Histogram of Earth's solid surface elevations relative to sea level using used data based on the ETOPO1 1-arc-minute global relief model (Amante and Eakins, 2009; NOAA National Geophysical Data Center, 2009).

crust. In turn, understanding continental genesis is central to understanding the first order topography of the solid earth surface, with its bimodal distribution reflecting compositional and thickness differences between oceanic and continental crust (Fig. 2).

Differences between more and less SiO_2-rich estimates for the composition of lower continental crust arise for several reasons, discussed in the next few sections of this paper.

Definitions of the middle and lower crust

There has been a tendency to define the lower crust as that portion of the crust that has a high seismic P-wave speed (Vp). This results in assigning different depth intervals and thicknesses to the lower crust in different regions. Thus, for example, Rudnick and Fountain (1995) inferred that the top of the lower crust is at an average depth of 28 and 30 km, with thicknesses of 14 and 10 km, in shields + platforms, and Paleozoic orogens respectively. Extending this to tectonically and volcanically active regions expands the Rudnick and Fountain range still further, with the top of the lower crust at 20–30 km, and the base at 25–50 km for Cenozoic orogens, rifted margins and volcanic arcs (e.g., CRUST1.0 (Laske et al., 2012, 2013)). This approach emulates studies of oceanic crust, with its relatively well-defined seismic layers, separated by sharp discontinuities in Vp, and the gradient of Vp with depth (e.g., Christensen, 1978; Christensen and Salisbury, 1975; Geological Society of America, 1972; Peterson et al., 1974; Raitt, 1963). However, as noted by, e.g., Christensen and Mooney (1995) and Sammon et al. (2022), continental crust generally lacks consistent, well-defined seismic discontinuities, and instead is characterized by smoothly increasing Vp with depth.

Here, we define the lower crust as extending from 25 km to the base of the crust, where a sharp increase in Vp generally defines the *Mohorovičić* discontinuity at the top of the continental upper mantle. Choice of a depth of 25 km for the top of the lower crust, at about 0.7 GPa, is based on equilibrium thermodynamic calculations showing that garnet becomes an important phase in thousands of granulite rock compositions at >700 °C and pressures greater than 0.7–0.9 GPa (e.g., Jull and Kelemen, 2001; Hacker et al., 2015). The assumption of equilibrium can be questioned, of course, because for example it is possible to sample garnet-bearing rocks at the Earth's surface, and conversely some "dry" granulites in metamorphic terrains have not formed garnet, even in in eclogite facies conditions, due to kinetic limitations (e.g., Austrheim and Griffin, 1985). However—based on metamorphic thermobarometry that does not involve garnet—garnet is present in the Talkeetna and Kohistan arc crustal sections where it is predicted, and absent where it is not predicted (Hacker et al., 2008). On this basis we infer that a close approach to equilibrium is common in lower arc and continental crust metamorphosed at >700 °C.

Following the CRUST1.0 model (Laske et al., 2012, 2013), we assign an average thickness of 39 km to average continental crust in shields, platforms, and Paleozoic to Mesozoic orogens (Supplementary Table 1 in the online version at https://doi.org/10.1016/B978-0-323-99762-1.00121-2). The range of 25–39 km yields an average depth of 32 km within the lower continental crust. In turn, the area-weighted average upper crust thickness for shields, platforms, and Paleozoic to Mesozoic orogens in CRUST1.0 is 14 km, leaving an 11 km thick mid-crust extending from 14 to 25 km, with an average depth of 19.5 km.

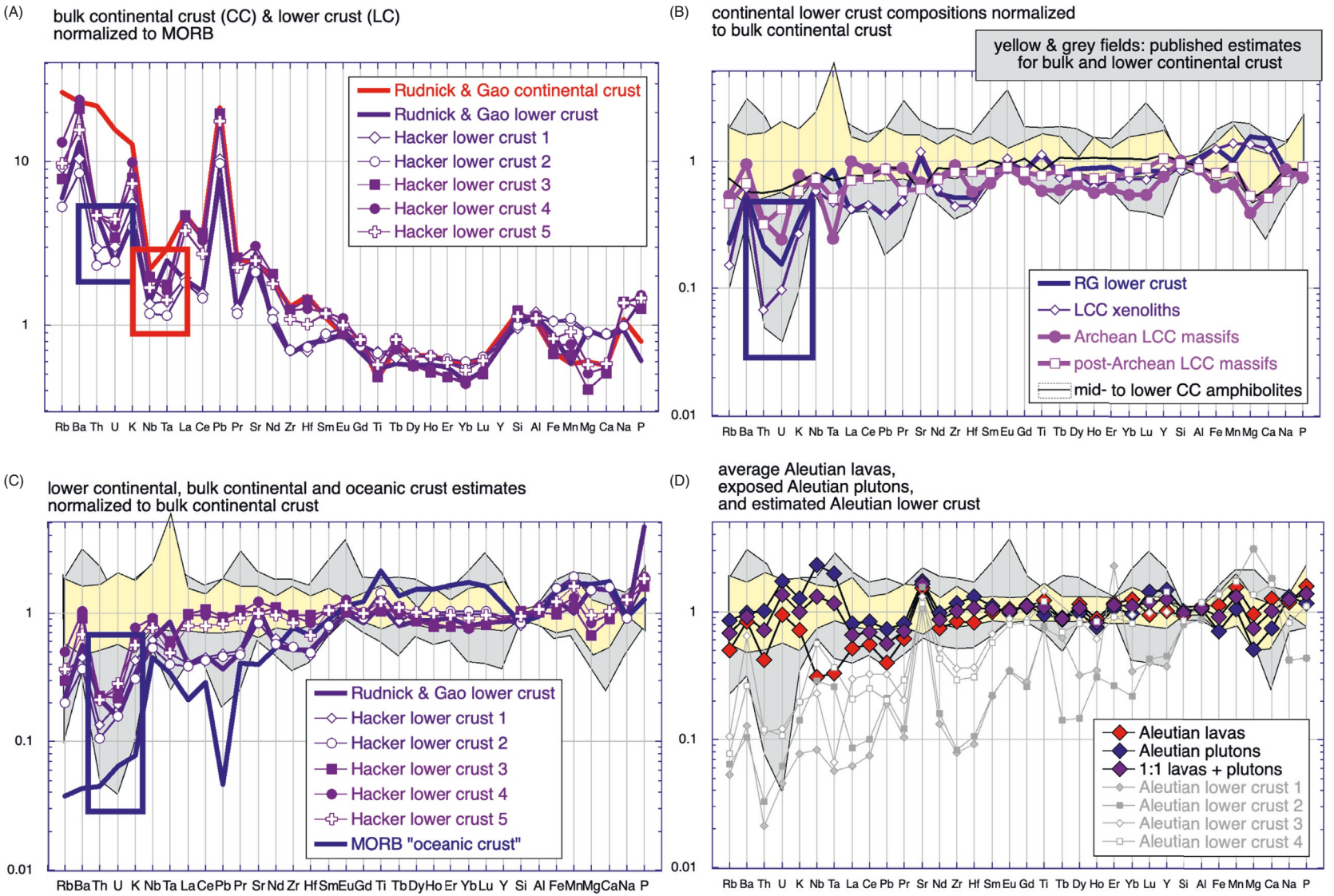

Fig. 3 Geochemical plots illustrating proposed compositions of lower and bulk continental crust. (A–D) Extended major and trace element plots, with compositions normalized to N-MORB in panel (A) (Gale et al., 2013) and to the bulk continental crust composition of Rudnick and Gao (2003, 2014) in panels (B–D). Yellow and grey fields illustrate maximum and minimum concentrations for published estimates of bulk and lower continental crust composition (references in Kelemen and Behn, 2016). Blue rectangles highlight depletions in Th and U relative to Rb, Ba, K and La in the lower continental crust, which are not present in MORB, arc lavas, or bulk continental crust. Red rectangle highlights depletions in Nb and Ta, relative to K and La, which are ubiquitous in arc lavas and in lower and bulk continental crust, but not in MORB or ocean island basalts. (A,C) Lower continental crust compositions

(Continued)

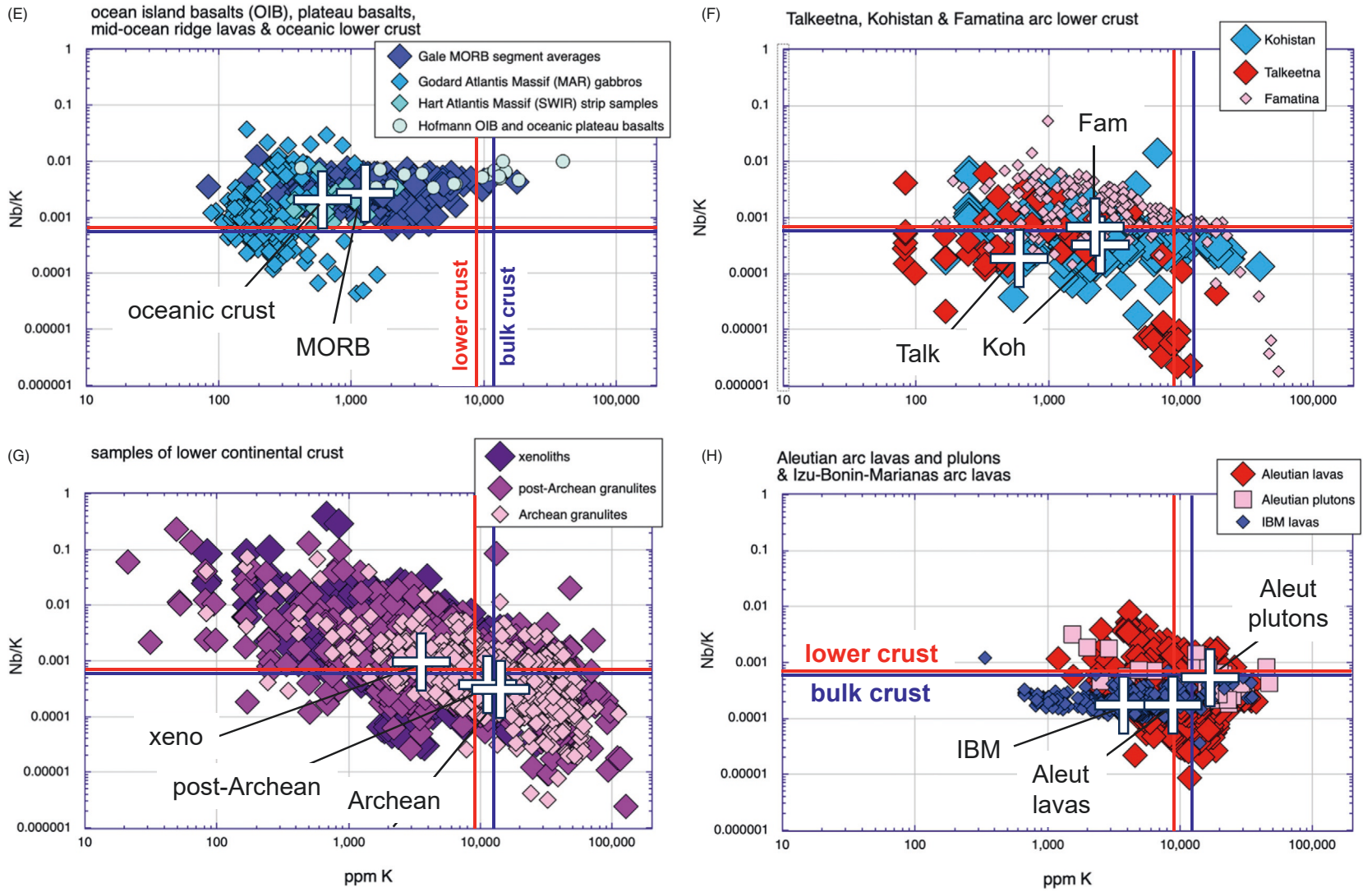

Fig. 3—Cont'd from Rudnick and Gao (2003, 2014) and Hacker et al. (2015). (B) Average compositions of samples from Archean terrains, post-Archean terrains and xenoliths recording lower crustal conditions, and of amphibolites proposed to be representative of the middle crust by Huang et al. (2013), together with the lower continental crust composition of Rudnick and Gao (2003, 2014). (D) Averages of compositions of lavas & exposed, upper to mid-crustal plutons in the Aleutian volcanic arc, together with estimated Aleutian lower crustal compositions. See Kelemen and Behn (2016) for Aleutian data sources. (E,H) Plots of K concentration vs Nb/K ratios. Red and blue lines in all panels indicate composition of our preferred lower and bulk continental crust compositions (geometric means). (E) MORB segment averages from Gale et al. (2013, omitting back arc basins), lower oceanic crust sample compositions from Godard et al. (2009) and Hart et al. (1999), and a compilation of averages for ocean island basalts and oceanic volcanic plateau from Hofmann et al. (2022). Crosses indicate the average composition of oceanic crust (VanTongeren et al., 2021) and MORB (Gale et al., 2013). (F) Sample (points) and average (crosses) compositions of volcanic arc lower crust. References as for Fig. 1. (G) Sample (points) and average (crosses) compositions of lower crustal granulites. References as for Fig. 1. (H) Sample (points) and average (crosses) compositions of lavas and exposed, upper to mid-crustal plutons in volcanic arcs (Jordan et al., 2012; Kelemen and Behn, 2016; Kelemen et al., 2003a, 2014).

Table 1 Recently published compositions of lower and middle continental crust.

		Rudnick and Fountain, 1995	*Rudnick and Gao, 2003, 2014*	*Hacker et al., 2015*	*Hacker et al., 2015*	*Hacker et al., 2015*	*Hacker et al., 2015*	*Hacker et al., 2015*	*Emo et al., 2021*	*Sammon and McDonough, 2021*	*Sammon et al., 2022*	*Pease et al., 2023*	*Cui et al., 2023*	*Cui et al., 2023*	*This paper*	*This paper*
		Lower crust	*Lower crust*	*Most mafic lower crust*	*Vp 7.1–7.3 lower crust*	*Most felsic lower crust*	*Vp 6.7–6.9 lower crust*	*Lower crust = middle crust*	*Refractory lower crust*	*Lower crust*	*Lower crust*	*Lower crust EarthChem Prior*	*Lower crust RF1.0*	*Lower crust RF0.5*	*Recommended lower crust 410 °C, 0.92 GPa*	*Recommended lower crust 510 °C, 0.92 GPa*
Density 410 °C, 0.92 GPa	kg/m^3	3147	3146	3225	3215	2930	2981	3014	3156	3088	3109	3076	3203	3102	2994	3024
Vp 410 °C, 0.92 GPa	km/s	7.16	7.16	7.25	7.24	6.69	6.80	6.83	7.18	7.08	7.01	6.94	7.29	7.02	6.86	6.89
Vs 410 °C, 0.92 GPa	km/s	4.15	4.15	4.10	4.15	3.92	3.93	3.95	4.17	4.08	4.08	3.99	4.19	4.06	3.98	3.99
Vp/Vs 410 °C, 0.92 GPa		1.72	1.72	1.77	1.74	1.71	1.73	1.73	1.72	1.74	1.72	1.74	1.74	1.73	1.71	1.72
wt%	SiO2	53.4	53.41	48.6	50.7	61.9	58.0	57.3	52.98	53.28	55.38	54.6	51.1	54.5	57.71	56.86
wt%	TiO2	0.8	0.82	1.40	1.24	0.78	0.91	0.99	0.90	0.98	0.88	1.09	0.9	0.9	0.92	0.95
wt%	Al2O3	16.9	16.90	18.1	16.5	16.1	17.5	16.8	17.89	17.19	17.45	15.9	16.5	16.4	16.64	16.71
wt%	FeOT	8.6	8.57	10.44	10.39	6.52	7.41	8.15	8.97	7.12	9.09	8.41	9.1	8.4	7.97	8.27
wt%	MnO	0.1	0.10	0.18	0.19	0.11	0.13	0.16		0.16	0.16				0.14	0.14
wt%	MgO	7.2	7.24	6.87	7.03	3.14	3.93	4.46	6.80	7.63	5.12	7.24	8.7	6.7	4.84	5.18
wt%	CaO	9.6	9.59	10.10	10.10	5.77	6.23	6.63	9.61	10.15	8.06	8.36	10.8	9.1	6.66	7.01
wt%	Na2O	2.7	2.65	2.85	2.80	3.92	3.82	3.89	2.42	2.63	2.86	3.21	2.4	2.9	3.08	3.03
wt%	K2O	0.6	0.61	1.22	0.79	1.54	1.86	1.42	0.43	0.70	1.00	1.23	0.5	1.0	1.58	1.50
wt%	P2O5	0.1	0.10	0.23	0.22	0.21	0.25	0.24		0.16					0.22	0.23
100 × molar Mg/(Mg + Fe)	molar	Mg# (%)	60	60	54	55	46	49	49	57	66	50	61	63	59	52
53																
Heat production	μW/m^3	0.16	0.16	0.14	0.11	0.18	0.19	0.20	0.10	0.14					0.60	0.58
	ppm Rb	11	11	17	10	14	24	18	7.14	10.6					41	39
	ppm Th	1.2	1.2	0.75	0.59	1.26	1.19	1.19	0.70	0.77					4.6	4.3
	ppm U	0.2	0.2	0.25	0.20	0.29	0.34	0.37	0.13	0.25					0.8	0.8
	ppm K	5083	5065	6434	4659	9292	11,617	8508	3570	5809	8280	10,228	4197	8335	12,950	12,354
	ppm Sm	2.8	2.8	2.9	3.1	4.1	4.2	4.1	2.57	3.57					5.1	5.0

Notes: Major element concentrations normalizzed to 100 wt%, volatile-free. FeOT = all iron as FeO.

Physical properties for all compositions EXCEPT this paper calculated using Perple_X 6.6.7 following methods described in Section "Methods."

Physical properties for our recommended lower crust compositions are Vp-weighted averages of individual sample values. Values for each sample were calculted using Perple_X 6.6.7 following methods described in Section "Methods."

Seismic properties of the middle and lower crust

Following past work, we use compilations of P-wave speed (Vp), shear wave speed (Vs), and their ratios (Vp/Vs) from Holbrook et al. (1992) and Hacker et al. (2015). We find that Vs is not well correlated with rock composition at lower crustal conditions, in the compositional range of interest, and so we focus on Vp.

The results of Holbrook et al. (1992) and Hacker et al. (2015) are very similar, and consistent with Vp of Christensen and Mooney (1995) at 30–35 km, suggesting that these values are well-determined, though updated compilations could be useful. These Vp compilations yield *median and average* Vp of 6.8–6.9 km/s at lower crustal depths. In contrast—partly due to definitions of lower crust that *depend* on high Vp rather than depth—many previous reviews of lower crust have inferred that the lower crust has Vp *substantially greater than* 6.9 km/s, for example with an *average* in situ Vp of 7.1 km/s (Huang et al., 2013, Table 4).

The compiled seismic data for the "lower crust" (Hacker et al., 2015; Holbrook et al., 1992) were originally calculated and reported in terms of 2D "layers"—vertically-oriented, horizontally-elongate polygons—typically with separate polygons for middle versus lower crust. As noted in the previous section, we define the top of the lower crust to be 25 km, whereas past studies have used different depths in different regions. Thus, in calculating our new averages for lower crustal wave speeds, we combined values from previously defined "lower crust" with a proportion of values from previously defined "middle crust", as detailed in Supplementary Table 1 in the online version at https://doi.org/10.1016/B978-0-323-99762-1.00121-2.

Holbrook et al. and Hacker et al. compiled the cumulative cross-sectional area of rocks with a given Vp (height × length in 2D seismic transects). We weighted these data according to the relative surface areas and crustal thickness of their different tectonic settings to produce an areally-weighted distribution of P-wave and Vp/Vs values (Fig. 4 and Supplementary Table 1 in the online version at https://doi.org/10.1016/B978-0-323-99762-1.00121-2).

The thickness of crust in tectonically active regions is variable, and in many cases includes little material below 25 km depth. For this reason, in calculating averages for both middle and lower crust (for Vp as well as for heat flow, Section "Temperatures and pressures in the middle and lower crust") we focus on shields, platforms and Paleozoic to Mesozoic orogens. Together, these have median and average Vp of 6.82 and 6.91 km/s, respectively. If we do not incorporate a proportion of previously defined mid-crust, the lower crust median and average values shift upward to 6.94 and 6.98 km/s, respectively. If we include young orogens, rifts and arcs, as well as older, stable crust, median and average values shift to 6.86 and 6.93 km/s, respectively.

The SiO_2 content of metamorphic rocks is negatively correlated with Vp. Thus, the inference that the average Vp of lower crust is 6.9 km/s yields a more SiO_2-rich composition than the inference that lower crust has an average Vp of 7.1 km/s.

Temperatures and pressures in the middle and lower crust

As can be seen in Fig. 5, the choice of lower crustal pressure and temperature has a significant influence on the inferred composition of the lower crust. Higher pressures and/or lower temperatures yield higher Vp for a given composition and mineral assemblage, while SiO_2 contents in most crustal rocks decrease with increasing Vp. As a result, choice of a relatively hot lower crustal temperature yields a relatively mafic lower crust composition at a given Vp.

Relationships of pressure, density and depth in the crust depend on the average composition of the crust as a function of depth. However, fortunately, the densities of inferred crustal compositions do not vary substantially from one study to another. For example, we calculate densities of 2748, 2789, and 3146 kg/m^3 for the upper, middle and lower crust compositions of Rudnick and Gao (2003, 2014),[2] and densities of about 2800 and 3000 kg/m^3 for the middle and lower crust in this study. Using either data set, and upper, middle and lower crust thicknesses in Section "Definitions of the middle and lower crust", yields 0.38 GPa for the top of the middle crust, 0.54 GPa for average middle crust, 0.69–0.70 GPa for the top of lower crust, 0.90–0.92 GPa for average lower crust, and 1.1 GPa for the base of the crust.

Unfortunately, in contrast to pressure, the relationship of temperature to depth in the continental crust is not well known, despite its importance. In principle, one could use estimates of heat production in crust compositions, together with heat flow from the mantle, to calculate steady state crustal temperatures as a function of depth. However, in practice, the uncertainties in both crust compositions and mantle heat flow yield unacceptably large uncertainties in temperature. Instead, crustal temperatures at a given depth can be estimated from surface heat flow, combined with inferences about variation in crustal composition and heat production as a function of depth.

Surface heat flow in young continental crust is highly variable. The recent compilation of Lucazeau (2019) includes values from less than 20 to more than 120 mW/m^2 for crust less than 200 million years old, and for older, thermally reactivated regions (most notably, the South Australian Heat Flow Anomaly, e.g., Lucazeau, 2019, Neumann et al., 2000). In young crust, this variability is due in part to high heat flow in continental rift zones (Lysak, 1992; Morgan, 1982), and to low heat flow in forearcs juxtaposed with high heat flow volcanic arcs (Blackwell et al., 1982; England and Molnar, 1983; Furukawa, 1993; Fyfe and McBirney, 1975; Molnar and England, 1990). In turn, these variations are due to advection of hot rocks and magmas upward, and advection of cold rocks downward, in tectonically active settings. Such relatively rapid advection of heat is not incorporated in calculated steady state geotherms, which generally account only for thermal diffusion and radioactive heat production.

Shallow magma chambers and volcanic necks cause high surface heat flow, potentially over a broad region due to hydrothermal convection. As noted by, e.g., Blackwell et al. (1982) and Rothstein and Manning, (2003), rapid thermal advection by magmas and

[2]We calculated the density of Rudnick & Gao upper and middle crust at average middle crust conditions of 280 °C and 0.54 GPa, and the density of Rudnick & Gao lower crust at average lower crust conditions of 410 °C and 0.92 GPa.

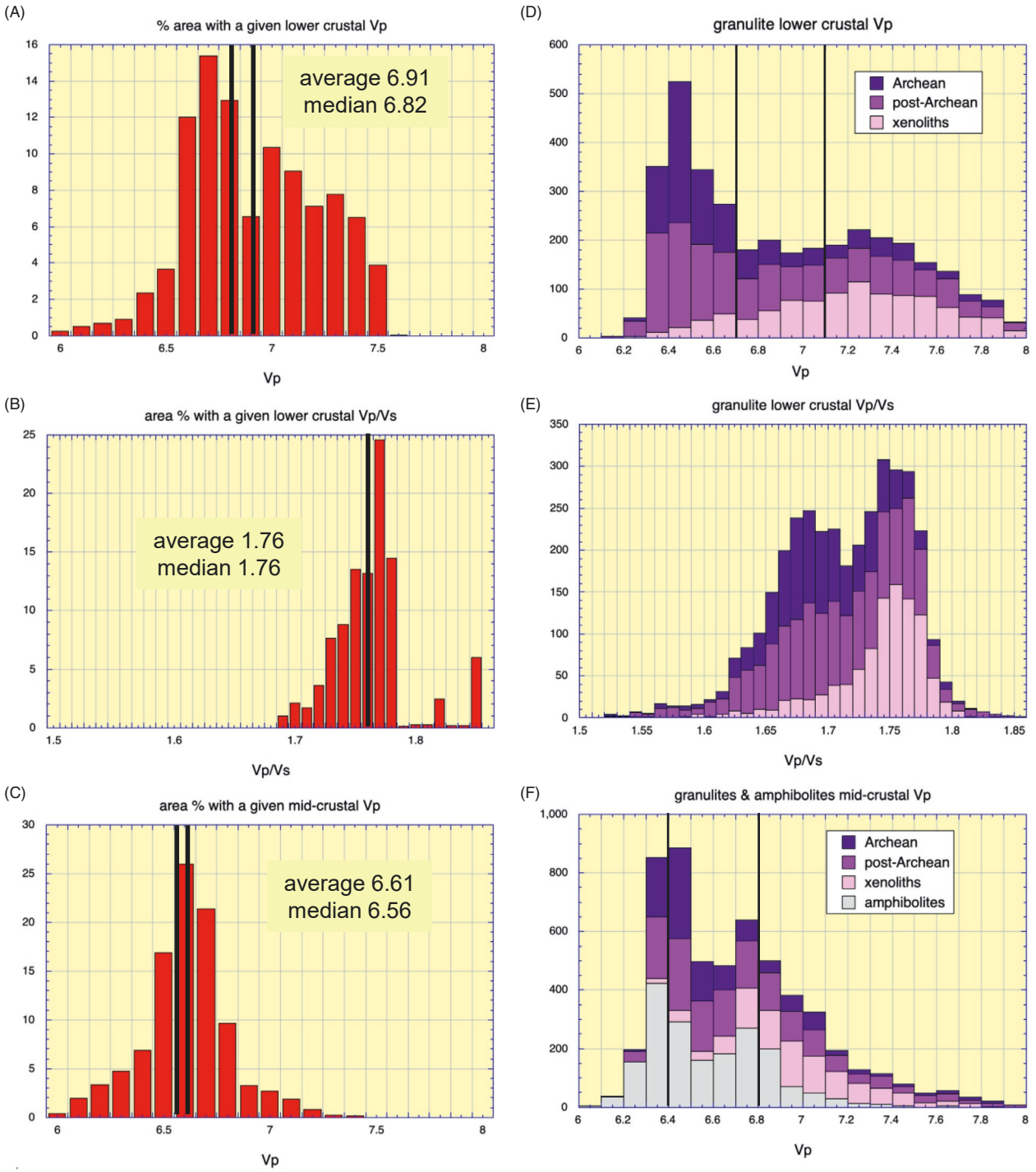

Fig. 4 Histograms of observed and calculated seismic wave speeds in the lower and middle continental crust. Compiled observations are reported in Supplementary Table 1 in the online version at https://doi.org/10.1016/B978-0-323-99762-1.00121-2. Calculated values for rock compositions are reported in Supplementary Table 2 in the online version at https://doi.org/10.1016/B978-0-323-99762-1.00121-2. (A–C) observed seismic wave speeds, based on cross sectional area-weighted observations for shields, platforms and Mesozoic to Paleozoic orogens (Hacker et al., 2015; Holbrook et al., 1992), weighted by the relative surface area of each setting from CRUST1.0 (see Supplementary Table 1 in the online version at https://doi.org/10.1016/B978-0-323-99762-1.00121-2). (D–F) Histograms of calculated lower crustal Vp and Vp/Vs for granulite compositions at 410 °C, 0.92 GPa, and of calculated Vp for granulite and amphibolite compositions at 280 °C, 0.54 GPa. Black vertical lines in panels D and F illustrate bounds of average lower- and mid-crustal Vp $\pm$ 0.2 km/s, used to choose Vp-filtered alternative lower and middle crust compositions in Table 2 and Supplementary Table 2 in the online version at https://doi.org/10.1016/B978-0-323-99762-1.00121-2.

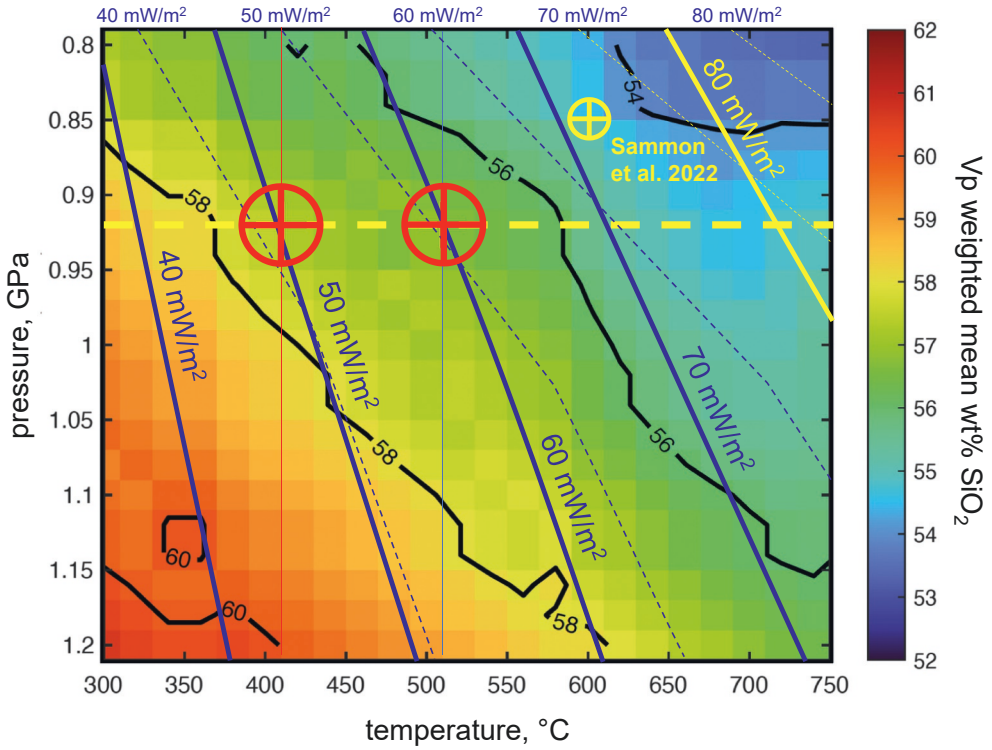

Fig. 5 Temperature and pressure, contoured for the SiO_2 content of Vp-weighted samples from granulite terrains and xenoliths, calculated as described in Sections "Relationship between rock composition and seismic P-wave speed" and "Methods." Solid blue isopleths illustrate geotherms for lower continental crust from Furlong and Chapman (2013) and Pollack and Chapman (1977) as a function of surface heat flow (blue labels in diagram). Blue dashed isopleths illustrate geothermals from Hasterok and Chapman (2011) as a function of surface heat flow (blue labels at top). Red circles with cross indicate the average lower crustal temperature and pressure we used to calculate Vp values for granulite compositions (Section "Temperatures and pressures in the middle and lower crust"). Smaller yellow circle with cross illustrates the temperature and pressure used by Sammon et al. (2022) to calculate Vp values for granulite compositions.

hydrothermal fluids could produce arc crust that is regionally hotter than 1000 °C at about 10 km depth, and nearly isothermal from there to the base of the crust. Indeed, there could be depth intervals in which temperature decreases with depth below shallow plutons (e.g., Fig. 1 in Kelemen et al., 2003b). The observation of shallow magmatism overlying or adjacent to regions of high lower crustal P-wave velocities suggests that lower arc crust could be colder than upper crust, and/or that the location and length scales of seismic observations do not sample the same rock volumes as heat flow measurements. For example, in the Aleutian arc, shallow magma chambers cause high surface heat flow within the volcanic chain. In contrast, seismic data collected over the adjacent forearc yield high P-wave speeds from 7.3 to 7.7 km/s with low Vp/Vs ratios in the lower crust, indicating that the lower crust is composed of relatively cold, mafic material containing little or no melt (Shillington et al., 2013, 2004).

Similarly, thrusting and rifting cause advection of high temperature material toward the surface, which is often faster than establishment of a steady state conductive geotherm. Thrusting can lead to transient inverted geothermal gradients, with hot hanging wall material overlying cold footwall rocks (e.g., Peacock, 1987, 1996; Molnar and England, 1990).

On the other hand, for crust more than 200 million years old, which has not been thermally reactivated by later tectonic events, surface heat flow is less variable, averaging about 52 ± 15 mW/m^2 (1 sigma) with a median of 49 mW/m^2 (data from Fig. 5 of Lucazeau, 2019), as illustrated in Supplementary Fig. 1A in the online version at https://doi.org/10.1016/B978-0-323-99762-1.00121-2 and previously noted in many reviews (Artemieva, 2006; Jaupart and Mareschal, 2003, 2014; Jaupart et al., 2016; Mareschal and Jaupart, 2013; Pollack et al., 1993; Sclater et al., 1980; Stein, 1995; Vitorello and Pollack, 1980). These regions account for about 60% of the total continental area. Presumably, the variability in regional heat production and surface heat flow over time is reduced via mechanical mixing and thermal diffusion. It is also useful to note that—among heat flow observations in younger crust that average 69 ± 23 mW/m^2 (1 sigma) with a median of 65 mW/m^2 (data from Fig. 5 of Lucazeau, 2019), 47% fall within the range of heat flow in older crust (Supplementary Fig. 1B in the online version at https://doi.org/10.1016/B978-0-323-99762-1.00121-2). Thus, about 79% of continental crust has heat flow of 52 ± 15 mW/m^2.

Using heat flow to estimate crustal temperature versus depth also requires assumptions about radioactive heat production versus depth. Given the consensus that the concentration of heat-producing elements decreases with depth, and the lack of seismic evidence for sharp layer boundaries, many workers use models in which heat production decreases exponentially with depth in the upper crust, below which it is constant and 40% lower than the upper crust in the middle to lower crust.

In keeping with this practice, we prefer the relationships between heat flow, temperature and depth developed by Furlong and Chapman (2013) for their Figs. 4A and 5, following the methodology of Pollack and Chapman (1977). We refer to this type of geotherm with the acronym FC,PC. For surface heat flow of 50 mW/m^2, FC,PC geotherms yield temperatures of 280 °C at 0.54 GPa and 410 °C at 0.92 GPa for the middle and lower crust, respectively (Fig. 5).

On the other hand, Hasterok and Chapman (2011) proposed an alternative model, with two crustal layers, each having constant heat production (Fig. 4b in Furlong and Chapman, 2013), with heat production in the lower layer equal to 26% of that in the upper layer. For the same surface heat flow of 50 mW/m^2, the Hasterok and Chapman (HC) approach yields average temperatures of 300 °C at 0.54 GPa and 510 °C at 0.92 GPa for the middle and lower crust, respectively. As we show in Section "Composition of the lower continental crust", for regions with surface heat flow of 50 mW/m^2, lower crustal compositions derived using an HC geotherm contain about 1 wt% less SiO_2 than compositions using an FC,PC geotherm.

For their thermodynamic calculations, Sammon et al. (2022) used lower crust conditions of 600 °C at 0.85 GPa (corresponding to a depth of ~29 km). As shown in Fig. 5, this choice lies near an FC, PC geotherm for surface heat flow of about 72 mW/m^2, higher than average continental surface heat flow, and an HC geotherm for heat flow of about 64 mW/m^2, similar to average continental heat flow (67 mW/m^2, Lucazeau, 2019) including arcs, rifts and other tectonically active regions, and higher than average heat flow for undisturbed crust more than 200 million years old. Along an HC 64 mW/m^2 geotherm, the Sammon et al. choice of 600 °C at 0.85 GPa corresponds to a temperature of more than 800 °C at the base of continental crust (1.1 GPa).

In their Bayesian approach, Pease et al. (2023) use a map of continental heat flow provinces, and a corresponding set of geotherms, developed by Artemieva (2006). Implicitly, because this map includes tectonically active regions, which Artemieva incorrectly interpreted as having steady state conductive geotherms, Pease et al. must have used significantly higher lower crustal temperatures than those along the 50 mW/m^2 geotherms of Pollack and Chapman, Hasterock and Chapman, or Furlong and Chapman.

Such high temperatures at the base of stable continental crust are inconsistent with a variety of data. For example, pressure/temperature trends recorded by suites of mantle xenoliths can be used to extrapolate to lower pressures, assuming that the xenoliths record PT points along a smooth, steady state geotherm. Rudnick et al. (1998) used mantle xenolith data to infer temperatures of about 340–550 °C at 25–40 km depths in stable continental regions with surface heat flow of 50 mW/m^2 (their Fig. 6B). Similarly, a recent review of continental geotherms by Goes et al. (2020) shows that compiled mantle xenolith PT data preclude temperatures greater than 550 °C at depths less than 40 km in stable continental regions. These authors also illustrate results of a full range of steady state geotherm models based on heat flow and assumptions about crustal heat production, which yield temperatures less than 550 °C at 40 km and less than 450 °C at 25 km, for regions with heat flow of 50 mW/m^2.

To reiterate, because the P-wave velocity for a given rock composition decreases with increasing temperature, and Vp at a given temperature and pressure increases with decreasing SiO_2 content, interpreting Vp in terms of composition will yield a more mafic, SiO_2-poor composition at a higher temperature and a more felsic, SiO_2-rich composition at a lower temperature (Fig. 5). This may be the main reason why our estimated lower crust compositions have higher SiO_2 contents than those of Sammon et al. and Pease et al.

Rock samples from the middle and lower crust

For over 50 years, scientists have inferred that granulite facies metamorphic rocks are samples of lower continental crust (e.g., Holland and Lambert, 1972), because these rocks record pressures of equilibration consistent with the depth and thickness of lower continental crust. For example, as illustrated in Supplementary Fig. 2 in the online version at https://doi.org/10.1016/B978-0-323-99762-1.00121-2, reviews of 375 tectonically exposed, granulite facies metamorphic suites yield median and average pressures of 0.95 and 1.05 ± 0.4 (1 sigma) GPa respectively (Brown, 2007; Brown and Johnson, 2019). An asymmetric distribution of pressures may reflect partial preservation of mineral assemblages formed at higher pressures during transient, orogenic crustal thickening events, as is thought to be currently occurring in southern Tibet.

Mineral assemblages in granulite facies metamorphic rocks record temperatures from ~500 to 1100 °C, with an average of 825 ± 113 °C (1 sigma) and a median of 840 °C (Brown, 2007, Brown and Johnson, 2019). These temperatures are higher than in stable lower continental crust more than 200 million years old. Moreover, some—perhaps most—of these are "closure temperatures," recorded during re-equilibration of minerals during cooling when temperatures fall below a "closure temperature" that depends on reaction kinetics and cooling rates (e.g., Dodson, 1973). Following past practice (e.g., Sammon and McDonough, 2021, and references cited therein), we infer that most granulite facies metamorphic rocks formed at high temperature in the lower crust during orogenic events, and then cooled isobarically to ambient lower crustal temperatures. However, we cannot rule out the possibilities that some granulites record pressures lower than their peak pressures of metamorphism, and/or that cooling from their closure temperatures to ambient crustal temperatures was accompanied by decompression.

Granulite suites, recording past metamorphism, are currently exposed on the surface, in areas with 30–50 km thick crust. This raises the question: What is beneath exposed granulite facies metamorphic terrains at the present time? This issue can be viewed in the context of different explanations for granulite facies metamorphism. In one view, granulite facies rocks form in the mid-crust, within ~80 km thick crust formed by transient thickening and radioactive heating during continental collisions, as may be occurring

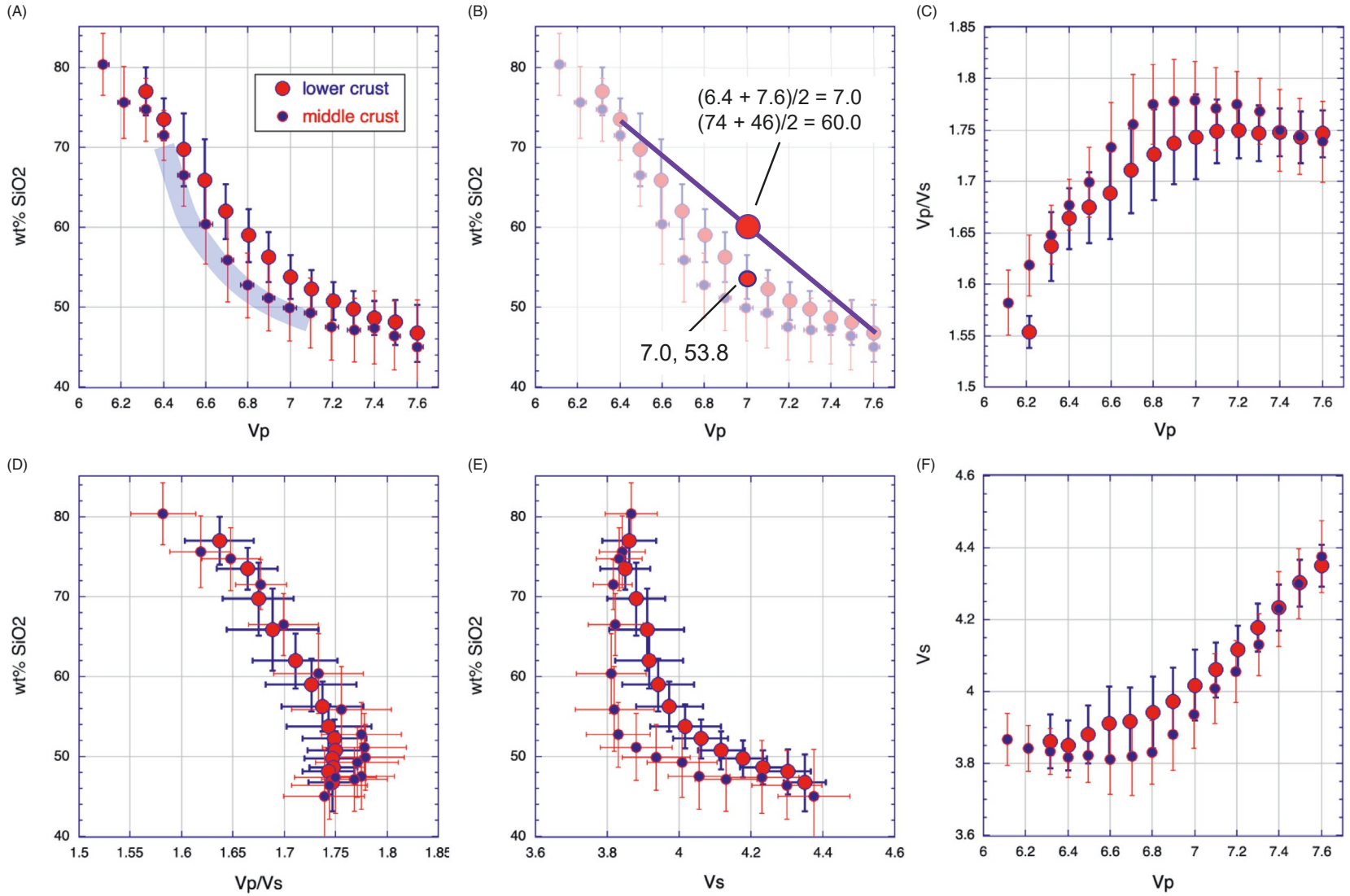

Fig. 6 Average SiO_2 contents, Vs and Vp/Vs ratios for a given Vp, for granulite compositions lower crustal conditions (410 °C, 0.92 GPa) and for granulite and amphibolite compositions at mid-crustal conditions (280 °C, 0.54 GPa). (A–F) Cross plots of arithmetic mean values of SiO^2 contents and seismic wave speeds in Supplementary Table 2 in the online version at https://doi.org/10.1016/B978-0-323-99762-1.00121-2, for lower crust (granulites at 410 °C, 0.92 GPa) and middle crust (granulites and amphibolites at 280 °C, 0.54 GPa) on an FC,PC style 50 mW/m^2 geotherm. Error bars illustrate 1 sigma variation from the arithmetic mean. (A) Shaded blue curve in panel A shows approximate trend of experimental Vp data (~25 °C, 0.6 GPa) vs SiO_2 from Huang et al. (2013, their Fig. 3), connecting their mafic, intermediate and felsic granulite averages, "corrected" to lower crustal temperature (410 °C, $\Delta T = 385$ °C) and pressure (0.92 GPa, $\Delta P = 0.32$ GPa) using their preferred derivatives of -0.0004 km/s/°C and 0.2 km/s/GPa. (B) Purple line shows that 1:1 mechanical mixing of felsic and mafic compositions with Vp of 6.4 and 7.6 km/s produces an intermediate composition with Vp of 7.0 km/s and 60 wt% SiO_2, significantly higher than the average SiO_2 content of granulite samples with Vp of 7.0 km/s.

(Continued)

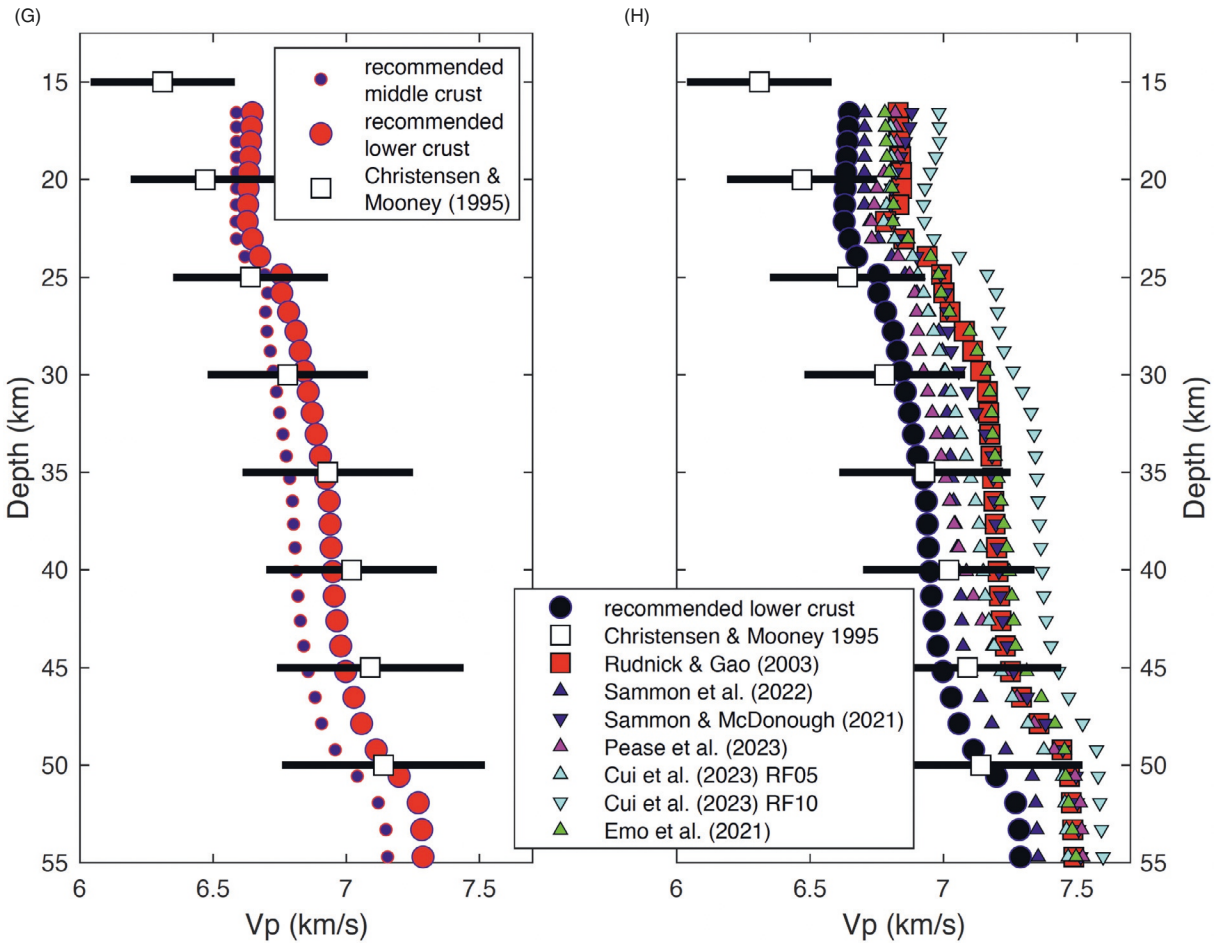

Fig. 6—Cont'd (G) Seismic P-wave speeds calculated for our recommended lower and middle crust compositions (Table 2 and Supplementary Table 2 in the online version at https://doi.org/10.1016/B978-0-323-99762-1.00121-2) as a function of depth, along a 50 mW/m^2 "FC,PC" continental geotherm as modeled by Furlong and Chapman (2013) and Pollack and Chapman (1977), compared to variation in Vp versus depth estimated by Christensen and Mooney (1995) shown with black bars and open squares. (H) Seismic P-wave speeds calculated for our recommended lower crust (black) and in lower crust compositions from Rudnick and Gao (2003, 2014), Sammon et al. (2022), Pease et al. (2023), Cui et al. (2023) and Emo et al. (2021).

in southern Tibet today (e.g, Jaupart et al., 1985; McKenzie and Priestley, 2008).[3] In another view, granulite facies metamorphism occurs near the base of normal thickness crust, during arc- or rift-related heating events (e.g., Miyashiro, 1961). In this latter scenario, the rocks beneath exposed granulite terrains must have been added to the underlying crust by thrusting or underplating after granulite metamorphism. Either way, we must use additional data to infer which, if any, granulite facies metamorphic rocks could be representative of present-day lower continental crust.

Granulite facies rock compositions are highly variable (e.g., Figs. 1E, 3B and 3G). Compiled compositions for Archean and post-Archean granulite terrains (Hacker et al., 2015; Huang et al., 2013; Sammon and McDonough, 2021) have average SiO_2 contents of 64 ± 9 and 60 ± 13 wt% SiO_2, respectively (1 sigma, Hacker et al., 2015). As discussed below, in agreement with prior work, we calculate that the average compositions of granulite terrains are too SiO_2-rich, with correspondingly low Vp, to represent average lower continental crust.

Compiled compositions for granulite-facies xenoliths from continental volcanic centers contain an average of 52 ± 7 wt% SiO_2 (1 sigma, Huang et al., 2013). Since xenoliths *might* sample rocks from the present-day lower crust, whereas exhumed metamorphic terrains do not, some workers have proposed that the granulite xenoliths are—on average—more representative of the present-day lower crust (e.g., Huang et al., 2013; Rudnick, 1992; Rudnick and Presper, 1990; Sammon and McDonough, 2021). However, as discussed below, we calculate that the average composition of the granulite xenoliths is too mafic, with a corresponding Vp too high, to correspond to average lower continental crust.

Some prior work treats amphibolite facies metamorphic rocks as representative of middle continental crust (Huang et al., 2013; Rudnick, 1992; Rudnick and Gao, 2003, 2014; Rudnick and Presper, 1990; Sammon and McDonough, 2021). We are not confident about the basis for this, but for this paper we consider the possibility that some amphibolite facies samples (compiled by Huang et al., 2013) together with some granulite facies samples, could be representative of rocks in the middle continental crust.

Relationship between rock composition and seismic P-wave speed

Prior to 2022, most studies inferring a mafic composition for the lower continental crust relied on experimental measurements of acoustic wave speeds (and in some cases shear wave speeds, Vs) for rocks at lab temperature and elevated pressure (typically, 0.6 GPa), together with empirical factors for dVp/dT and dVp/dP, to extrapolate laboratory measurements to lower crustal temperatures and pressures. As discussed more extensively by Hacker et al. (2015), such experimental approaches have weaknesses that limit their application, as follows:

(a) In whole or in part, samples selected for experiments often contained mineral assemblages inconsistent with equilibration at lower crustal depths. Many contained less garnet—with its high seismic wave speeds—than calculated to be present in rocks with their bulk composition at ~0.9 GPa. Moreover, most acoustic wave speed measurements aimed at understanding lower crust were made at 0.6 GPa. As demonstrated by, e.g., Jull and Kelemen (2001), the equilibrium proportion of garnet in metamorphic rocks, and thus their density, varies dramatically between 0.6 and 0.9 GPa. Also, many samples selected for laboratory investigation contained minerals formed by alteration during or after exhumation to the surface. As a result of these factors, some samples had experimental wave speeds lower than those of rocks with the same bulk composition, equilibrated in the lower crust.

(b) Similarly, decompression of lower crustal rocks during transport to the surface, via rapid ascent as xenoliths in lavas or slow tectonic exhumation, forms microcracks which can irreversibly reduce wave speeds, compared to those for the same bulk composition at lower crustal conditions (e.g, Fig. 14 and related text in Behn and Kelemen, 2003).

(c) Many mafic samples were selected for experimental study based in part on the assumption that relatively high seismic wave speeds in lower continental crust, compared to upper crust, indicated that the lower crust was mafic. In contrast, relatively few intermediate to felsic samples were selected for experimental measurements (e.g., Supplementary Fig. 2 in Hacker et al., 2015).

(d) Extrapolation of experimental wave-speeds (almost all at 20–25 °C) to the in situ seismic properties of lower continental crust requires "correction" of the in situ observations to experimental temperature and pressure, or vice versa. The nature of this correction is approximate and uncertain. Single values of of dVp/dT of –0.0004 km/s per °C and dVp/dP of 0.2 km/s per GPa are often used. However, Korenaga et al. (2002), using the elastic properties of minerals and mixture theory, found that these derivatives for mafic rocks at 400 °C and 0.6 GPa ranged from 0.00035 to 0.00043 and from 0.175 to 0.225, respectively, for rocks with in situ Vp of 6.7–7.1.

To avoid such biases, some recent studies relating physical properties and rock compositions rely on thermodynamically calculated mineral proportions in a bulk composition at a given pressure and temperature, together with the elastic properties of those minerals, and then use mixture theory to estimate the physical properties of polymineralic rocks.

This methodology yields systematically higher Vp, and Vp/Vs, for mafic, intermediate and felsic bulk compositions, compared with empirical fits based on the experimental data described above. The lower crustal mineral assemblages and physical properties

[3]It is noteworthy that thickened crust in southern Tibet has seismic P-wave speeds much *lower* than average Vp at a given depth in stable continental crust (Kind et al., 2002; Zhao et al. 2002; Schulte-Pelkum et al., 2005; Monsalve et al., 2006, 2008; Nabelek et al., 2009; Wittlinger et al., 2009), while temperatures at the base of the crust in southern Tibet are estimated to be ~600 °C at 80 km (e.g., Craig et al., 2020 and references therein). Thus, the low Vp in the lower crust of southern Tibet is probably indicative of relatively SiO_2-rich compositions compared to average lower continental crust. This is not consistent with the idea that granulite terrains are metamorphosed in the middle crust during orogenic thickening,and are underlain by a more mafic lower crust.

used by Behn and Kelemen (2003, 2006), Hacker et al. (2015), Kelemen and Behn (2016), Sammon et al. (2022), Pease et al. (2023) and this paper use this thermodynamically-based methodology.

A recent study (Sui et al., 2022) derived a contour diagram and associated lookup table relating SiO_2 content in samples to Vs and Vp/Vs at lower crustal conditions, based on experimental data. They also used a thermodynamic method, similar to those discussed in the previous paragraph. Though it is not clear in the text of their paper, 80% of their text and figures relied on the contoured experimental data. As can be seen in their Fig. 17, their compositional estimates for North American lower continental crust, based on Vs and Vp/Vs observations, differ by 6–8 wt%, from 51 to 52 wt% SiO_2 based on experimental data, to 58–59 wt% SiO_2 based on thermodynamically-calculated values. Similar, though smaller, differences are another important reason why our average lower crustal SiO_2 content is higher than in prior studies relying solely on experimental data.

Constraints on lower crust composition from surface heat flow, revisited

Some past studies relied on surface heat flow as an important constraint on the composition of lower continental crust, inferring that the concentration of heat producing elements must be low in the lower crust, to be consistent with mantle heat flow plus high heat production in the middle and upper crust. For example, Rudnick and Gao (2003, 2014) used values of mantle heat flow of 17 mW/m^2 (citing Jaupart and Mareschal, 2003, 2014), upper crust heat production of 1.6 $\mu W/m^3$, middle crust heat production of 1.0 $\mu W/m^3$, and surface heat flow of 50 mW/m^2, to infer that heat production in the lower crust must be 0.2 $\mu W/m^3$, consistent with the low U, Th and K contents of mafic granulite xenoliths.

However, given that the range of likely mantle heat flow is 11–18 mW/m^2 as reported in the reviews by Jaupart and Mareschal (2003, 2014), and that composition of the middle crust is uncertain, Hacker et al. (2011, 2015) showed that surface heat flow of 49–51 mW/m^2 could be produced by lower crust with heat production ranging from 0.17 to 0.72 $\mu W/m^3$. We conclude that surface heat flow is not a strong constraint on the composition of the lower continental crust. It is the case, however, that the temperature of the lower continental crust is constrained by both surface heat flow, and heat production as a function of depth in the crust. Though it is beyond the scope of this paper, future studies could ensure that these values are internally consistent.

Composition of the lower continental crust

Following the general approach of Jull and Kelemen (2001) and Hacker et al. (2011, 2015), we calculated equilibrium mineral assemblages in the compiled compositions of granulite samples (Hacker et al., 2015) at closure conditions of 0.5 wt% H_2O, 700 °C, 0.92 GPa for the lower crust, and 0.5 wt% H_2O, 700 °C, 0.54 GPa for the middle crust. Similarly, we calculated equilibrium mineral assemblages in the compiled compositions of amphibolite samples (Huang et al., 2013) at 1.0 wt% H_2O, 650 °C, 0.54 GPa for the mid-crust. We then assumed that these rocks underwent isobaric cooling to temperatures along steady state, 50 mW/m^2 geotherms, of 410–510 °C in the lower crust, and 280–300 °C in the middle crust, as described in Section "Seismic properties of the middle and lower crust." We calculated physical properties for the mineral assemblages at these lower temperatures, using the elastic properties of minerals, and mixture theory, to estimate density, Vp and Vs (Figs. 4D–F, and Supplementary Table 2 in the online version at https://doi.org/10.1016/B978-0-323-99762-1.00121-2).

Using this suite of samples, we calculated average compositions for each P-wave speed (Fig. 6), and multiplied these values by the proportions of each P-wave speed observed in the lower and middle crust (Fig. 4A, C and Supplementary Table 1 in the online version at https://doi.org/10.1016/B978-0-323-99762-1.00121-2) to determine weighted average lower crust compositions with 56.9–57.7 wt% SiO_2, respectively (Figs. 1C, 1D and 7, Table 2, and Supplementary Table 2 in the online version at https://doi.org/10.1016/B978-0-323-99762-1.00121-2). These are our preferred estimates, because they incorporate the compositional variability represented by the full range of lower crustal Vp observations. For simplicity, in Figs. 6–8 and 11 we use the weighted average composition for Vp calculated at 410 °C and 0.92 GPa along an FC,PC 50 mW/m^2 geotherm.

In addition to our preferred estimates, discussed in the previous paragraph, alternative compositions for the lower crust are presented in Table 2, and Supplementary Table 2 in the online version at https://doi.org/10.1016/B978-0-323-99762-1.00121-2. These result from averaging all of the compiled granulite rock compositions with Vp between 6.7 and 7.1 at 410 °C or 510 °C, 0.92 GPa with 0.5 wt% H_2O. These alternatives are similar to our preferred, weighted average compositions, with 55.7–56.6 wt% SiO_2, about 1 wt% lower than in our preferred compositions.

Using *both* the preferred and alternative estimates, the average lower continental crust (Table 2, and Supplementary Table 2 in the online version at https://doi.org/10.1016/B978-0-323-99762-1.00121-2) has an intermediate composition with 55.7–57.7 wt% SiO_2, an Mg# of 48–50, a density of 3000 kg/m^3, radioactive heat production of 0.58–0.65 $\mu W/m^3$, Vp of 6.9 km/s, and a Vp/Vs ratio of 1.72. With the exception of average Vp/Vs, which does not vary much over the relevant range of compositions, our lower crustal compositions are significantly different from most previous estimates for the average lower crust (e.g., lower crust 53.4 wt% SiO_2, Mg# 60, 3150 kg/m^3; 0.16 $\mu W/m^3$, Vp 7.15 km/s, Vp/Vs ~ 1.72, Rudnick and Gao, 2003, 2014). Since before 1995, other than the work of Hacker et al. (2015), no estimates of the composition of lower continental crust contain more than 55 wt% SiO_2, or yield heat production greater than 0.20 $\mu W/m^3$, and only the lower crust of Sammon et al. (2022) has an Mg# less than 60 (Table 1).

The histograms of estimated Vp for granulites and amphibolites and lower and middle crust conditions, (Fig. 4D–F) are strikingly bimodal, as are histograms for SiO_2 in these suites (Hacker et al., 2015). It is likely that in some regions, lower continental

Table 2 Recommended and alternative lower, middle and bulk continental crust compositions.

Lower and middle crust compositions calculated for a Pollack and Chapman (1977), Furlong and Chapman (2013) style 50 mW/m^2 geotherm

		Reccomended lower crust granulites				*Reccomended mid-crust granulites & amphibolites*				*Reccomended bulk crust*	*Alternative granulites with Vp 6.7–7.1*				*Alternative granulites & amphibolites with Vp 6.4–6.8*				*Alternative bulk crust*					
		Vp weighted average	*std dev (±)*	*N*	*std error (±)*	*Vp weighted average*	*std dev (±)*	*N*	*std error (±)*	*Vp weighted LC, MC upper crust from RG*	*Vp filtered average*	*std dev (±)*	*N*	*std error (±)*	*Vp filtered average*	*std dev (±)*	*N*	*std error (±)*	*Vp filtered LC, MC upper crust from RG*	*Rudnick & Gao compositions*				*Gale et al.*
																				Lower crust	*Middle crust*	*Upper crust*	*Bulk crust*	*Normal* ***MORB***
																				Physical properties from PerpleX				**Perple_X**
Density 280 °C, 0.54 GPa	kg/m^3					2786	57	5392	0.78						2820	61	1052	1.9			2789	*2748*		*3055*
Vp 280 °C, 0.54 GPa	km/s					6.47	0.10	5392	0.0014						6.58	0.065	1052	0.0020			6.71			*6.99*
Vs 280 °C, 0.54 GPa	km/s					3.75	0.17	5392	0.0023						3.82	0.074	1052	0.0023			3.80			*3.91*
Vp/Vs 280 °C, 0.54 GPa						1.69	0.11	5392	0.0014						1.72	0.023	1052	0.0007			1.77			*1.79*
Density 410 °C, 0.92 GPa	kg/m^3	2994	70	3295	1.2						3005	93	737	3.4						3146				*3171*
Vp 410 °C, 0.92 GPa	km/s	6.86	0.029	3295	0.00050						6.90	0.11	737	0.0041						7.16				*7.29*
Vs 410 °C, 0.92 GPa	km/s	3.98	0.089	3295	0.0015						3.98	0.10	737	0.0038						4.15				*4.12*
Vp/Vs 410 °C, 0.92 GPa		1.71	0.037	3295	0.00065						1.74	0.04	737	0.0015						1.72				*1.77*
Arithmetic mean values	Normalized to 100 wt% volatile free																							
wt%	SiO_2	57.71	3.55	3295	0.062	61.28	4.66	5392	0.064	61.78	56.57	4.03	737	0.15	62.31	5.79	1052	0.18	61.93	53.40	63.50	66.62	60.60	50.42
wt%	TiO_2	0.92	0.47	3276	0.0083	0.86	0.57	5371	0.0077	0.81	0.93	0.44	735	0.016	0.81	0.59	1049	0.0182	0.80	0.82	0.69	0.64	0.72	0.14
wt%	Al_2O_3	16.64	3.18	3295	0.055	15.86	2.92	5392	0.040	16.00	18.07	3.22	737	0.12	16.02	2.26	1052	0.070	16.66	16.90	15.00	15.40	15.90	15.13
wt%	FeOT	7.97	2.85	3295	0.050	7.16	2.55	5392	0.035	6.73	7.87	2.76	737	0.102	6.64	2.68	1052	0.083	6.59	8.57	6.02	5.04	6.71	9.81
wt%	MnO	0.14	0.11	3201	0.0020	0.13	0.21	5285	0.0029	0.12	0.14	0.076	731	0.0028	0.12	0.208	1041	0.0065	0.12	0.10	0.10	0.10	0.10	0.17
wt%	MgO	4.84	2.23	3289	0.039	3.79	1.68	5384	0.023	3.73	4.43	1.93	737	0.071	3.24	1.69	1051	0.052	3.44	7.24	3.59	2.48	4.66	7.76
wt%	CaO	6.66	2.87	3295	0.050	5.61	2.18	5392	0.030	5.31	6.69	3.04	737	0.11	5.16	2.30	1052	0.071	5.22	9.59	5.25	3.59	6.41	11.35
wt%	Na_2O	3.08	1.23	3293	0.021	3.20	1.29	5386	0.018	3.18	3.44	1.35	737	0.050	3.44	1.22	1050	0.037	3.40	2.65	3.39	3.27	3.07	2.83
wt%	K_2O	1.58	1.39	3287	0.024	1.90	1.60	5379	0.022	2.09	1.56	1.33	736	0.049	2.05	1.68	1050	0.052	2.13	0.61	2.30	2.80	1.81	1.53
wt%	P_2O_5	0.22	0.22	3051	0.0040	0.21	0.31	5105	0.0043	0.19	0.26	0.22	699	0.0083	0.20	0.304	984	0.0097	0.21	0.1	0.15	0.15	0.13	0.16
100 × molar Mg/(Mg + Fe)	Molar Mg# (%)	48	12.1	3289	0.21	45	10.2	5384	0.14	47	49	11.7	737	0.43	44	6.7	1051	0.21	47	60	52	47	55	59
Thickness	km	14				11				39	14				11				39	Ours 14, RG 12	11	Ours 14, RG 17	40	
Heat production (μW/m^3) from arithmetic mean	0.60					0.61					0.65				0.65					0.16	0.83	1.49		
Surface heat flow (mW/m^2)									Mantle 14	50								Mantle 13	50			Mantle 14	50	
Range of surface heat flow (mW/m^2) w mantle contributing 11–18 mW/m^2										*47–54*									*48–55*				47–54	
															0.65									
Arithmetic mean values																								
ppm	Rb	41	60	2728	1.16	55	60	4598	0.89	60	39	52	592	2.1	62	29	917	0.97	61	11	65	84	49	1.8
ppm	Th	4.6	11.0	1613	0.27	4.8	7.3	2564	0.14	6.7	5.2	13.3	364	0.70	5.4	4.2	481	0.19	7.1	1.2	6.5	10.5	5.6	0.25
ppm	U	0.8	1.7	1402	0.045	0.93	1.4	2324	0.028	1.50	0.82	1.61	309	0.092	0.88	0.78	450	0.037	1.49	0.20	1.3	2.7	1.3	0.083
ppm	K	12,950	11,454	3292	200	15,328	12,541	5352	171	17,173	12,883	10,969	737	404	16,964	5979	1051	184	17,676	5064	19,093	23,244	15,025	1162
ppm	Sm	5.1	4.5	1722	0.11	5.0	4.3	3308	0.075	4.9	5.4	4.9	424	0.24	5.3	2.2	616	0.09	5.2	2.8	4.6	4.7	3.9	3.5

Lower and middle crust compositions calculated for a Hasterok and Chapman (2011) style 50 mW/m^2 geotherm

		Reccomended lower crust Vp weighted granulites				*Reccomended middle crust Vp weighted granulites & amphibolites*				*Reccomended bulk crust*	*Alternative lower crust granulites with Vp 6.7–7.1*				*Alternative middle crust granulites & amphibolites with Vp 6.4–6.8*				*Alternative bulk crust*
		Vp weighted average	*std dev (±)*	*N*	*std error (±)*	*Vp weighted average*	*std dev (±)*	*N*	*std error (±)*	*Vp weighted LC,MC upper crust from RG*	*Vp filtered average*	*std dev (±)*	*N*	*std error (±)*	*Vp filtered average*	*std dev (±)*	*N*	*std error (±)*	*Vp filtered LC,MC upper crust from RG*
Density 300 °C, 0.54 GPa	kg/m^3					2799	57	5396	0.78						2827	73	2422	1.5	
Vp 300 °C, 0.54 GPa	km/s					6.50	0.10	5396	0.0014	Concentrations: layer thickness & density weighted sum					6.59	0.232	2422	0.0047	Concentrations: layer thickness & density weighted sum
Vs 300 °C, 0.54 GPa	km/s					3.76	0.17	5396	0.0023						3.81	0.170	2422	0.0034	
Vp/Vs 300 °C, 0.54 GPa						1.70	0.11	5396	0.0014						1.73	0.130	2422	0.0026	
Density 510 °C, 0.92 GPa	kg/m^3	3024	71	3361	1.2						3018	92	742	3.4					
Vp 510 °C, 0.92 GPa	km/s	6.89	0.029	3361	0.00049						6.90	0.11	742	0.0042					
Vs 510 °C, 0.92 GPa	km/s	3.99	0.092	3361	0.0016					Heat production: volume weighted sum	3.97	0.11	742	0.0040					Heat production: volume weighted sum
Vp/Vs 510 °C, 0.92 GPa		1.72	0.039	3361	0.00068						1.74	0.04	742	0.0016					
Arithmetic mean values	Normalized to 100 wt% volatile free																		
wt%	SiO_2	56.86	3.44	3361	0.059	60.97	4.59	5396	0.063	58.59	55.67	3.82	742	0.14	61.75	5.78	2422	0.12	61.56
wt%	TiO_2	0.95	0.50	3342	0.0086	0.87	0.57	5375	0.0078	0.92	0.96	0.50	741	0.018	0.84	0.59	2418	0.012	0.82
wt%	Al_2O_3	16.71	3.35	3361	0.058	15.87	2.38	5396	0.032	16.36	18.18	3.29	742	0.12	16.10	2.27	2422	0.046	16.76
wt%	FeOT	8.27	2.91	3361	0.050	7.27	2.50	5396	0.034	7.85	8.11	2.56	742	0.094	6.87	2.69	2422	0.055	6.76
wt%	MnO	0.14	0.11	3266	0.0020	0.13	0.21	5289	0.0028	0.14	0.14	0.072	737	0.0026	0.12	0.208	2378	0.0043	0.12
wt%	MgO	5.18	2.32	3355	0.040	3.89	1.68	5388	0.023	4.64	4.73	2.02	742	0.074	3.37	1.69	2421	0.034	3.60
wt%	CaO	7.01	2.96	3361	0.051	5.72	2.15	5396	0.029	6.47	7.11	3.14	742	0.12	5.33	2.34	2422	0.048	5.44
wt%	Na_2O	3.03	1.22	3359	0.021	3.20	1.22	5390	0.017	3.10	3.36	1.32	742	0.048	3.41	1.22	2418	0.025	3.37
wt%	K_2O	1.50	1.33	3353	0.023	1.86	1.58	5383	0.021	1.65	1.45	1.26	741	0.046	2.01	1.69	2419	0.034	2.08
wt%	P_2O_5	0.23	0.23	3112	0.0041	0.21	0.31	5108	0.0043	0.22	0.26	0.24	701	0.0089	0.21	0.290	2289	0.0061	0.21
100 × molar Mg/(Mg + Fe)	Molar Mg# (%)	49	12	3355	0.21	45	9.4	5388	0.13	48	50	12	742	0.43	45	9.6	2421	0.20	48
Thickness	km	14				11				39	14				11				39
Heat production (μW/m^3) from arithmetic mean	0.58					0.58					0.53				0.62				
Surface heat flow (mW/m^2)									Mantle	15 50								Mantle	15 50
Range of surface heat flow (mW/m^2) w mantle contributing 11–18 mW/m^2										*47–54*									*48–55*
Arithmetic mean values																			
ppm	Rb	39	56	2778	1.07	54	57	4630	0.83	45	34	44	599	1.8	61	63	2139	1.37	59
ppm	Th	4.3	9.7	1644	0.24	4.6	8.3	2582	0.16	4.4	4.2	7.9	374	0.41	5.2	9.9	1124	0.30	6.7
ppm	U	0.8	1.5	1423	0.039	0.90	1.5	2338	0.030	0.83	0.68	1.28	323	0.071	0.86	1.36	1025	0.043	1.43
ppm	K	12,354	10,984	3358	190	15,079	11,327	5393	154	13,502	12,001	10,440	742	383	16,584	12,530	2421	255	17,264
ppm	Sm	5.0	4.4	1763	0.11	5.0	3.9	3337	0.067	5.0	5.2	4.6	439	0.22	5.3	4.6	1373	0.12	5.1

Notes.: Major element concentrations normalizzed to 100 wt%, volatile-free. FeOT = all iron as FeO.

Physical properties for MORB and Rudnick & Gao compositions calculated using Perple_X 6.6.7 following methods described in Section "Methods."

Physical properties for our new lower crust compositions are Vp-weighted or Vp-filtered averages of individual sample values. Values for each sample were calculated using Perple_X 6.6.7 following methods described in Section "Methods."

For lower crust = LC, middle crust = MC and upper crust = UC, and layer thicknesses in meters, and densities in kg/m^3, bulk crust compositions calculated as:

(LC thickness in m × LC density × LC concentration + MC thickness × MC density × MC concentration + UC thickness (14,000 m in this paper) × Rudnick & Gao UC density × Rudnick & Gao UC compostion) ÷ (LC thickness × LC density + MC thickness × MC density + UC thickness × Rudnick & Gao UC density)

Heat production in various crustal volumes calculated as density x 0.000001 x (0.000003387 x ppm K + 0.01139 x ppm Rb + 0.04595 x ppm Sm + 26.18 x ppm Th + 98.29 x ppm U) as recommended by McDonough et al. (2020).

Surface heat flow for bulk crust compositions calculated as LC thickness in m × LC heat production + MC thickness in m × MC heat production + Rudnick & Gao UC heat production × UC thickness (14,000 m in this paper) + mantle heat flow values between 11 and 18 mW/m^2 recommended by Jaupart and Mareschal (2014).

See Supplementary Table 2 in the online version at https://doi.org/10.1016/B978-0-323-99762-1.00121-2 for calculation of Vp-weighted (recommended) and Vp-filtered (alternative) arithmetic mean values, arithmetic standard deviations, geometric mean values and geometric standard deviations for our lower and middle crust compositions.

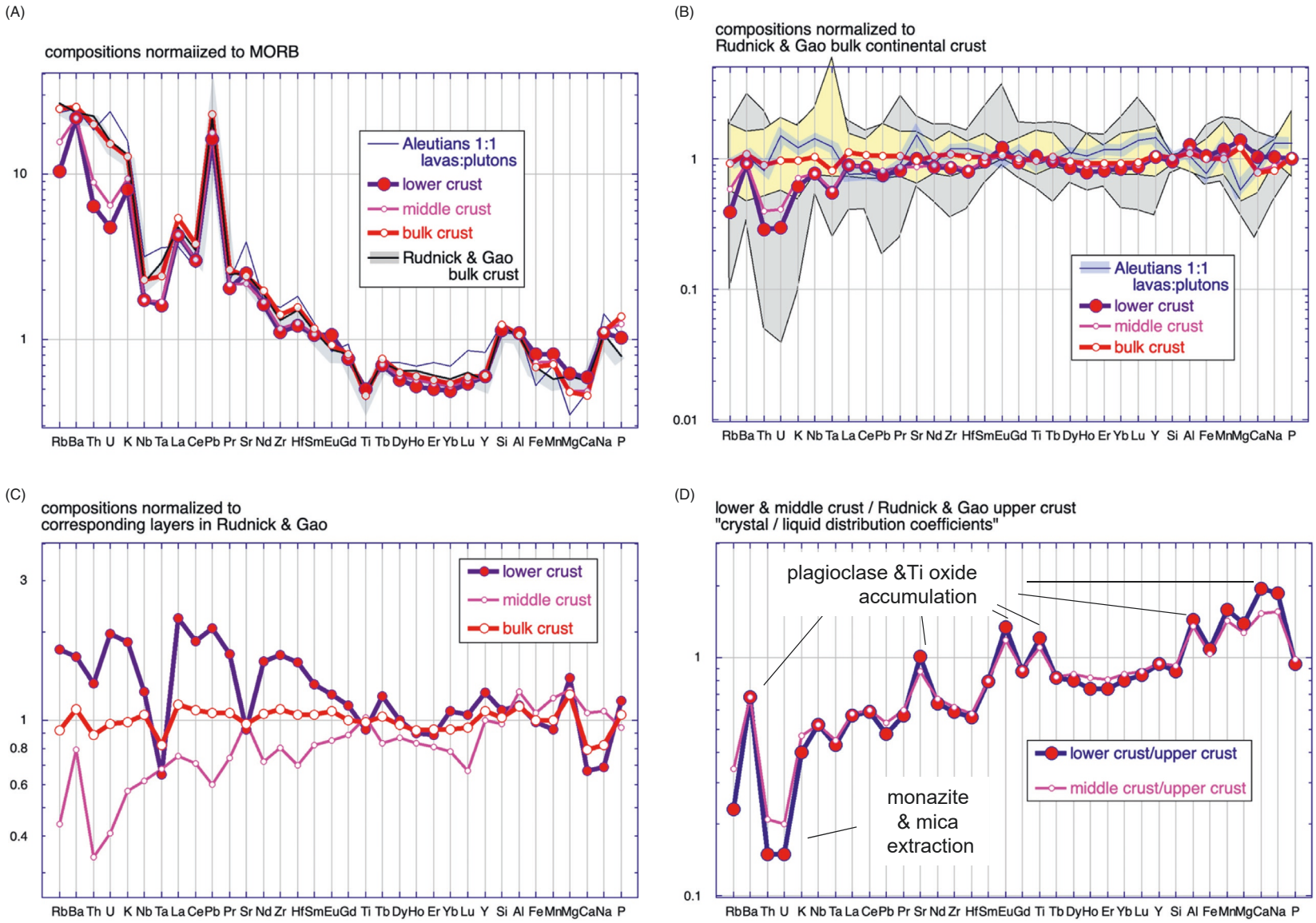

Fig. 7 Extended major and trace element diagrams for our preferred lower, middle and bulk continental crust compositions at 410 °C, 0.92 GPa, compared to other compositions. Values are arithmetic means for major elements, geometric means for trace elements. (A) Compositions normalized to normal MORB (Gale et al., 2013). (B) Compositions normalized to the bulk continental crust composition of Rudnick and Gao (2003, 2014). Shaded fields enclose published estimates for lower (grey) and bulk (yellow) continental crust, as compiled by Kelemen and Behn (2016). (C) Compositions of lower, middle and bulk continental crust from this paper, divided by the compositions of the same layers from Rudnick and Gao (2003, 2014). (D) Compositions of lower and middle crust, divided by the upper continental crust composition of Rudnick and Gao (2003, 2014).

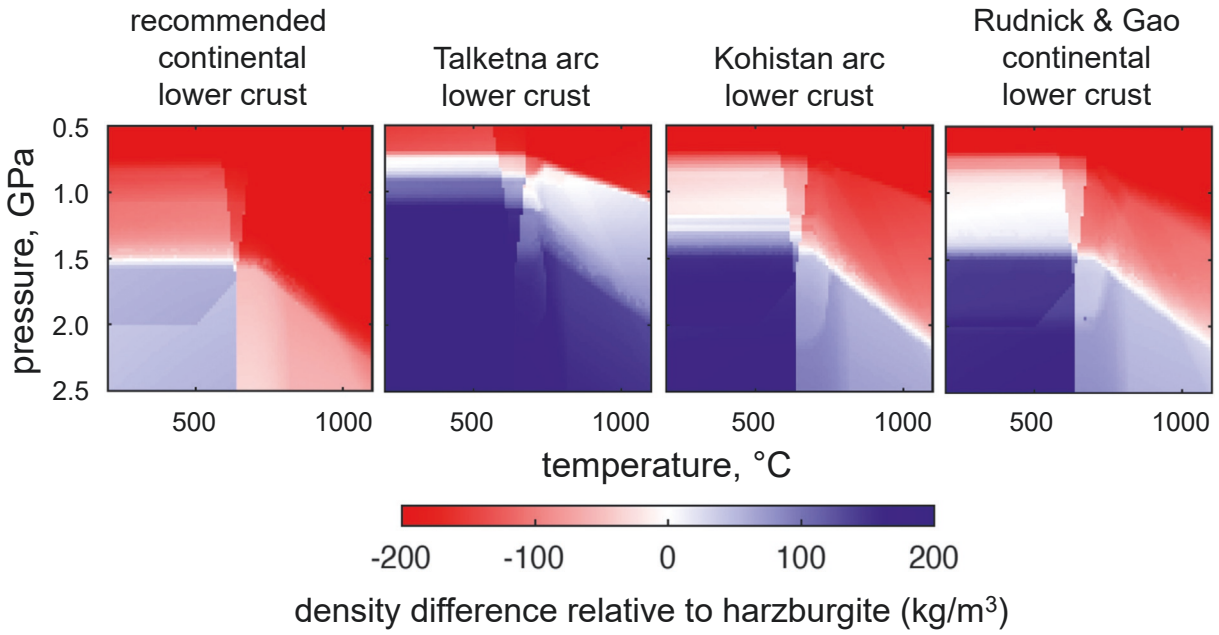

Fig. 8 Density of depleted arc mantle peridotite subtracted from densities of different lower crustal compositions (Table 2 and Supplementary Tables 2 and 3 in the online version at https://doi.org/10.1016/B978-0-323-99762-1.00121-2). Densities calculated using Perple_X.

crust is composed of mixtures of low-SiO_2, high-Vp lithologies and high-SiO_2, low-Vp rocks, on scales ranging from hundreds of kilometers to less than a few meters (in "banded gneisses"). This is one reason why we prefer our Vp weighted average lower crust compositions, which incorporate proportions of low- and high-Vp compositions, to the alternative compositions derived by averaging only those samples with Vp between 6.7 and 7.1 km/s.

Mixtures on length scales smaller than a "seismic wavelength" will have Vp intermediate between the different components. In turn, because the relationship of Vp to SiO_2 in granulites is curved, concave upward (Fig. 6A), the SiO_2 content of simple mixtures will fall above the curve (Fig. 6B). Thus, if simple mixtures of SiO_2-rich and SiO_2 poor lithologies are ubiquitous in lower continental crust, *all of our estimated SiO_2 contents for lower continental crust in Table 2 could be systematically too low*. For the end member scenario in Fig. 6B, the SiO_2 content of a mixture with Vp of 7 km/s is 60 wt% SiO_2, whereas the relationship between SiO_2 and Vp derived in this study yields about 54 ± 2 wt% SiO_2 at 7 km/s. In the future, systematic studies of the length scale and magnitude of compositional banding in gneiss terrains could help to quantify the effect of such mixing on crustal SiO_2 estimates.

Geochemists generally interpret trace element concentrations using a logarithmic scale encompassing several orders of magnitude. Viewed through this lens, the trace element contents of our new lower and middle crust compositions are similar to most previously published estimates for lower, middle and bulk continental crust (Fig. 7). As noted by Kelemen et al. (1993), compared to average mid-ocean ridge basalts, all such estimates—including those for the lower crust—have depletions of Nb and Ta relative to U, Th, K and La, all are Rb, Ba, Th, U, Nb, Ta, K and light rare earth element (REE) enriched, and heavy REE depleted, and all have high Pb/Ce (Fig. 3). They share these characteristics with most arc lavas and have compositions that are rare or absent among samples of MORB, lower oceanic crust, ocean island basalts, and oceanic plateaux.

In detail, when compared to the Rudnick and Gao (2003, 2014) lower crust composition (Fig. 7C), the concentrations of Rb, Th, U, K, Pb and the light REE's in our lower crust compositions are 20 to 220% higher. Higher concentrations of the heat producing elements (U, Th, K, Rb, Sm) in our lower crust are balanced by lower concentrations of these elements in our middle crust, so that total crustal heat production is similar in our bulk crust compositions, compared with the bulk crust of Rudnick & Gao. Rb/Sr in our lower crust is higher, while U/Pb, Th/Pb, Sm/Nd and Lu/Hf ratios are lower than those of Rudnick & Gao. These variations in radiogenic parent/daughter ratios may have significant consequences for the long-term isotopic evolution of the lower continental crust, and the residue of its extraction from the mantle.

Composition of the middle continental crust

Using the same methods as described in Section "Composition of the lower continental crust", we calculated average compositions for the middle crust (Table 2, and Supplementary Table 2 in the online version at https://doi.org/10.1016/B978-0-323-99762-1.00121-2). Whereas we are confident that granulite facies metamorphic rocks generally record lower crustal conditions, and are likely to be representative of lithologies in the lower crust, we are less confident that the compositions of granulites and

amphibolites are representative of the middle crust. As a result, we are less confident about our estimated middle crust compositions, compared to the lower crust compositions discussed in Section "Composition of the lower continental crust."

Our recommended middle crust compositions—calculated as a weighted average of compositions with Vp from 6.0 to 7.6 km/s at 280–300 °C and 0.54 GPa—are quite similar to the middle crust composition of Rudnick & Gao, as is evident in Fig. 7C. Ours have 61 wt% SiO_2, Mg# of 45, a density of 2800 tons/m^3, Vp of 6.5 km/s, and Vp/Vs of 1.69–1.70. Alternative middle crust compositions—the average of all compositions with Vp between 6.5 and 6.8 km/s at 280 °C to 300 °C and 0.54 GPa—are almost identical to our preferred compositions, with 62 wt% SiO2, Mg# of 44–45, a density of 2800 kg/m^3, Vp of 6.6 km/s, and Vp/Vs of 1.72–1.73.

As noted above, Rb, Th, U, K and Sm concentrations, and corresponding heat production of 0.58–0.62 μW/m^3, in our middle crust compositions are similar to those in our lower crust, and much lower than in Rudnick and Gao (2003, 2014) middle crust, which has heat production of 0.84 μW/m^3. The ratio of heat production in our middle and lower crust compositions, to heat production in well-characterized, Rudnick & Gao upper crust, is about 40%, consistent with the partitioning value of Pollack and Chapman (1977) used in Figs. 4A and 5 of Furlong and Chapman (2013). In contrast, heat production in the lower crust composition of Rudnick & Gao is 20% of that in their middle crust, and 10% of that in their upper crust. These partitioning values are lower than those used by Hasterok and Chapman (2011). Despite these differences, and differences in layer thickness (17 vs 14 km upper crust and 12 km vs 14 km lower crust, in Rudnick & Gao and our work, respectively) both sets of layer compositions and depths yield very similar bulk crustal heat flow (Table 2).

Combining our lower and middle crust compositions with the upper crust of Rudnick and Gao (2003, 2014) yields bulk continental crust with 59–62 wt% SiO_2. If heat flow from the mantle is 11–18 mW/m^2, our values yield surface heat flow of 47–55 mW/m^2, consistent with observational bounds for stable continental regions older than 200 Ma.

Discussion of crustal compositions

An intermediate composition for the lower crust

As noted above, since 1995, most papers have estimated an average lower crust composition with 51–55 wt% SiO_2 (Cui et al., 2023; Emo et al., 2021; Pease et al., 2023; Rudnick and Fountain, 1995; Rudnick and Gao, 2003, 2014; Sammon and McDonough, 2021; Sammon et al., 2022), while one paper advocates a lower crust with 47.1 wt% SiO2 (Huang et al., 2013). In contrast, our preferred lower crust compositions contain 56.9–57.7 wt% SiO_2. A difference of 2–4 wt% SiO_2 may seem small, but from the point of view of crustal genesis, it is important. By definition, "mafic" igneous rocks have less than 55 wt% SiO_2. In contrast, igneous rocks with 55–65 wt% SiO_2 are termed "intermediate."

Mantle derived magmas at mid-ocean ridges and ocean islands are almost all mafic basalts ($\leq$ 52 wt% SiO_2). Lower oceanic crust is primarily composed of olivine-pyroxene-plagioclase "cumulates" with Mg# > 0.7, produced by crystal fractionation of cooling, mantle-derived magma, after which the remaining melt was extracted to form sheeted dikes and lavas. These cumulates commonly have less than 50 wt% SiO_2. As can be seen in Fig. 1, oceanic crust is composed almost entirely of rocks with <53 wt%, while those with >53 wt% are absent among with molar Mg/(Mg + Fe), aka Mg#, greater than 0.35. Thus, the bulk and lower oceanic crust are certainly mafic.

The hypothesis that the lower continental crust is mafic arose in part by analogy to oceanic crust, where refractory cumulates in the lower crust underlie more evolved, genetically related lavas in the upper crust. This analogy with oceanic crust was supported by the observations that seismic wave speeds in lower continental crust are higher in the lower crust compared to the upper crust, and that—all other things being equal—SiO_2-poor, mafic rocks have higher seismic wave speeds than SiO_2-rich, felsic rocks. Correlation between bulk rock SiO_2 contents and laboratory measurements of Vp at mid- to lower-crustal pressures (typically, 0.6 GPa) provided a quantitative basis for this hypothesis (Christensen and Mooney, 1995; Holbrook et al., 1992; Huang et al., 2013; Rudnick and Fountain, 1995; Rudnick and Gao, 2003, 2014; Rudnick and Presper, 1990), which has been extended to include functions relating laboratory observations of Vs and Vp/Vs ratios to SiO_2 contents (e.g., Sui et al., 2022).

In contrast, as noted above, our average lower crust compositions fall within the compositional range of intermediate arc lavas and plutonic rocks (e.g., compilations in Kelemen et al., 2003a, 2014). To summarize, it has long been known that oceanic crust is mafic while ***bulk*** continental crust has an intermediate composition. In this context, our new average ***lower*** continental crust compositions are also ***intermediate***, and in this way—as well as in its trace element contents—lower continental crust resembles arc lavas, batholiths, and bulk continental crust (Fig. 7).

Moreover, (with the exception of U, Th, Sr, Eu and Ti, discussed below) the average composition of the lower crust is "liquid-like." It does not resemble mafic and ultramafic cumulate rocks—formed by partial crystallization of primitive (Mg# > 0.6), mantle-derived mafic magmas, followed by removal of most of the remaining melt—nor does it resemble residues of partial melting and melt extraction from primitive, mafic rocks. Cumulates produced by crystallization of mantle-derived, mafic magmas, and restites produced by partial melting of mantle-derived mafic rocks, typically have Mg# > 0.7, MgO and/or CaO contents >10 wt%, calcic plagioclase, and substantial enrichments in Eu/Sm compared to mid-ocean ride basalts and the mantle. Differentiation of mantle-derived, mafic magmas into cumulates, restites and evolved melts has undoubtedly occurred in forming the building blocks of continental crust. However, average lower continental crust does not represent a mafic, cumulate or residual complement, recording crystal fractionation from a mafic mantle-derived parental melt to produce felsic, average upper continental crust, or intermediate, average bulk continental crust.

A caveat here is that — like the compositions of average granulite xenoliths, average granulite terrains and most estimates of the trace element content of lower continental crust (Fig. 3)—the average lower continental crust compositions derived in this study are depleted in U and Th compared to upper and bulk continental crust (Fig. 7). Moreover, mantle or MORB normalized concentrations of U and Th are depleted with respect to similarly incompatible elements Ba, K and La. And, when we divide the lower crust compositions by upper continental crust (Fig. 7D), we see that the lower crust is relatively enriched in Sr, Eu and Ti, and has a high Ba/Rb ratio, suggesting that the lower crust is enriched in Ca-rich plagioclase and Fe-Ti oxides relative to the upper crust. This may be due to removal of small amounts of U- and Th-rich, anatectic, felsic melt from the intermediate lower crust, which subsequently crystallized in the upper crust. Such a global relationship was proposed by Reid et al. (1989) based on analyses of lower crustal xenoliths from Kilbourne Hole, and modeled as a consequence of underplating of buoyant lithologies at the base of arc crust at high temperature by Hacker et al., (2011).

The density of continental lower crust is significantly less than that of lower crust in the two best preserved arc crustal sections (Supplementary Table 3 in the online version at https://doi.org/10.1016/B978-0-323-99762-1.00121-2), supporting the idea that—though arc and continental crust are surely related—the densest part of arc crust has been removed by one or more post-magmatic process (Section "Genesis and evolution of lower continental crust"). Our new lower crust composition is more buoyant than underlying mantle harzburgite at $\leq$1.5 GPa at ambient temperature, and more buoyant than the mantle at 2.5 GPa or more at >700 °C. In contrast, lower arc crust and the lower continental crust composition of Rudnick & Gao are denser than the mantle at >1.2 GPa at ambient conditions, and > 1.8 GPa at arc Moho conditions (Fig. 8).

To summarize, our new lower crustal composition is not consistent with widely held views of a "mafic lower crust", based on prior, geophysically-based estimates and on analogies to mafic oceanic and lower arc crust (Christensen and Mooney, 1995; Holbrook et al., 1992; Huang et al., 2013; Pease et al., 2023; Rudnick and Fountain, 1995; Rudnick and Gao, 2003, 2014; Rudnick and Presper, 1990; Sammon et al., 2022; Sui et al., 2022). The significant differences in our estimated lower crust composition, compared to most previous studies, arise for three main reasons:

1. First, as noted in Section "Constraints on lower crust composition from surface heat flow, revisited", qualitative assumptions about the composition of the middle crust, inferred to contain abundant K, U and Th, combined with observed surface heat flow and assumptions about heat flow from the underlying mantle, resulted in the inference that the lower crust had low K, U and Th contents, as found in mafic igneous rocks. As shown by Hacker et al. (2011, 2015), and again here, a critical assessment of the heat flow constraints yields a much broader range of potential compositions for lower continental crust.
2. Second, as noted in Section "Relationship between rock composition and seismic P-wave speed", prior to 2022, most geophysically constrained estimates of lower continental crust composition relied on experimental data relating whole rock composition to acoustic wave speeds with the exception of Behn and Kelemen (2003), and Hacker et al. (2015).
3. Third, Sammon et al. (2022) used hot average lower crust conditions of 600 °C and 0.85 GPa, corresponding to surface heat flow of 64–74 mW/m^2, whereas we use 410 °C and 510 °C at 0.92 GPa along geotherms corresponding to surface heat flow of 50 mW/m^2. Our choice is based on average heat flow in stable continental crust more than 200 million years old. Incorporating younger crust, especially at tectonically and magmatically active continental margins, would result in a higher average heat flow, and correspondingly a higher average temperature in the lower crust if the heat flow data were interpreted in terms of a steady state geotherm.

The surface heat flow in crust less than 200 million years old varies dramatically, from less than 20 to more than 120 mW/m^2, and lower crustal Vp in those areas is also highly variable. Some areas of young crust have relatively low Vp in the lower crust, for example in the Sierra Nevada batholith (Fliedner et al., 2000) and southern Tibet (Kind et al., 2002; Monsalve et al., 2008; Monsalve et al., 2006; Nabelek et al., 2009; Schulte-Pelkum et al., 2005; Shi et al., 2015; Wittlinger et al., 2009; Zhao et al., 2001), while others have relatively high Vp (e.g., Aleutian arc, Fliedner and Klemperer, 1999, Holbrook et al., 1999, Shillington et al., 2004). In some cases, this variability may be ascribed mainly to temperature, while in others it probably involves more and less SiO_2-rich lower crust. It could be that these younger regions have not yet undergone the density sorting discussed in Section "Genesis and evolution of lower continental crust", and thus still contain more mafic material than older crust. Also, mechanical mixing and thermal diffusion may reduce the variability of heat production and heat flow variability over time, producing a more robust average.

Thus, to some extent, the recent papers proposing lower crustal compositions, including this one, may be comparing apples and oranges, with some incorporating tectonically or magmatically active crust with higher heat flow, and perhaps a mafic lower crust, while ours is focused on stable crust more than 200 million years old, with lower heat flow and an intermediate lower crust. However, cratons, platforms and Paleozoic to Mesozoic orogens comprise 60% of the continental area, while 47% of heat flow observations in the remaining 40%, tectonically active crust, fall within the same range as heat flow in stable crust (Supplementary Fig. 1 in the online version at https://doi.org/10.1016/B978-0-323-99762-1.00121-2). In this sense, the composition we recommend may be a robust average for preserved lower continental crust formed during 95% of its history, covering 79% of the present continental area.

In turn, compared to previous, mafic estimates, our new average composition is closer to the average composition of granulite facies metamorphic terrains. Though samples from these terrains are more numerous than mafic granulite xenoliths, and the terrains themselves are orders of magnitude larger in area and volume compared to the xenoliths, prior studies commonly suggested

that the granulite terrains are not representative of lower continental crust, based on interpretations of seismic data and heat flow. Here, following Hacker et al. (2011, 2015) and Sammon and McDonough (2021), we suggest that this approach and its conclusions were in error, and that granulite terrains *are* representative of a significant proportion of lower continental crust.

Sources of uncertainty in the composition of lower continental crust

Some recent studies of continental lower crust have emphasized quantitative uncertainty in their compositional estimates, most notably Tang et al. (2015), Sammon et al. (2022) and Pease et al. (2023). While estimated compositions for the lower crust are certainly uncertain (!), and we do present standard deviations of average values in Table 2 and Supplementary Table 2 in the online version at https://doi.org/10.1016/B978-0-323-99762-1.00121-2, we feel that some of the formal uncertainty estimates in recent papers are misleading.

Based on our calculations, for temperatures and pressures along 50 mW/m^2 geotherms, *all* the lower crust compositions from Rudnick and Fountain (1995) Rudnick and Gao (2003, 2014), Emo et al. (2021) Sammon and McDonough (2021), Sammon et al. (2022), Cui et al. (2023), and Pease et al. (2023), and the average xenoliths of Huang et al. (2013), have Vp that is *systematically* faster than values for average continental crust from Christensen and Mooney (1995) and this study (Fig. 6H). Fig. 5 shows that choices of an average value for surface heat flow, and the variation of heat production with depth, the thickness of crustal "layers", and the crustal domains to use when averaging Vp can each lead to changes of several weight percent in the resulting SiO_2 content of the lower crust. Poor choices can lead to systematic errors that are not captured by the formalism of the average and standard deviation for normally or log-normally distributed data.

An ongoing conundrum that illustrates the importance of these considerations is the observation of very high Vp—more than 7.5 km/s, up to 7.7 km/s, over 50 km along strike at depths of 20–35 km—in Aleutian lower crust (Shillington et al., 2004). If the high Vp crust is at arc Moho temperatures (900 to 1100 °C, e.g., Hacker et al., 2008, Kelemen et al., 2003b), much of this material must be ultramafic rock containing little or no melt. Alternatively, since the arc parallel refraction line underlying the Vp data spanned a transect south of the volcanic front, perhaps these data sampled cold forearc crust, rather than arc crust. Two cross-lines show steep gradients in lower crustal Vp—from 7.2 to 7.0 km/s (Holbrook et al., 1999) and from 7.3 to 6.9 km/s (Lizarralde et al., 2002)—over distances of about 50 km perpendicular to the volcanic front, from the forearc to the active arc. The Aleutian example shows why locations and spatial scales of seismic observations and heat flow measurements must be closely matched in order to draw meaningful conclusions about the composition of the lower crust in tectonically active regions.

Similarly, calculations of mineral assemblages corresponding to rock compositions can produce different results, depending not only on the current temperature at a given depth, discussed above, but also on the conditions at which mineral assemblages equilibrate, including temperature, pressure, water content, and even oxygen fugacity. All of these factors are uncertain, though it is difficult to quantify the range of "best" values, and their impact on resulting compositional estimates. We have found that, all other things being equal, higher equilibration temperatures yield mineral assemblages with higher Vp upon subsequent cooling. The compiled data equilibration temperatures for granuites (Brown, 2007; Brown and Johnson, 2019) average 845 ± 95°C (1 sigma), whereas for the thermodynamic calculation of mineral proportions used in this paper we used an equilibration temperature of 700°C. If we used a higher temperature, this would probably yield a higher SiO^2 content for the lower crust, though the magnitude of this effect has not been fully quantified.

Once mineral assemblages are calculated, and cooled to a steady state temperature, physical properties for minerals and mixture theory are used to calculate physical properties for polymineralic rock compositions. We have found that the temperature dependence of Vp in "alpha quartz", dVp/dT, is variable and poorly quantified in thermodynamic models. This introduces uncertainty related to the temperature of the lower crust, as described above, but also indicates that the thermodynamic model results themselves incorporate systematic uncertainties that have not been fully quantified.

A related technical issue is that mineral equilibration kinetics may vary from one rock composition to another and may vary from one kind of equilibration reaction to another within a single rock. An end-member example again involves SiO_2 minerals. SiO_2-rich mineral assemblages equilibrated near the base of arc crust (e.g., 900 °C, 1.2 GPa) include the polymorph beta quartz, which has Vp about 1 km/s faster than low temperature, alpha quartz. The alpha-beta transition is rapid, and beta quartz is not observed in slowly cooled metamorphic rocks. Thus, while we may choose to use relatively high temperatures of metamorphic equilibration to calculate mineral assemblages in granulites, this probably should not apply to beta quartz.

While the formal uncertainties for most other mineral physical properties, and for mixture theory, are better quantified than those for quartz, they have not been consistently incorporated in formal estimates of uncertainty for crustal compositions. In addition, Pease et al. (2023) include estimated uncertainties related to porosity (cracks), rock alteration, and preservation of metastable high PT mineral assemblages at lower pressure, while this study and Sammon et al. (2022) do not.

Seismic properties of rock volumes are commonly used to infer rock compositions, but it is difficult to quantify the uncertainty of each seismic "measurement" for a given rock volume, and uncertainties in Vp have not been used consistently in formal error propagation, to infer the uncertainty in average Vp values for the crust at various depths, and hence the uncertainty in the resulting compositions. Again, Pease et al. (2023) implicitly adopt a global approach that incorporates inferred steady state geotherms from Artemieva, (2006) for young, tectonically and magmatically active crust that probably does not lie on steady state geotherms and has (i) high variability in both Vp and heat flow over short length scales, and (ii) seismic scale lengths that are different from the

heat flow data that inform the global thermal model of Artemieva (2006). Moreover, as noted in Section "An intermediate composition for the lower crust" and illustrated in Fig. 6B, mixtures of different rock compositions, on a scale smaller than the "seismic wavelength", probably lead to systematic underestimates of SiO_2 content in the middle and lower crust, and this hard-to-quantify factor has not been included in any formal estimates of uncertainty for crustal compositions.

In general, choices of constraints on the composition of lower continental crust can potentially lead to systematic errors that are not captured by conventional methods of estimating variance around the mean or a normal (or log-normal) distribution of observational data. As for Bayesian approaches, as Pease et al. (2023) would readily agree, the resulting bounds on possible solutions are only as good as the input constraints.

The upshot of all this, in our opinion, is that recent estimates of lower and middle crust compositions should be viewed as the result of successful forward models, that satisfy various constraints derived from geophysical and geochemical data. The constraints vary from one study to another. Most importantly, none of these estimates can be used to rule out all possible, alternative models, that could meet all reasonable constraints, even if results from one set of models lie outside formal uncertainty bounds developed using another set of models. In this context . . . will we ever know the average composition of continental lower crust with certainty? Perhaps not, but we hope this paper will persuade readers that the range of possibilities is larger than might be inferred from the large number of recent studies advocating a mafic composition for the lower crust.

Tectonic provenance of lower continental crust

Continental crust shares its major and trace element characteristics with average lavas erupted in subduction-related volcanic arcs (Figs. 1 and 3). Strikingly, as noted in Section "Composition of the lower continental crust", the trace element patterns for lower continental crust are very similar to trace element patterns for upper continental crust (e.g., Fig. 1 in Kelemen et al., 1993). And the major and trace element compositions of bulk, upper, middle and lower continental crust, while uncertain, fall into the same range as those of intermediate arc lavas and plutonic rocks (55–65 wt% SiO_2)—compositions that are not present in oceanic crust (Fig. 1).

In turn, compared to MORB, ocean island basalts, and the estimated composition of bulk silicate earth, relative depletions of Nb and Ta with respect to U, Th and K, and elevated Ba, U, Th, K and light rare earth element concentrations in arc magmas and bulk, upper, middle and lower continental crust are all best understood as deriving from a "subduction component" (melt, fluid and/or supercritical liquid) that is extracted from subducting oceanic crust and sediments (e.g., Armstrong, 1968; Armstrong, 1971; Coats, 1962; Gill, 1974; Kay, 1980; Kay et al., 1978; Marschall and Schumacher, 2012; Tatsumoto, 1969) and reacts with the overlying mantle (flux melting, Kelemen et al., 2003a, 2014) or mixes with mantle melts. The specific trace element characteristics of this component, particularly the Nb and Ta depletions, are attributed to extraction of the subduction component from a residue composed of subducting, rutile- and garnet-rich eclogite via dehydration or low temperature, hydrous melting of subducting oceanic crust (e.g., Ayers and Watson, 1993; Brenan et al., 1994; Brophy and Marsh, 1986; Green, 1981; Kay, 1978; Kelemen et al., 1993; Morris and Hart, 1983; Ryerson and Watson, 1987; Saunders et al., 1980; Tatsumi et al., 1986; Yogodzinski et al., 1995; Yogodzinski et al., 1994). Thus, it is generally held that the building blocks of continental crust were derived primarily from arc magmatism.

A persistent, alternative viewpoint is that Archean continental crust formed prior to the initiation of subduction and arc magmatism (e.g., Condie, 2018; Hamliton, 2003; Laurent et al., 2014; Tang et al., 2016). In this view, the trace element characteristics of Eoarchean continental crust, including Nb and Ta depletions in mafic, intermediate and felsic magmas, might have derived from partial melting of eclogite, heating as it foundered into the mantle in negatively buoyant diapirs (e.g., Bédard, 2006). However, the "eclogite signature" in arc magmas is best understood as the outcome of low temperature anatexis that forms hydrous, SiO_2-rich melts (or fluids, or supercritical liquids) from garnet-rich eclogite with residual rutile, as outlined in the references cited above. Anatexis of high temperature eclogites involves less garnet, because more Al is dissolved in residual pyroxenes, and may lack residual rutile saturation during formation of hotter, drier melts (Pertermann et al., 2004).

Another persistent alternative idea is that formation of continental crust involved flood basalt volcanism (e.g., Albarède, 1998; Condie, 1997; Schubert and Sandwell, 1989; Stein and Goldstein, 1996; White et al., 1999). Indeed, oceanic plateaux, interpreted as large igneous provinces, could have formed a tectonic nucleus for subsequent subduction of adjacent oceanic crust and resulting arc magmatism (Abbott and Mooney, 1995; Nair and Chacko, 2008). However, our Fig. 3 (and Fig. 1 in Hofmann et al. (2022)) indicates that ocean island basalts and oceanic plateau basalts—at least, with their present characteristics—have trace element ratios that are typical for MORB, and are distinct from ratios in average lower and bulk continental crust. This suggests that accreted ocean island basalts and continental flood basalts, though they are present in continental crust, had a relatively minor role in forming average lower and bulk continental crust. We briefly return to this topic in Section "A role for oceanic plateaux, after all?."

No vestige of a beginning . . .

In addition to the similarity of average granulite compositions to arc magmas, another striking feature of lower continental crustal samples is the lack of systematic temporal variation in key trace element ratios. While the average Archean granulite concentrations for most incompatible trace elements are about two times lower than the post-Archean granulite averages, both sample groups have

similar, large depletions in Nb and Ta relative to U, Th, K and La, both are Rb, Ba, Th, U, Nb, Ta, K and light rare earth element (REE) enriched and heavy REE depleted, with a flat middle- to heavy REE pattern, and both have high Pb/Ce compared to MORB. Based on these data, we infer that, since the Hadean, most of the currently preserved lower continental crust formed as a result of volcanic arc magmatism, together with the density sorting processes discussed later in this paper. This hypothesis is consistent with inferences based on similar trace element characteristics in intermediate to felsic Eoarchean rocks (e.g., Hoffmann et al., 2011; Nutman et al., 2021; Polat et al., 2011; Sotiriou et al., 2022; Turkina, 2023) and even Hadean zircons (Grimes et al., 2007; Harrison, 2009; Hopkins et al., 2010).

As a caveat, we note that the trace element characteristics of samples from granulite terrains are highly variable, probably as a result of igneous differentiation and/or fluid alteration processes, so that the characteristics outlined here for average values are not evident in many individual samples, or even in groups of samples from specific studies or localities. For example, low K granulites have relatively high Nb/K compared to continental crust, with compositions similar to cumulate gabbros in lower oceanic crust (Fig. 3), perhaps indicative of the presence of mafic, oxide-bearing gabbros in both suites. Thus, whereas arc magmatism has produced most of the building blocks of continental crust, it is evident that other processes have played a role and generated regional heterogeneity.

Genesis and evolution of lower continental crust

The composition of the oceanic crust arises from crystallization of mantle-derived basalts, formed by polybaric decompression melting of DMM rising beneath oceanic spreading ridges, in a relatively well understood process. As a result, bulk oceanic crust has the composition of a mantle-derived, primitive magma. In contrast, despite its first-order importance, there is a lack of consensus about the processes that form continental crust in general, and lower continental crust in particular, as reviewed in many recent studies (Arndt, 2013; Castro et al., 2013; Chen et al., 2020; Collins et al., 2020; Condie and Kröner, 2013; Dhuime et al., 2015; Gaschnig et al., 2016; Gómez-Tuena et al., 2018; Hacker et al., 2011; Hacker et al., 2015; Hawkesworth et al., 2010; Hawkesworth and Kemp, 2006; He et al., 2018; Jagoutz and Behn, 2013; Jagoutz and Kelemen, 2015; Jagoutz et al., 2011; Jagoutz and Schmidt, 2012; Jagoutz and Schmidt, 2013; Puetz et al., 2017; Qin et al., 2022). While it is not our intent to provide another comprehensive review here, the next few paragraphs outline some of the ongoing uncertainties.

Ascribing a dominant role for arc magmatism in creating the basic ingredients for continental crust raises a long-standing problem, because primitive, mantle-derived arc lavas are dominantly mafic (< 55 wt% SiO2, e.g. Fig. 5 in Kelemen et al., 2003a, 2014), with an Mg# greater than 0.6. Lower arc crust commonly contains mafic material with a P-wave speed greater than 7.2 km/s (e.g., in the Aleutians, Shillington et al., 2004), and mafic cumulates with Mg# greater than 0.7 and less than 51 wt% SiO_2 (Jagoutz and Schmidt, 2012; Kelemen et al., 2003a, 2014; DeBari and Coleman, 1989; DeBari and Sleep, 1991; Dhuime et al., 2007, 2009; Greene et al., 2006). In contrast, to reiterate, lower, middle and bulk continental crust are intermediate in composition (55–65 wt% SiO_2) with an Mg# between 0.4 and 0.6, and lower continental crust has P-wave speeds averaging about 6.9 km/s.

To explain the evolution from primitive, basaltic arc magmas to intermediate bulk and lower continental crust, various workers have proposed the following ideas[4]:

(i) Arc magmatism in some times and places is dominated by direct melts of subducting eclogite, with intermediate to felsic compositions that are preserved during limited reaction with mantle peridotite (e.g., Brophy and Marsh, 1986; Defant and Drummond, 1990; Drummond and Defant, 1990; Gómez-Tuena et al., 2018; Kay, 1978; Kelemen, 1995; Kelemen et al., 2003a; Kelemen et al., 1998; Kelemen et al., 1993; Marsh, 1979; Martin, 1986; Myers et al., 1985; Rapp et al., 2003; Rapp et al., 1999; Schiano et al., 1995; Yogodzinski et al., 1995; Yogodzinski et al., 1994).

(ii) Dense, mafic, high Mg# lithologies (mafic and ultramafic cumulates) "delaminate" or "founder" into less dense, underlying mantle peridotite (e.g., Arndt and Goldstein, 1989; Behn et al., 2007; Behn and Kelemen, 2006; Bowman et al., 2021; DeBari and Coleman, 1989; DeBari and Sleep, 1991; Ducea and Saleeby, 1998a; Ducea and Saleeby, 1998b; Ducea, 2002; Ducea et al., 2021a; Ducea et al., 2021b; Ducea and Saleeby, 1996; Herzberg et al., 1983; Jagoutz and Behn, 2013; Jagoutz and Kelemen, 2015; Jagoutz and Schmidt, 2012; Jagoutz and Schmidt, 2013; Jull and Kelemen, 2001; Kay and Kay, 1991; Kelemen et al., 2003a, 2014; Lee and Anderson, 2015; Lee et al., 2006; Müntener et al., 2001; Tilhac et al., 2016; Xiao et al., 2019; Zandt et al., 2004).

(iii) Buoyant, subducting materials are thrust into, or underplated beneath, arc crust in a process known as "relamination" (Hacker et al., 2011, 2015). As defined by Hacker et al. (2011, 2015) relamination processes may include

  (a) imbrication of material beneath the crust in the upper plate (e.g., Angiboust et al., 2013; Angiboust et al., 2022; Calvert, 2004; Calvert et al., 2003; Calvert et al., 2011; Calvert et al., 2006; Chapman, 2017; Chin et al., 2013; Ducea and Chapman, 2018; Gordon et al., 2017; Hanson et al., 2022; Henrys et al., 2013; Jacobson et al., 1996; Kimbrough and Grove, 2007; Klein, 2019; Klein et al., 2016; Kotowski et al., 2022; Matzel et al., 2004; Pearson et al., 2017; Quick et al., 1995; Sauer et al., 2017; Sauer et al., 2018; Scholl, 2021; Tewksbury-Christle et al., 2021; Tozer et al., 2017)

[4]These concepts have not been comprehensively reviewed in the past, and thus we include references to numerous seminal studies.

(b) buoyant ascent from mantle depths to the base of the crust along a "subduction channel" (e.g., Andersen and Austrheim, 2008; Andersen et al., 1991; Brueckner and van Roermund, 2004; Chemenda et al., 2000; Chemenda et al., 1995; Cloos and Shreve, 1988a; Cloos and Shreve, 1988b; Gerya et al., 2007; Gerya et al., 2002; Hacker and Gerya, 2013; Li and Gerya, 2009; Warren et al., 2008), and/or

(c) ascent of buoyant diapirs through the mantle wedge to the base of the crust (e.g., many of the references cited in (i) plus Behn et al., 2011, Cruz-Uribe et al., 2018, Currie et al., 2007, Gerya and Meilick, 2011, Gerya and Yuen, 2003, Gorczyk et al., 2006, Kelemen et al., 2003a, 2014, Klein and Behn, 2021, Marschall and Schumacher, 2012, Miller and Behn, 2012, Nielsen and Marschall, 2017, Wang et al., 2022, Yan et al., 2019, Yin et al., 2007, Zhu et al., 2009).

Most of the literature on low temperature, hydrous partial melting of eclogite—without reaction with the mantle—emphasizes the unusual trace element characteristics of such melts, which are expected to be dacites that are more strongly light REE enriched, and heavy REE depleted than typical arc magmas and continental crust, with much higher ratios of Dy/Yb and Sr/Y (e.g., Gill, 1974). However, Kelemen et al. (2003c) showed that, when reacting with mantle peridotite, the trace element characteristics of eclogite melts would change, producing depleted, flat middle to heavy REE patterns and lower Sr/Y ratios, typical of arc magmas. Still, such hybrid products would have the major element characteristics of primitive (Mg# > 0.6) mantle-derived magmas, and thus would have to undergo processes (ii) and/or (iii) in order to produce intermediate bulk and lower continental crust compositions with Mg# < 0.6 (see, e.g., Supplementary Fig. S4A in Kelemen and Behn, 2016). Thus, this paper focuses on processes (ii) and (iii), though we briefly return to recent work on process (i) in Section "Diapirs revisited."

Processes (ii) and (iii) are similar in that they involve density sorting: At some stage(s), or perhaps at steady state, magmatic differentiation of mantle-derived melts produced dense mafic compositions—solidified primitive magmas, crystalline cumulates or residues of partial melting—that have been removed, so that the remaining crust retains a bulk composition that closely resembles intermediate arc lavas and mid-crustal plutons. Using experimental data on crystal fractionation, Kelemen and Behn (2016), (Supplementary Fig. 4 and Supplementary Table 2) estimated the proportion of removed material to be 25–80 wt% of the initial mantle-derived magma, depending on the composition of the parental magma (basalt, basaltic andesite, primitive andesite or dacite, mixed magma), pressure, temperature and oxygen fugacity.

In the following sections, we evaluate processes (ii) and (iii) a,b,c in more detail.

One-stage delamination of oceanic arc crust does not form lower continental crust

What processes might have removed a significant proportion of the mafic residues of magmatic differentiation that are present in lower arc crust? One idea is that dense, mafic lithologies formed near the base of the crust, where they were denser than the underlying mantle, and ultimately "foundered"or "delaminated" due to viscous, compositional convection. However, though relatively intact crustal sections from oceanic, volcanic arcs do show compositional evidence for such "delamination" (e.g., DeBari and Coleman, 1989; DeBari and Sleep, 1991; Greene et al., 2006; Kelemen et al., 2003a, 2014), gabbroic lower arc crust at depths less than about 40 km is buoyant compared to the mantle, but remains significantly more mafic, and depleted in incompatible trace elements, compared to lower continental crust (Fig. 9 in this paper, and Kelemen and Behn, 2016). Thus, delamination of arc crust probably occurs, but in preserved oceanic arc crustal sections, the delamination process has not been sufficient to produce continental crust from arc crust. Moreover, granulite terrains and xenoliths derived from lower continental crust contain tens of percent metasedimentary rocks (Hacker et al., 2011, 2015), which are almost absent from oceanic arc lower crustal sections studied to date (Kelemen et al., 2003a, 2014; Jagoutz and Schmidt, 2012; DeBari and Coleman, 1989; DeBari and Sleep, 1991; Dhuime et al., 2007, 2009; Greene et al., 2006).

Models of relamination reproduce lower continental crust composition

As noted above, the estimated compositions of lower continental crust, bulk continental crust, arc upper crust (lavas, pyroclastic rocks, volcanoclastic sediments) and arc middle crust (intermediate plutons and batholiths) are very similar. Thus, while foundering or "delamination" of dense lithologies from the base of arc crust has probably occurred, available data indicate that this process alone does not produce lower and bulk arc crust with the composition of lower continental and bulk crust. Instead, Kelemen and Behn (2016) argued that substantial proportions of lower continental crust are composed of intermediate to felsic lavas and plutons from arc upper and middle crust, that were subducted, rose buoyantly, and were emplaced at or near the base of arc and continental crust. Similarly, Hacker et al. (2011, 2015) argued that "relamination" processes provide a good explanation for the presence of metasediments among granulite xenoliths and within granulite terrains, where some are juxtaposed with lenses of mantle peridotite. In this section, we review relamination processes (iii) b and c, and provide a new model for process (iii)a in Section "Density filtering of underthrust material in at the base of arc crust."

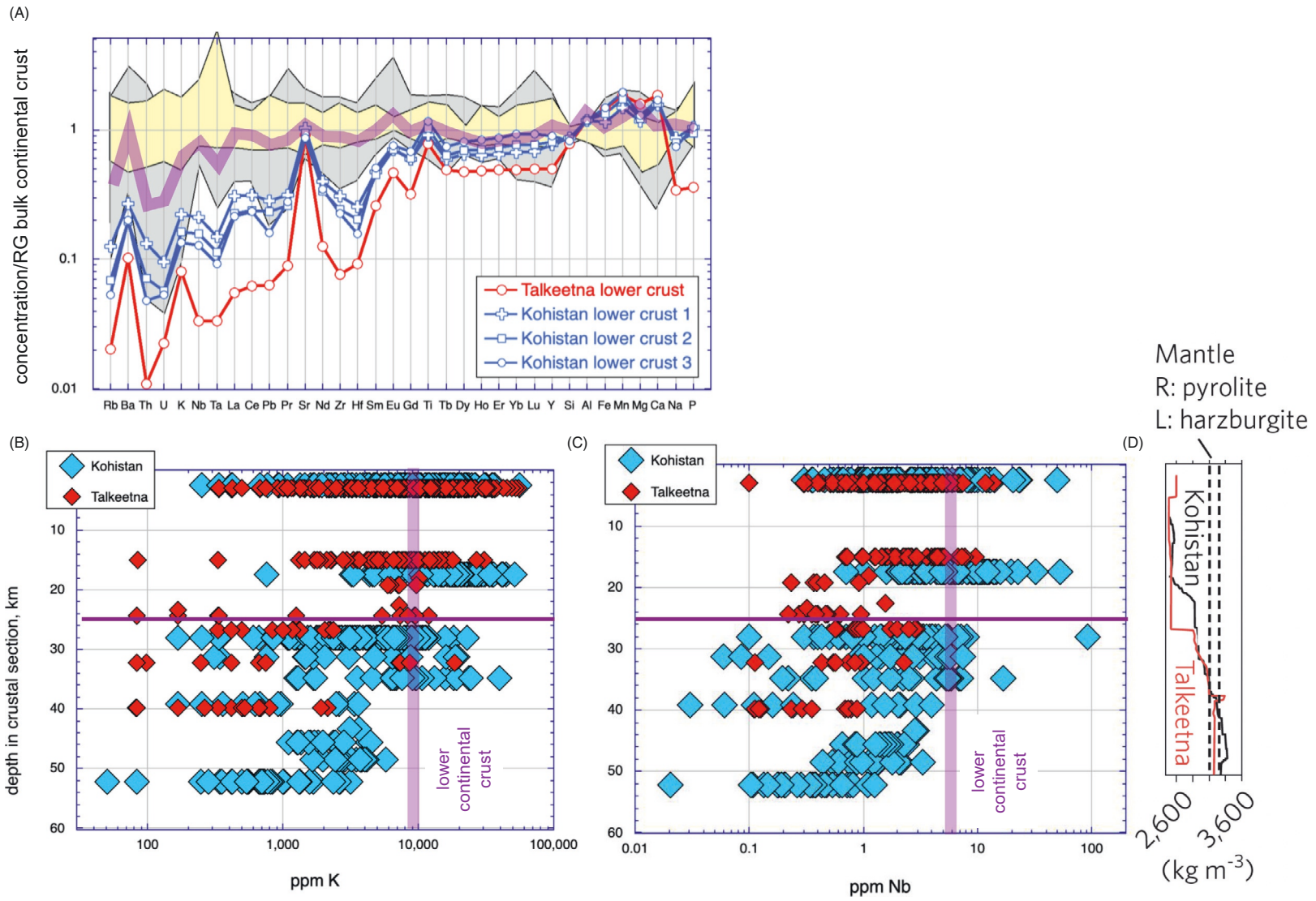

Fig. 9 Comparison of lower continental crust to lower arc crust compositions. Purple shaded lines illustrate our preferred lower continental crust compositions (geometric means). (A) Extended major and trace element diagram illustrating the compositions of lower crust from the Talkeetna and Kohistan arc crustal sections. *See grey lines in Fig. 3D for similar estimates of the composition of Aleutian arc lower crust.* (B and C) Compositions of samples from the Talkeetna (blue) and Kohistan (red) arc sections as a function of depth. (D) Densities of average Talkeetna and Kohistan samples as a function of depth along an arc geotherm, compared to the density of mantle peridotite compositions at the base of arc crust. For both arc sections, average compositions at a given depth are less dense than the underlying mantle, down to depths of about 40 km. (A) and (D) modified from Kelemen PB, Behn MD. 2016. Formation of lower continental crust by relamination of buoyant arc lavas and plutons. *Nature Geoscience* 9: 197–205, Fig. 3

Density sorting of subducting material in eclogite facies

Kelemen and Behn (2016) evaluated "relamination" processes (iii)b and (iii)c by calculating eclogite facies mineral assemblages for arc magmatic rock compositions from the Talkeetna and Kohistan arc crustal sections, and from the active Aleutian and Izu-Bonin-Mariana arcs. In our calculations, we assumed that subduction erosion of arc-derived lithologies would continue until they were heated above 700–800 °C, at a depth of 3–4 GPa. At these conditions, and at higher temperatures and pressures, prior calculations indicate that low viscosities lead to density instabilities, in which material more buoyant than mantle peridotite rises, and denser material founders (e.g., Behn et al., 2011, and several other references cited in Section "Genesis and evolution of lower continental crust").

In Kelemen and Behn (2016), we did not include calculations of the density of continentally-derived sediments. Instead, we envisioned an Archean world, prior to the formation of abundant terrigenous sediments via weathering of mature continental crust. In this early world, subducting sediments would have been dominated by immature trench greywackes, with compositions similar to arc upper crust (Linn et al., 1992; Wang et al., 2022). Trench sediments would have been supplemented by blocks of magmatic arc crust entrained via "subduction erosion." Over geologic time, subducted blocks of forearc crust, typically composed of magmatic rocks formed by arc magmatism, have probably been more voluminous than subducting trench sediments. In any case, our previous density calculations for a suite of subducting sediment compositions (Fig. 2 in Behn et al., 2011) indicate that a majority of present-day, subducting sediments are less dense than mantle peridotite and would rise buoyantly through mantle peridotite, at both subduction zone conditions (700–800 °C, 3–4 GPa) and the crust-mantle transition in arcs (700–1000 °C, 1.0–1.4 GPa).

Kelemen and Behn (2016) calculated mineral assemblages and densities for our comprehensive suite of arc lithologies, and then separated them into a group that is less dense than mantle peridotite at the same pressure and temperature, and a group that is denser than peridotite. Using a mantle density of 3377 kg/m^3, based on the estimated density of primitive mantle ("pyrolite") at 700 °C, 3 GPa (and similar densities at 700 °C, 4 GPa, 800 °C, 3 GPa, and 800 °C, 4 GPa), we found that average density sorted buoyant compositions for each arc lie within the range defined by average compositions of Archean granulite terrains, post-Archean granulite terrains, and granulite xenoliths for all elements considered, except Nb in two of the four arc suites. In turn, in the context of this paper, the density filtered, buoyant arc compositions from the Kelemen and Behn (2016) model fall within one standard deviation of our preferred lower crust composition for all elements considered. Thus, modeling of relamination via processes (iii)b and (iii)c yielded a quantitative fit to the composition of lower continental crust, suggesting that these processes could have formed the lower crust.

Density filtering of underthrust material at the base of arc crust

In this paper, we follow the same approach as Kelemen and Behn (2016), but model relamination via process (iii)a, thrusting of subducted material into or just beneath lowermost arc crust. High temperatures at 1.0–1.4 GPa at the base of arc crust are recorded by arc heat flow and metamorphic PT records (e.g., Hacker et al., 2008, Jagoutz and Behn, 2013, Jagoutz and Schmidt, 2012, Kelemen et al., 2003b and references cited therein). Many granulite terrains may represent forearc and subducted material that has been "underplated" by thrusting into the arc crust-mantle transition zone. For example, Quick et al. (1995) proposed that the granulite facies rocks of the Ivrea Zone—commonly invoked as a representative section of lower continental crust—were derived via subduction erosion and underplating of an accretionary prism. In support of this hypothesis, Quick et al. noted the juxtaposition of metasediments with tectonic slivers of mantle peridotite and mafic orthogneisses, in an assemblage common in modern accretionary prisms.

Similarly, many other granulite terrains worldwide include felsic and pelitic metasediments juxtaposed with variably altered mantle peridotite and orthogneisses—the Skagit, Swakane and Napeequa high pressure metamorphic rocks in the North Cascades of Washington State (Miller et al., 2009; Misch and Rice, 1975; Sauer et al., 2018; Whitney, 1992), the Teton gneisses (Frost et al., 2018; Swapp et al., 2018; Zartman and Reed Jr, 1998), the Gruf granulites (Galli et al., 2013), the Malenco pelitic gneisses (Hermann et al., 1997; Müntener and Hermann, 1996), and outcrops in Fjordland in New Zealand (Czertowicz et al., 2016; Dwight et al., 2019; Scott, 2020). The Skagit and Swakane examples have been interpreted as forming via underplating of forearc and/or back-arc material near the crust-mantle transition during arc magmatism (Gordon et al., 2017; Hanson et al., 2022; Matzel et al., 2004; Sauer et al., 2017; Sauer et al., 2018). On the basis of structural mapping and geochronological data, underplating has also been invoked for other metasedimentary suites in North America that record lower crustal pressures, including the Pelona-Orocopia-Rand suite (Chapman, 2017; Chapman, 2021; Grove et al., 2003; Jacobson et al., 1996), the Condrey Mountain schist (Tewksbury-Christle et al., 2021), the Central Gneiss Complex (Pearson et al., 2017), and the southern Sierra Nevada (Klein, 2019; Klein et al., 2016). In a complement to these geological observations, underplated lenses of subducted, forearc material are imaged in seismic studies (Calvert, 2004; Calvert et al., 2003; Calvert et al., 2011; Calvert et al., 2006; Henrys et al., 2013; Tozer et al., 2017).

As an aside, only very minor, shallow metasedimentary lenses were found in the Talkeetna and Kohistan, oceanic arc sections (DeBari and Coleman, 1989; DeBari and Sleep, 1991; Dhuime et al., 2007; Dhuime et al., 2009; Garrido et al., 2006; Greene et al., 2006; Jagoutz and Kelemen, 2015; Jagoutz and Schmidt, 2012; Jagoutz et al., 2009; Kelemen et al., 2003a, 2014), whereas they

appear to be abundant in many lower crustal sections (Ducea et al., 2015; Gordon et al., 2017; Hanson et al., 2022; Liao et al., 2013; Matzel et al., 2004; Otamendi et al., 2009; Pearson et al., 2017; Saleeby et al., 2003; Saleeby, 1990; Saleeby et al., 1987; Sauer et al., 2017; Sauer et al., 2018; Todd, 2015; Todd, 2016; Whitney, 1992). The incorporation of abundant metasediments in continental arc lower crust may arise due to underthrusting of lenses derived from the thick aprons of volcanoclastic and terrigenous sediment that form in forearcs and trenches adjacent to continental margins.

It is likely that tectonic underplating also emplaces intermediate to felsic magmatic rocks near the base of the crust in active arcs. This could explain the metamorphic and tectonic processes that formed the abundant orthogneisses that are common in granulite suites. It is relatively easy to identify underplated pelitic metasediments and marbles, though we wonder how many "banded gneisses" classified as orthogneisses are actually metamorphosed greywackes. In any case, compared to pelites and marbles, it is harder to identify underplated igneous lithologies, particularly if high temperature metamorphism has erased prior history, and/or if old zircons are interpreted as having been inherited during assimilation or melting of surrounding crust. Based on the evidence from underplated metasediments, we propose that tectonic underplating, of intermediate to felsic, arc magmatic rocks has been an important process during the formation and evolution of continental crust. In this context, older zircons might record the crystallization of plutons, while younger overgrowths might form during metamorphism at high temperature conditions, such as at the base of volcanic arc crust.

Accordingly, for this paper, we calculated densities of the same suite of arc magmatic samples as Kelemen and Behn (2016), but in this case at lower pressure and somewhat higher temperature (800 °C, 1 GPa; 900 °C, 1.2 GPa), based on thermobarometry of samples from just above the crust-mantle transition in exposed arc sections, and supported by estimates based on heat flow observations, as summarized by Kelemen et al. (2003b). Compositions used, and references for data sources, are provided in Supplementary Table 3 in the online version at https://doi.org/10.1016/B978-0-323-99762-1.00121-2, which in turn is based on compilations of data on Aleutian lavas and shallow plutons from Gene Yogodzinski (personal communication) as well as Kelemen et al. (2003c) and Cai et al. (2015), compositions of samples of the Kohistan arc crustal section from Jagoutz and Schmidt (2012), compositions of samples from the Talkeetna arc crystal section from Kelemen et al. (2003a, 2014),[5] and lavas from the Izu-Bonin-Marianas arc from Jordan et al. (2012).

For this paper, we separated the samples into groups more and less dense than 3250 kg/m^3, a value chosen on the basis of the density of highly depleted mantle peridotites (harzburgite) observed just below the crust-mantle transition in the Talkeetna arc section (Kelemen et al., 2003a, 2014). In turn, we envisioned a process in which dense, underthrust lithologies reach the Moho and then founder into the underlying, hot, low viscosity sub-arc mantle, while buoyant lithologies accumulate in an intermediate composition lower crust (Fig. 10).

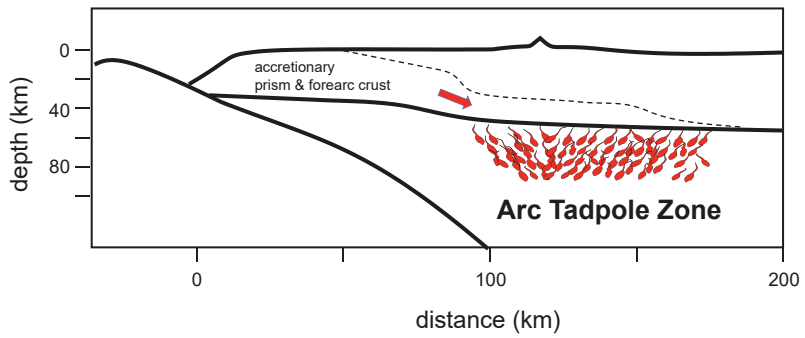

Fig. 10 Schematic cross-section illustrating underthrusting of fore-arc material along the crust-mantle boundary beneath a volcanic arc, accompanied by foundering of lithologies denser than the underlying mantle. Foundering material is schematically illustrated with red diapirs, informally termed "tadpoles" by Kelemen and Hacker (2016). Note that the red shapes are two to three orders of magnitude larger than the likely 100–1000 m diameter of dense diapirs foundering into the arc mantle (e.g., Behn et al., 2011; Jull and Kelemen, 2001).

[5]While revising this paper, we found that among tabulated compositions of Talkeetna arc samples in the Supplementary Table of Kelemen et al., Treatise on Geochemistry, 2003, 2014, 41 with compositions originally reported by Clift et al. (1995) had transposed values for MgO and CaO, and for Na_2O and K_2O. 33 of these are included in Supplementary Table 3 in the online version at https://doi.org/10.1016/B978-0-323-99762-1.00121-2 with corrected compositions. 6 of the 41 also had transposed values for TiO_2 and Al_2O_3. None of these 6 are included in Supplementary Table 3 in the online version at https://doi.org/10.1016/B978-0-323-99762-1.00121-2. In addition to the 41 samples from Clift et al. (1995) an additional 15 samples from Hacker et al. JGR 2008 had transposed values for Na_2O and K_2O. All of these are included in Supplementary Table 3 in the online version at https://doi.org/10.1016/B978-0-323-99762-1.00121-2 with corrected compositions. Corrected values are marked with a green highlight in the Table. Densities calculated for all these samples could be incorrect.

The results of this model are illustrated in Fig. 11 and reported in Supplementary Table 3 in the online version at https://doi.org/10.1016/B978-0-323-99762-1.00121-2. The average compositions of buoyant arc lithologies at 800–900 °C and 1–1.2 GPa provide a close match for the composition of lower continental crust, falling within one geometric standard deviation (GSD) of our preferred lower continental crust composition for all elements considered (Fig. 11 D and E).[6] And in fact, the trace element systematics of these compositions are quite similar to the composition of bulk continental crust.

It is notable that, compared to the eclogite facies density filter of Kelemen and Behn (2016), the arc Moho density filter we used here yielded a smaller proportion of dense versus buoyant compositions, and correspondingly slightly less SiO_2-rich average compositions for the buoyant fraction from each arc suite. However, this difference may not be very significant. If we had used a depleted harzburgite density, rather than a fertile lherzolite density, in the 2016 model, it would have yielded buoyant compositions with lower SiO_2 and incompatible element concentrations, more similar to the results of the model presented here.

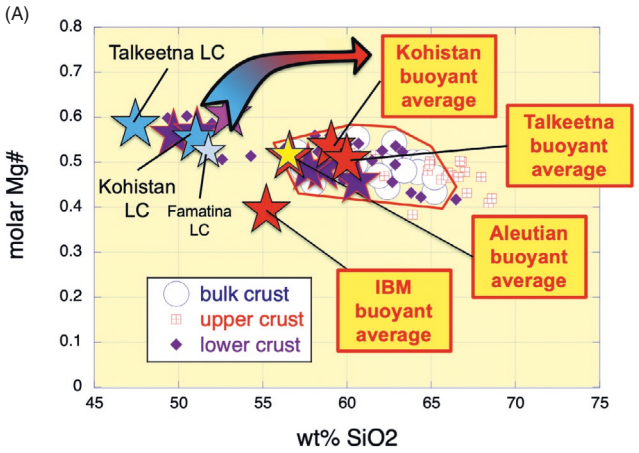

Fig. 11 Results of density filtering at the base of arc crust (900 °C, 1.2 GPa), in which compositions more buoyant than depleted mantle peridotite (3250 kg/m^3) are retained, while denser compositions founder into the underlying mantle. Compositions of samples in the buoyant group, and their averages, are reported in Supplementary Table 3 in the online version at https://doi.org/10.1016/B978-0-323-99762-1.00121-2. (A) Wt% SiO_2 versus Mg# diagram with symbols for arc lower crust as in Fig. 1D with buoyant compositions for various arcs added as red stars. Density filtering of subducting upper, middle and lower arc crust removes dense lower arc crust lithologies and retains buoyant compositions in the lower continental crust. (B and C) Extended major and trace element diagrams for buoyant arc compositions, normalized to the bulk continental crust composition of Rudnick and Gao (2003, 2014). Purple shaded line illustrates our preferred lower continental crust composition at 410 °C and 0.92 GPa. For all data sets plotted, values are geometric means. (D and E) Extended major and trace element diagrams for buoyant arc compositions, with a linear vertical scale, normalized to our preferred lower crust composition at 410 °C and 0.92 GPa. All values are geometric means. Grey shaded lines outline one geometric standard deviation of our preferred lower crust composition. Grey dashed lines illustrate bounds for two geometric standard deviations. (F–H) Histograms of compositions of lower crustal granulites with Vp from 6.7 to 7.1 km/s at 410 °C, 0.92 GPa. (I–K) Histograms of compositions of volcanic arc samples with densities less than 3250 kg/m^3 at 900 °C, 1.2 GPa, which are more buoyant than depleted mantle peridotite at the same conditions. Dark polygons in outline the distributions of granulite compositions from panel (F–H). Dashed polygons outline the compositional distributions of MORB segment averages and ocean island basalt centers (Gale et al., 2013; Hofmann et al., 2022).

(Continued)

[6]U concentrations in average, buoyant Aleutian lavas and plutons are higher than the bounds for *two* GSD, as are Th, K, Nb and Ta in Aleutian lavas. Nb, Ta and Pb concentrations lie just below the *two* GSD bounds for Talkeetna and IBM datasets.

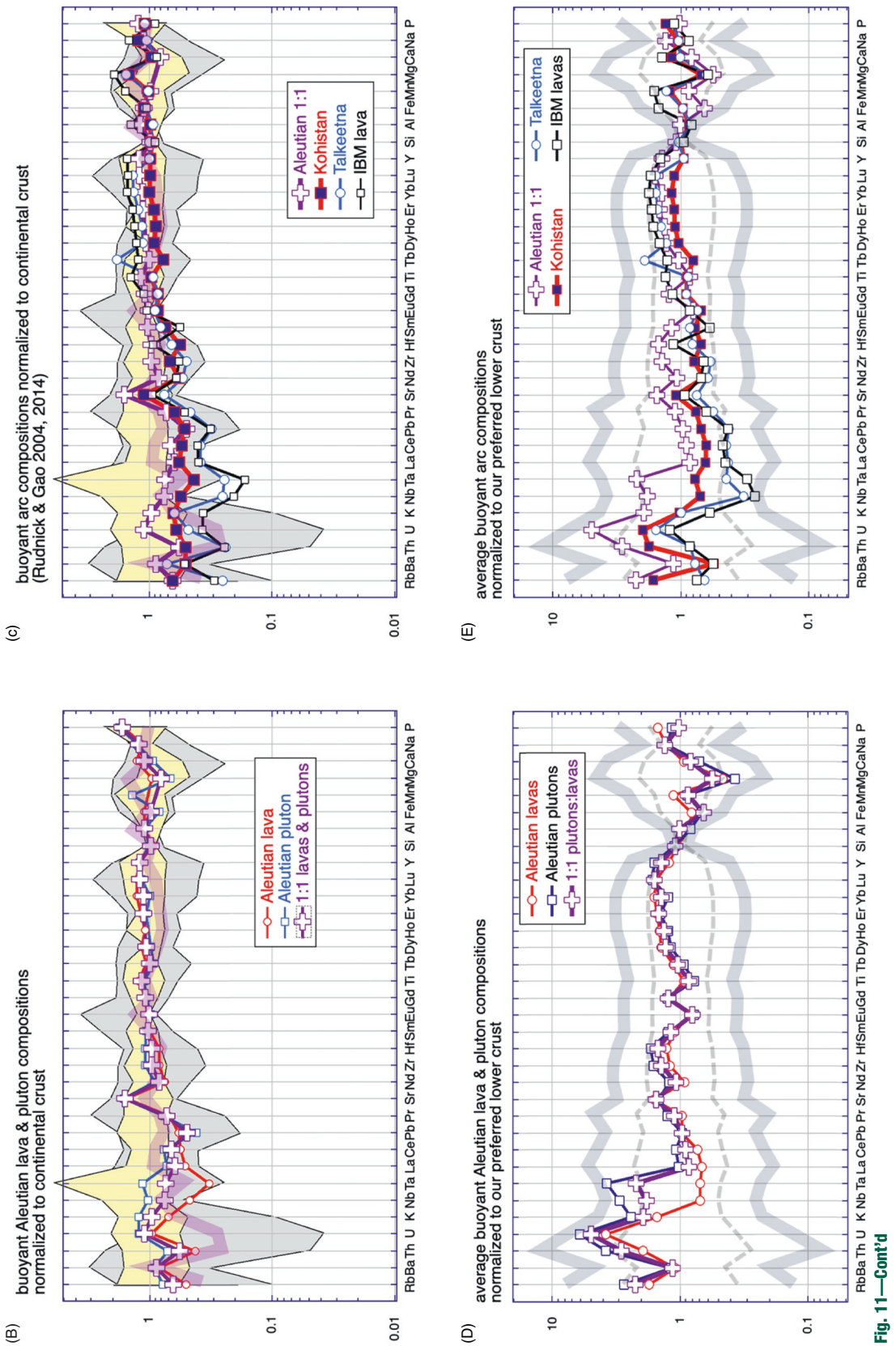
(B)
buoyant Aleutian lava & pluton compositions
normalized to continental crust
Aleutian lava
Aleutian pluton
1:1 lavas & plutons
(C)
buoyant arc compositions normalized to continental crust
(Rudnick & Gao 2004, 2014)
Aleutian 1:1
Kohistan
Talkeetna
IBM lava
(D)
average buoyant Aleutian lava & pluton compositions
normalized to our preferred lower crust
Aleutian lavas
Aleutian plutons
1:1 plutons:lavas
(E)
average buoyant arc compositions
normalized to our preferred lower crust
Aleutian 1:1
Kohistan
Talkeetna
IBM lavas
10
1
0.1
0.01
Rb Ba Th U K Nb Ta La Ce Pb Pr Sr Nd Zr Hf Sm Eu Gd Ti Tb Dy Ho Er Yb Lu Y Si Al Fe Mn Mg Ca Na P

Fig. 11—Cont'd

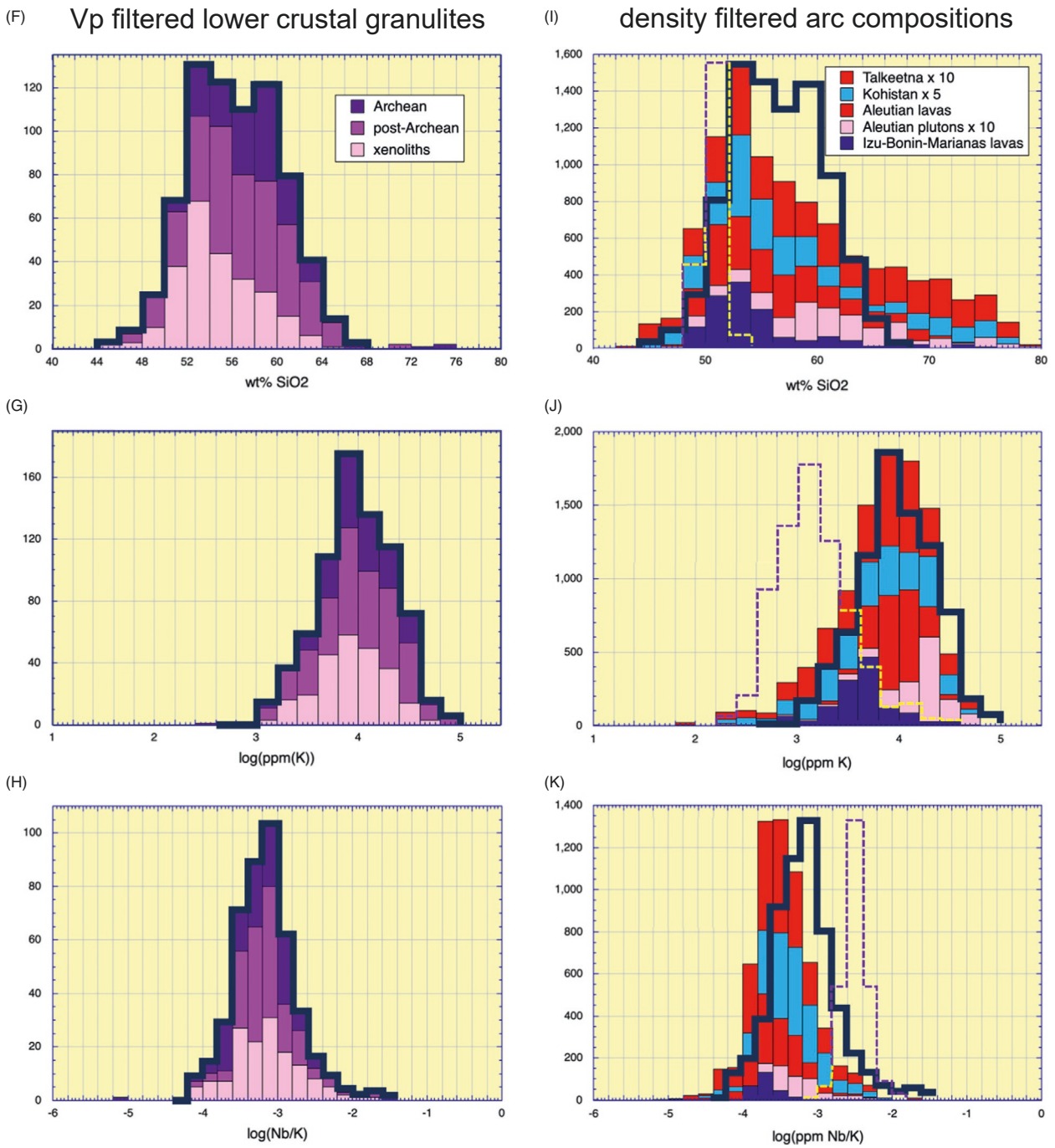

Fig. 11—Cont'd

Density filtering of underthrust material during continental collisions

We were originally inspired to investigate density filtering of underthrust material at the base of the crust by observations and hypotheses related to collision of the Indian and Asian continents in southern Tibet, northern Nepal and northern India. In this collision zone, some combination of thickening via pure shear, and simple shear via thrusting of Indian crust beneath Asian crust, has created doubly thick continental crust, about 80 km thick, with seismic Vp less than 7.0 down to more than 70 km depth (Kind et al., 2002; Monsalve et al., 2008; Monsalve et al., 2006; Nabelek et al., 2009; Schulte-Pelkum et al., 2005; Shi et al., 2015; Wittlinger et al., 2009; Zhao et al., 2001).

A notable feature of this thick crust is the lack of high P-wave speeds in most of the lower crust. To explain this, Le Pichon et al. (1992, 1997) proposed that mafic lower crust of the Indian plate transforms into eclogite at high pressure and temperature along the crust-mantle transition at 80 km, and then founders into the underlying mantle. Envisioning this process, we sketched a model of foundering diapirs along the Moho in southern Tibet (Fig. 12), that we termed the "South Tibetan Tadpole Zone" (Kelemen and Hacker, 2016). Such Tadpole Zones[7] could produce efficient density sorting, retaining compositions that are buoyant with respect to the mantle, and removing those that are denser than the mantle.

With this said, it is unclear how common Tibetan-style continental collisions have been in Earth history. McKenzie and Priestley (2008) proposed that such collisions form most metamorphic granulite terrains, as a result of high temperature metamorphism in radioactively-heated, thickened, felsic middle and lower crust. These granulites are then exhumed due to isostasy and erosion of the thickened orogen, resulting in normal thickness continental crust. If so, then based on seismic data, and the relationship of Vp to rock composition, we infer that exposed granulite terrains are underlain by similar granulites, formed at about the same time, extending to the base of the present-day crust.

Alternatively, granulite facies metamorphic rocks may form in "Arc Tadpole Zones" near the base of lower arc crust (Fig. 10), as outlined in Section "Rock samples from of the middle and lower crust." Based on present-day geological observations, Arc Tadpole Zones are likely to have been more common than Tibetan style continental collisions. Arc Tadpole Zones would have temperatures similar to the Tibetan Tadpole Zone, but would undergo density sorting at a lower pressure. If so, however—since exposed granulite terrains rarely if ever overlie anomalously thin continental crust—*the crustal material underlying lower crustal granulite terrains must have been added later*, perhaps in part via pure shear (thickening), but perhaps more commonly by continued underplating of younger, buoyant lithologies, and/or emplacement of magmatic rocks.

Delamination revisited

The processes described in Sections "One-stage delamination of oceanic arc crust doesn't form lower continental crust", "Density filtering of underthrust material at the base of arc crust" and "Density filtering of underthrust material during continental collisions" are quite similar, since they involve density sorting at the base of arc crust. The key difference is that density sorting of underplated material involves lithologies derived from lavas, pyroclastic deposits, volcanoclastic sediments and trench sediments, as well as felsic to intermediate, mid- and upper-crustal plutonic rocks, whereas delamination of arc crust, as generally envisioned, only affects mafic plutonic rocks formed at the base of the crust, such as those that comprise the lower crust of the oceanic Talkeetna and Kohistan arc crustal sections. As a result, the buoyant fraction produced by density sorting of underplated material closely resembles arc upper crustal lavas and plutonic rocks, whereas abundant mafic rocks are preserved after a single phase of delamination of oceanic arc sections like Talkeetna and Kohistan.

However, perhaps long-term burial, combined with extensive, ongoing delamination, could eventually transport upper crustal rocks to the base of arc crust, forming compositions similar to lower continental crust. Such a scenario was proposed, on a

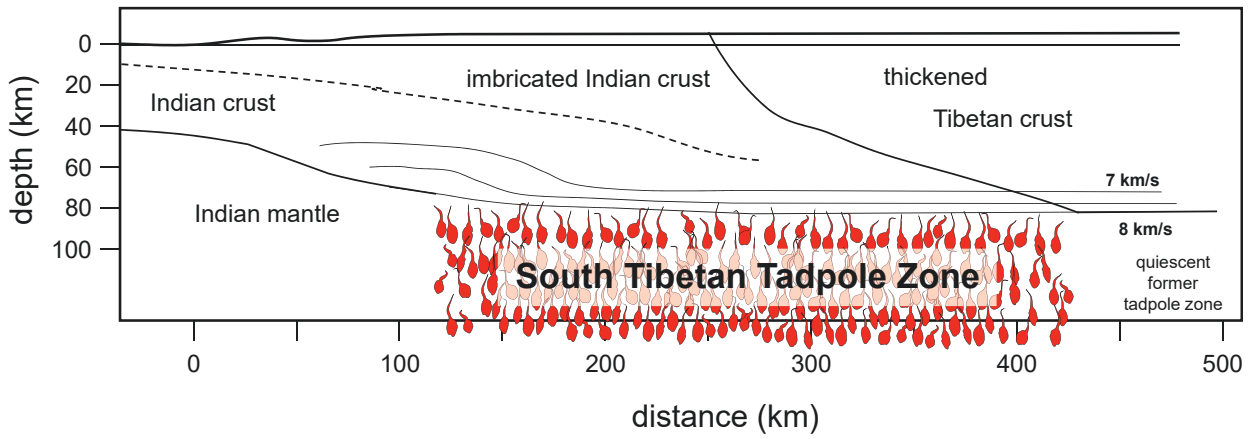

Fig. 12 Schematic cross-section illustrating a Tibetan-style continental collision, with underthrusting Indian crust along the crust-mantle boundary beneath Tibetan crust, accompanied by foundering of lithologies denser than the underlying mantle, as proposed by Le Pichon et al. (1992, 1997). Retained, accumulating buoyant material forms thick, intermediate to felsic crust with Vp less than 7 km/s extending to depths of more than 70 km. Foundering material is schematically illustrated as red diapirs, informally termed "tadpoles" by Kelemen and Hacker (2016). Note that the red shapes in the Figure are two to three orders of magnitude larger than the likely 100–1000 m diameter of dense diapirs foundering into the arc mantle (e.g., Behn et al., 2011, Jull and Kelemen, 2001).

[7]Here, "tadpole" refers to foundering blobs of dense material, which in models resemble the shapes of tadpoles. However, note that the tadpole shapes in Figs. 10 and 12 are two to three orders of magnitude larger than the likely size of foundering diapirs, on the order of 100–1000 m in diameter (Behn et al., 2011).

qualitative basis, to explain the presence of evolved, low Mg# quartz diorites near the base of the Talkeetna arc crustal section, and of banded amphibolites with arc andesite compositions in the Talkeetna arc mid-crust (Fig. 26 and related text, Kelemen et al., 2003a, 2014).

A good, though labor intensive, way to distinguish gradual burial and delamination beneath oceanic arcs from density sorting of underplated lithologies will be to determine the provenance of lower crustal metasediments, and—in the ideal case—to determine whether, on average, detrital zircons become increasingly young with increasing depth in continental crust, indicative of underplating, or increasingly old, indicative of gradual burial.

Yet another delamination scenario may arise where arcs along continental margins become so thick that lower crustal magmatism forms dense, garnet rich cumulate rocks at temperatures greater than 1000 °C and pressures greater than 0.9 GPa. In such a setting, highly depleted but density stable cumulates—such as those that comprise the lower crust in the oceanic Talkeetna and Kohistan arc sections—might never form. Instead, dense, garnet-rich cumulates might founder almost continuously from the arc Moho at magmatic temperatures. Mafic to intermediate lavas in such thick, continental arcs should record fractionation of igneous garnet, as may happen in central Chile as recorded by lavas with intermediate Mg# and high Dy/Yb produced by fractionation of abundant, low Dy/Yb garnet (e.g., Bourdon et al., 2000; Matteini et al., 2002).

Diapirs revisited

Behn et al. (2011) proposed that subducting metasediments are dominantly buoyant with respect to the overlying mantle, and as a consequence that sedimentary layers more than about 200 m thick will rise into the mantle wedge upon heating to more than 700–800 °C. We imagined that these diapirs, heating as they decompress along a super-adiabatic PT path, undergo extensive partial melting and reaction with surrounding mantle peridotite, causing fluxed melting and providing the "sediment component" in some primitive, mantle-derived arc magmas.

Recently, however, several papers have proposed that some diapirs of subducting, intermediate to felsic material (metasediments and buoyant arc lithologies undergoing subduction erosion) may be sufficiently large, and may rise sufficiently fast, to undergo closed system melting with little or no interaction with the mantle wedge, forming intermediate to felsic magmatic rocks in arcs (e.g. Gómez-Tuena et al., 2018; Marschall and Schumacher, 2012; Santa Cruz et al., 2023). This hypothesis is similar to some early papers on light REE enriched, Sr enriched, heavy REE depleted arc dacites, termed "adakites", cited in Section "Genesis and evolution of lower continental crust" (i). However, the more recent work applies the diapir hypothesis to intermediate arc magmas that lack the distinctive trace element characteristics of "adakites", and that more closely resemble the composition of bulk continental crust and lower continental crust. An end-member scenario for this process might be as follows: Ongoing tectonic erosion subducts intermediate to felsic arc magmatic rocks, such as batholiths. They are then returned to the crust via thrusting into or just beneath existing crust, ascent up a subduction channel, or in large diapirs rising though the mantle wedge, unaffected by reaction with surrounding peridotite. In some cases they may be recognizable as deformed tectonites. In others, they may melt, partially or completely, and appear to be newly formed magmatic rocks.

A role for oceanic plateaux, after all?

As noted in Section "Uncertainties in crustal composition", it has been proposed that oceanic plateaux could have formed a tectonic nucleus for subsequent subduction of adjacent oceanic crust and resulting arc magmatism (e.g., Abbott and Mooney, 1995; Albarède, 1998; Condie, 1997; Nair and Chacko, 2008; Schubert and Sandwell, 1989; Stein and Goldstein, 1996; White et al., 1999). Here we revisit this idea. Figs. 11 I, J and K show that granulites with lower crustal Vp from 6.7 to 6.9 km/s (at 410 °C, 0.92 GPa) have slightly higher average SiO_2, and slightly lower average K and Nb/K, than the buoyant arc compositions derived from the model of underplating of buoyant lithologies presented in Section "Density filtering of underthrust material in at the base of arc crust."

Dashed lines in Figs. 11 I, J and K outline the shape of histograms of MORB and OIB compositions (Gale et al., 2013; Hofmann et al., 2022), with lower SiO2, lower K, and higher Nb/K than the buoyant arc material. Addition of small amounts of MORB + OIB compositions to the buoyant arc material might yield a slightly better fit to the granulite data, as proposed for similar reasons by Rudnick (1995). A fully quantitative re-evaluation of this hypothesis is beyond the scope of our paper, but given that MORB + OIB averages have about ten times less K and ten times higher Nb/K than the buoyant arc lithologies (∼ 100 times higher Nb), a mixture of about 90% buoyant arc lithologies and 10% MORB + OIB lithologies might yield a distribution of compositions that is somewhat closer to the Vp-filtered granulite distribution.

Rates of continental formation and evolution

As discussed by Hacker et al. (2011), the present rate of sediment subduction, subduction erosion, and continental collision, coupled with the proportion of buoyant lithologies in these settings, is sufficient to accumulate the observed volume of lower continental crust by relamination over about two billion years. In their simplest form, these ideas require continuous accumulation of newly formed, compositionally buoyant lithologies. It is not clear how such hypotheses can be reconciled with proposed models for rapid formation of the current volume of continental crust in the early Archean or even the Hadean, followed by steady-state production rates equal to the rates of recycling of crust into the convecting mantle (e.g., Armstrong, 1981; Guo and Korenaga, 2020; Guo and Korenaga, 2023; Rosas and Korenaga, 2018). It is beyond the scope of this paper to address this problem, but perhaps (1)

the isotope evidence interpreted as requiring early Archean/Hadean formation of the entire volume of present-day continental crustal can be interpreted in other ways, or (2) some large fraction of the earliest "continental crust" was compositionally different from today, less buoyant and more easily recycled.

As noted above, Figs. 1 and 3, and many similar diagrams in the literature, show that Archean and post-Archean granulite terrains have similar compositions, as do xenoliths interpreted as sampling present-day lower continental crust. In particular, they all share Nb and Ta depletions relative to Th, U, K and La. These depletions are generally interpreted as being derived from a subduction component formed by low temperature, hydrous partial melting of subducting, mafic crust in eclogite facies. This can be taken as an indication that the processes forming granulites involved low temperature, hydrous partial melting of eclogite in subduction zones over 4 billion years.

However, our approach in this paper applies only to rocks preserved in continental crust. Archean rocks are exposed on Earth, but perhaps a more voluminous component of compositionally different, early continental crust has largely disappeared. As is evident from the dramatic geochemical variability of granulites seen in Figs. 1 and 3, use of averages may over-emphasize the importance of accumulated, buoyant "survivors" of erosion and relamination processes. Remnants remain that record other components of continental crust that are relatively rare today, but perhaps such rare compositions were common in the past, formed via different processes, and have been almost completely recycled during crustal evolution. Interpretation of crustal evolution using isotope data depends on the assumption that ancient continental crust had known isotopic parent and daughter ratios and concentrations. Often, models of complementary crust and mantle evolution in deep time use values for Sm, Nd, Lu, Hf, Rb, Sr, U, Th and Pb based on the present-day, average composition of continental crust. One wonders whether models using different assumptions might yield significantly different results.

Conclusions

The lower continental crust is intermediate rather than mafic, and resembles intermediate arc lavas and plutons with liquid-like compositions. The average lower crust does not have the composition of a cumulate produced from a primitive, mantle-derived, mafic magma by crystal fractionation or partial melting. Instead, though there are some indications that it has lost a partial melt enriched in Th and U, and depleted in Sr, Eu and Ti, the lower continental crust has a composition that is almost identical to many intermediate arc lithologies and is more similar to upper continental crust than previous estimates.

Density sorting processes (Fig. 13) are almost certainly required to remove dense, mafic, lower arc crust, and produce buoyant, intermediate continental crust from arc crust. Whereas multiple episodes of delamination of dense, garnet-bearing lithologies from the base of thickened arc crust remain a possibility, it is likely that the density sorting processes of "relamination" have resulted in selective underplating of buoyant lithologies that accumulated to form the main component in lower continental crust.

Combined with our previous work, these results indicate that simple models of density sorting can *quantitatively* account for the evolution of arc crust to produce lower and bulk continental crust, in the sense that these processes reproduce estimated lower crust compositions within one standard deviation. Of course, the origin and evolution of the continental crust has been complex and variable, in both time and space, and certainly involved other processes, for example flood basalt magmatism. However, we have taken a simple approach in order to develop quantitative models for the origin of average continental crust, via arc magmatism followed by density sorting and relamination. Our results suggest that these processes may have dominated crustal formation and evolution. However, though they satisfy geochemical constraints, these forward models do not rule out alternatives. We await development of other, similarly *quantitative*, necessarily simplified, explanations for the composition, genesis and evolution of continental crust.

Avenues for future investigation

Numerous avenues for further research are suggested by the results presented here, and by the contrast of our results with the more mafic lower crust compositions presented in many recent papers. For those who espouse alternative theories of crustal genesis, with a lesser role for arc magmatism, an impactful approach would be to develop compositional models whose results are statistically similar to estimated lower crust compositions. Even if there is not a consensus on the major element contents of lower continental crust, the trace element characteristics of most estimates are quite similar and offer a robust target for forward modeling.

As noted in Section "Delamination revisited", where thick granulite sections are exposed, recording a range of crustal pressures and depths, it would be valuable to determine whether metasediments in these suites become younger upward, consistent with gradual thickening via burial, or become younger downward, consistent with successive relamination events. Similar studies might be possible where extensive xenolith suites record a range of crustal pressures, and metasedimentary xenoliths retain identifiable, detrital zircon grains.

As noted in Section "Composition of the lower continental crust", mixing of SiO_2-rich and SiO_2-poor lithologies on a length scale smaller than a seismic wavelength (e.g., "banded gneisses") could lead to a systematic underestimate of SiO_2 contents in the lower crust as inferred from regional seismic data. Outcrop-scale studies of the length scale and amplitude of compositional banding in granulite terrains would help to quantify the extent to which this may have led to an underestimate of the SiO_2 content of the lower crust, in this and other papers. Intriguingly, if this effect were ubiquitous, it could reconcile the relatively high SiO_2

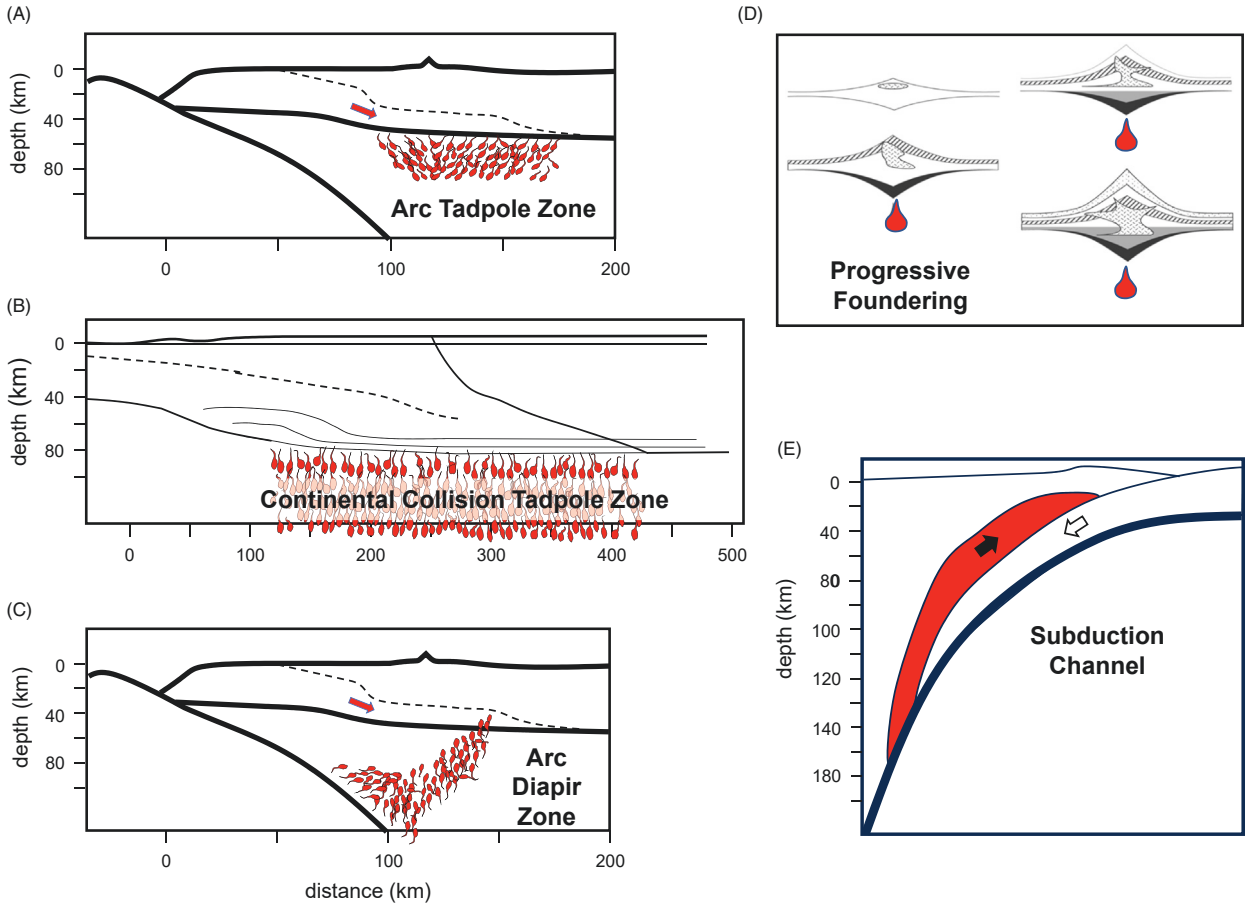

Fig. 13 Schematic summary of possible processes that remove mafic, lower arc crust and accumulate intermediate, buoyant lower continental crust via density sorting. (A and B) Tadpole zones, in which imbricated material undergoes density sorting at the crust-mantle boundary. (C) Rise of buoyant diapirs through sub-arc mantle, with or without extensive melting. (D) Progressive burial coupled with ongoing foundering of dense lithologies at the base of arc crust. (E) Rise of buoyant material up a subduction channel, with or without partial melting. (D) modified from Fig. 26 in Kelemen et al., (2003a, 2014). (E) modified from Fig. 2 in the Geopoem of Chemenda et al., (2000).

content of metamorphic granulite terrains based on the average composition of hand samples (globally, 60–63 wt% SiO_2, Fig. 1E) with the somewhat lower SiO_2 contents in our preferred lower crust compositions (56.9–57.7 wt% SiO_2) based on averages of seismic observations large crustal volumes.

While there are recent, comprehensive reviews of the temperatures and pressures recorded in granulite terrains, it would be instructive to make similar compilations for amphibolite suites, and for granulite xenoliths, preferably using a consistent set of thermobarometers. Also worthwhile would be additional comprehensive studies of the bulk composition of granulite facies metamorphic rocks, and their potential variation as a function of age, temperature and pressure. Many big metamorphic terrains in stable crust have received a lot of attention already, but there are fewer whole rock geochemical analyses on younger suites—with known tectonic provenance—such as the Skagit gneiss and Central Gneiss Complex in western North America and similar suites in Japan (Hidaka, Higo, ..) and New Zealand. In this context, a comprehensive study of isotope ratios in granulites—not only for Pb, Nd, Sr and Hf, but also for oxygen and other stable isotope systems—would be valuable.

Much hinges on the uncertainty in present-day, lower crustal temperatures in stable continental crust, and their corresponding use in interpreting Vp in terms of rock composition. A comprehensive study of the relationship between surface heat flow, crustal thickness, and Vp in the lower crust might yield useful relationships, particularly in crust less than 200 million years old, and in older crust in tectonically reactivated regions. However, it is important to be mindful of the spatial scale of the various observations involved, from "seismic wavelengths" and local heat flow observations to the composition of rock samples, and the natural scale of heterogeneity in temperature and composition. For an example of the importance of these considerations, please refer to the discussion of Vp in the Aleutian arc in Section "Uncertainties in crustal composition." It may be too much to ask, but if possible it would be particularly valuable to define the spatial scale and cause of high heat flow in tectonically active crust and older, "reactivated" crust, and to quantify how lower crustal Vp varies between these, and adjacent regions with normal heat flow.

Methods

Mineral assemblages and physical properties

Much of this paper is based on calculations of equilibrium mineral proportions and compositions at a given temperature and pressure using using Perple_X 6.6.7 (Connolly, 2005; Connolly, 2009) with thermodynamic data and solution models appropriate for subduction zone mineral assemblages (Hacker, 2008; Holland and Powell, 2003; Holland and Powell, 1998) listed in Table 3.

Mineral proportions and physical properties were calculated for compilations of granulite-facies Archean ($N = 1090$) and Post-Archean ($N = 1571$) terrains (Hacker et al., 2015) and xenoliths ($N = 1001$) (Huang et al., 2013) and amphibolite-facies terrains ($N = 1919$) (Huang et al., 2013). We assumed 0.5 and 1 wt% H_2O for the granulite and amphibolite samples, respectively. We set $Fe^{3+}/\Sigma Fe = 0.25$ based on the value found in melt inclusions from Agrigan volcano in the Mariana arc, which is approximately equivalent to an oxygen fugacity 1.5 log units higher than the Fayalite-Quartz-Magnetite oxygen buffer at 700 °C and 3 GPa (Kelley and Cottrell, 2012; Kress and Carmichael, 1991).

Physical properties (density, Vp, Vs, Vp/Vs) were calculated for the lower crust at 410 and 510 °C and 0.92 GPa for phase assemblages equilibrated at 650 °C (amphibolites) or 700 °C (granulites) and 0.92 GPa and for the middle crust at 280 and 300 °C and 0.54 GPa for phase assemblages equilibrated at 650 °C (amphibolites) or 700 °C (granulites) and 0.54 GPa. For the elastic moduli of quartz, we used values for alpha-quartz at 410 and 510 °C, 0.92 GPa in the lower crust, and 280 and 300 °C, 0.54 GPa in the middle crust.

Physical properties were calculated for arc magmatic suites (Supplementary Table 3 in the online version at https://doi.org/10.1016/B978-0-323-99762-1.00121-2) at 800 °C, 1 GPa, and 900 °C, 1.2 GPa, with 2 wt% H_2O and $Fe^{3+}/\Sigma Fe = 0.25$. The 900 °C, 1.2 GPa conditions were used for density filtering calculations at arc Moho conditions, wherein buoyant compositions have density less than underlying arc mantle. For the arc mantle, we used average mantle harzburgite from the base of the Talkeetna arc section (Kelemen et al., 2003a, 2014) with 44.63 wt% SiO_2, 0.00 wt% TiO_2, 0.60 wt% Al_2O_3, 7.91 wt% FeOT, 46.0 wt% MgO, 0.54 wt% CaO, 0.15 wt% Na_2O, and 0.00 wt% K_2O, assuming it contains 2 wt% H_2O.

Heat production in rock volumes was calculated using compositions and densities as recommended by McDonough et al. (2020), using arithmetic mean concentrations of heat producing elements, for compositions in Tables 1 and 2, and Supplementary Table 2 in the online version at https://doi.org/10.1016/B978-0-323-99762-1.00121-2.

Area and volume weighted proportions of lower and middle crust with a given Vp or Vp/Vs

Vp and Vp/Vs distributions for middle and lower continental crust were calculated as follows. Holbrook et al. (1992) and Hacker et al. (2015) made pre- and post-1992 compilations of seismic observations, for the different tectonic settings in CRUST1.0 (Laske et al., 2012, 2013): (a) shields & platforms, (b) Paleozoic and Mesozoic orogens, (c) India-Asia collision, and (d) rifts + continental shelves + margin-continent transitions. In keeping with our emphasis on average heat flow data for shields, platforms and older orogens, we only used the seismic data compilations for tectonic settings (a) and (b). omitting data for (c), (d), oceanic continental plateaux, and continental slopes.

Our definition of the lower continental crust (>25 km depth) differs from the definitions used previously, e.g., in the layer thicknesses of CRUST1.0. For tectonic settings (a) and (b), the CRUST1.0 lower crust starts at depths of 26.7 and 29.7 km, and extends to the base of the crust at 38.8 and 39.7 km, with lower crust thicknesses of 12.1 and 10 km, respectively. We added a proportion of data from the middle crust compilation for each tectonic setting adding 1.7 km of a total of 13.8 km lower crust, extending from 25 to 38.8 km for (a), and adding 4.7 km of a total of 14.7 km lower crust, extending from 25 to 39.7 km for (b). Thus, our average Vp for the lower crust in settings (a) and (b) includes 12.3 and 32.0% mid-crustal Vp values, respectively.

Table 3 Perple_X solution models used.

Abbreviation	*Mineral*	*References*
Atg	antigorite	ideal
Chl(HP)	chlorite	Holland et al. (1998)
Ctd(HP)	chloritoid	White et al. (2000)
Cpx(HP)	clinopyroxene	Holland and Powell (1996)
Ep(HP)	epidote	Holland and Powell (1998)
GlTrTsPg	clinoamphibole	Wei and Powell (2003); White et al. (2003)
Gt(HP)	garnet	Holland and Powell (1998)
O(HP)	olivine	Holland and Powell (1998)
Opx(HP)	orthopyroxene	Holland and Powell (1996)
Pheng(HP)	mica	"parameters from Thermocalc"
Pl(h)	plagioclase	Newton et al. (1980)
San	sanidine	Waldbaum and Thompson (1968)
Sp(HP)	spinel	Holland and Powell (1998)
T	talc	ideal

Combining Holbook et al. and Hacker et al. data yielded cumulative sums of cross-sectional area (length x height) for rock sections with a given Vp (bins of 0.1 km/s) or Vp/Vs (bins of 0.01) reported in the literature. These cumulative distributions were then multiplied by the proportions of surface areas for settings (a) and (b) (82% a 18% b) to calculate cross-sectional-area weighted average Vp or Vp/Vs.

Additional information

In addition to the description of methods in this Section, Supplementary Tables 1, 2 and 3 in the online version at https://doi.org/10.1016/B978-0-323-99762-1.00121-2 are Excel Workbooks, which retain the formulae used to calculate area- and provenance-weighted distributions of lower and middle crustal Vp and Vp/Vs, average compositions and physical properties for granulites, amphibolites and crustal layers at various pressures and temperatures together with different constraints from Vp, together with estimates of formal uncertainty arising from calculation of all of the average values.

Acknowledgments

This paper arises from many years of collaborative research supported in part by NSF Research Grants EAR-1841806, EAR-1844340, EAR-1855430, EAR-1457293, EAR-1316333, OCE-1144759, EAR-0742368, EAR-0727013, EAR-0632774, OCE-0242233, OCE-0533226, EAR-0125919, EAR-0087706, EAR-9910899, EAR-9419240, EAR-9005306 and EAR-8600534 to Behn, Hacker, Kelemen, Gene Yogodzinski, and their colleagues. Kelemen's effort on this particular paper was supported in part by the Arthur D. Storke and Thomas Alva Edison Chairs at Columbia University. We thank George Bergantz and Juan Otamendi for providing a compilation of geochemical data on the Famatina arc section, collected with funding from NSF EAR-1049884, Mike Brown for providing compiled data on pressures and temperatures recorded by granulite facies metamorphic rocks, and Francis Lucazeau for providing his compiled, global heat flow dataset. As always, we continue to benefit from data and insights generously shared by Gene Yogodzinski. We are sincerely grateful to Bill McDonough, editor Matt Kohn, and an anonymous reviewer, for comments and suggestions that very substantially improved this paper.

References

Abbott D and Mooney W (1995) The structural and geochemical evolution of the continental crust: support for the oceanic plateau model of continental growth. *Reviews of Geophysics* 33: 231–242.

Albarède F (1998) The growth of continental crust. *Tectonophysics* 296: 1–14.

Amante C and Eakins BW (2009) ETOPO1 1 Arc-minute global relief model: Procedures, data sources and analysis. In: *NOAA Technical Memorandum NESDIS NGDC-24, National Geophysical Data Center, NOAA*. https://doi.org/10.7289/V5C8276M.

Andersen TB and Austrheim H (2008) The Caledonian infrastructure in the fjord-ergion of western Norway: With special emphasis on formation and exhumation of high-and ultrahigh-pressure rocks, late-to post-orogenic tectonic processes and basin formation. In: *Field Trip Guidebook 33 IGC excursion No 29*. pp. 88.

Andersen TB, Jamtveit B, Dewey JF, and Swensson E (1991) Subduction and eduction of continental crust: Major mechanisms during continent-continent collision and orogenic extensional collapse, a model based on the south Norwegian Caledonides. *Terra Nova* 3: 303–310.

Angiboust S, Agard P, De Hoog JCM, Omrani J, and Plunder A (2013) Insights on deep, accretionary subduction processes from the Sistan ophiolitic "mélange"(Eastern Iran). *Lithos* 156: 139–158.

Angiboust S, Menant A, Gerya T, and Oncken O (2022) The rise and demise of deep accretionary wedges: A long-term field and numerical modeling perspective. *Geosphere* 18: 69–103.

Armstrong RL (1968) A model for the evolution of strontium and lead isotopes in a dynamic earth. *Reviews of Geophysics* 6: 175–199.

Armstrong RL (1971) Isotopic and chemical constraints on models of magma genesis in volcanic arcs. *Earth and Planetary Science Letters* 12: 137–142.

Armstrong RL (1981) Radiogenic isotopes: the case for crustal recycling on a near-steady-state no-continental-growth Earth. *Philosophical Transactions. Royal Society of London* A301: 443–472.

Arndt NT (2013) The formation and evolution of the continental crust. *Geochemical Perspectives* 2: 405.

Arndt NT and Goldstein SL (1989) An open boundary between lower continental crust and mantle: its role in crust formation and crustal recycling. *Tectonophysics* 161: 201–212.

Artemieva IM (2006) Global $1° \times 1°$ thermal model TC1 for the continental lithosphere: Implications for lithosphere secular evolution. *Tectonophysics* 416: 245–277.

Austrheim H and Griffin WL (1985) Shear deformation and eclogite formation within granulite-facies anorthosites of the Bergen Arcs, western Norway. *Chemical Geology* 50: 26281.

Ayers JC and Watson EB (1993) Rutile solubility and mobility in supercritical aqueous fluids. *Contributions to Mineralogy and Petrology* 114: 321–330.

Bédard J (2006) A catalytic delamination-driven model for coupled genesis of Archaean crust and sub-continental lithospheric mantle. *Geochimica et Cosmochimica Acta* 70: 118–1214.

Behn MD and Kelemen PB (2003) Relationship between seismic P-wave velocity and the composition of anhydrous igneous and meta-igneous rocks. *Geochemistry, Geophysics, Geosystems* 4.

Behn MD and Kelemen PB (2006) Stability of arc lower crust: Insights from the Talkeetna arc section, south central Alaska, and the seismic structure of modern arcs. *Journal of Geophysical Research - Solid Earth* 111.

Behn MD, Hirth G, and Kelemen PB (2007) Trench-parallel anisotropy produced by foundering of arc lower crust. *Science* 317: 108–111.

Behn MD, Kelemen PB, Hirth G, Hacker BR, and Massonne HJ (2011) Diapirs as the source of the sediment signature in arc lavas. *Nature Geoscience* 4: 641–646.

Blackwell DD, Bowen RG, Hull DA, Riccio J, and Steele J (1982) Heat flow, arc volcanism, and subduction in northern Oregon. *Journal of Geophysical Research* 87: 8735–8754.

Bourdon B, Woerner G, and Zindler A (2000) U-series evidence for crustal involvement and magma residence times in the petrogenesis of Parinacota Volcano, Chile. *Contributions to Mineralogy and Petrology* 139: 458–469.

Bowman EE, Ducea MN, and Triantafyllou A (2021) Arclogites in the subarc lower crust: Effects of crystallization, partial melting, and retained melt on the foundering ability of residual roots. *Journal of Petrology* 62.

Brenan JM, Shaw HF, Phinney DL, and Ryerson FJ (1994) Rutile-aqueous fluid partitioning of Nb, Ta, Hf, Zr, U and Th: implications for high field strength element depletions in island-arc basalts. *Earth and Planetary Science Letters* 128: 327–339.
Brophy JG and Marsh BD (1986) On the origin of Hi-Alumina arc basalt and the mechanics of melt extraction. *Journal of Petrology* 27: 763–790.
Brown M (2007) Metamorphic conditions in orogenic belts: A record of secular change. *International Geology Review* 49: 193–234.
Brown M and Johnson T (2019) Time's arrow, time's cycle: Granulite metamorphism and geodynamics. *Mining Magazine* 83: 323–338.
Brueckner HK and van Roermund HL (2004) Dunk tectonics: A multiple subduction/eduction model for the evolution of the Scandinavian Caledonides. *Tectonics* 23.
Cai Y, Rioux ME, Kelemen PB, Goldstein SL, and Bolge L (2015) Distinctly different parental magmas for calc-alkaline plutons and tholeiitic lavas in the central and eastern Aleutian arc. *Earth and Planetary Science Letters*. in press.
Calvert AJ (2004) Seismic reflection imaging of two megathrust shear zones in the northern Cascadia subduction zone. *Nature* 428: 163–167.
Calvert AJ, Fisher MA, Ramachandran K, and Tréhu AM (2003) Possible emplacement of crustal rocks into the forearc mantle of the Cascadia Subduction Zone. *Geophysical Research Letters*: 30.
Calvert AJ, Ramachandran K, Kao H, and Fisher MA (2006) Local thickening of the Cascadia forearc crust and the origin of seismic reflectors in the uppermost mantle. *Tectonophysics* 420: 175.
Calvert AJ, Preston LA, and Farahbod AM (2011) Sedimentary underplating at the Cascadia mantle-wedge corner revealed by seismic imaging. *Nature Geoscience* 4: 545–548.
Castro A, Vogt K, and Gerya T (2013) Generation of new continental crust by sublithospheric silicic-magma relamination in arcs: a test of Taylor's andesite model. *Gondwana Research* 23: 1554–1566.
Chapman AD (2017) The Pelona–Orocopia–Rand and related schists of southern California: A review of the best-known archive of shallow subduction on the planet. *International Geology Review* 59: 664–701.
Chapman JB (2021) Diapiric relamination of the Orocopia Schist (southwestern US) during low-angle subduction. *Geology* 49: 983–987.
Chemenda AI, Mattauer M, Malavieille J, and Bokun AN (1995) A mechanism for syn-collisional rock exhumation and associated normal faulting: results from physical modelling. *Earth and Planetary Science Letters* 132: 225–232.
Chemenda AI, Burg JP, and Mattauer M (2000) Evolutionary model of the Himalaya–Tibet system: Geopoem based on new modelling, geological and geophysical data. *Earth and Planetary Science Letters* 174: 397–409.
Chen K, Rudnick RL, Wang Z, Tang M, Gaschnig RM, Zou Z, He T, Hu Z, and Liu Y (2020) How mafic was the Archean upper continental crust? Insights from Cu and Ag in ancient glacial diamictites. *Geochimica et Cosmochimica Acta* 278: 16–29.
Chin EJ, Lee CTA, Tollstrup DL, Xie L, Wimpenny JB, and Yin QZ (2013) On the origin of hot metasedimentary quartzites in the lower crust of continental arcs. *Earth and Planetary Science Letters* 361: 120–133.
Christensen NI (1978) Ophiolites, seismic velocities and oceanic crustal structure. *Tectonophysics* 47: 131–157.
Christensen NI and Mooney WD (1995) Seismic velocity structure and composition of the continental crust; a global view. *Journal of Geophysical Research, B, Solid Earth and Planets* 100: 9761–9788.
Christensen NI and Salisbury MH (1975) Structure and constitution of the lower oceanic crust. *Reviews of Geophysics* 13: 57–86.
Cloos M and Shreve RL (1988a) Subduction-channel model of prism accretion, melange formation, sediment subduction, and subduction erosion at convergent plate margins: 1. Background and description. *Pure and Applied Geophysics* 128: 455–500.
Cloos M and Shreve RL (1988b) Subduction-channel model of prism accretion, melange formation, sediment subduction, and subduction erosion at convergent plate margins: 2. Implications and discussion. *Pure and Applied Geophysics* 128: 501–545.
Coats RR (1962) Magma type and crustal structure in the Aleutian arc. In: *The crust of the Pacific Basin*, vol. 6, pp. 92–109. Geoiphysical Monograph.
Collins WJ, Murphy JB, Johnson TE, and Huang HQ (2020) Critical role of water in the formation of continental crust. *Nature Geoscience* 13: 331–338.
Condie KC (1997) Contrasting sources for upper and lower continental crust: the greenstone connection. *Journal of Geology* 105: 729–736.
Condie KC (2018) A planet in transition: The onset of plate tectonics on Earth between 3 and 2 Ga? *Geoscience Frontiers* 9: 51–60.
Condie KC and Kröner A (2013) The building blocks of continental crust: evidence for a major change in the tectonic setting of continental growth at the end of the Archea. *Gondwana Research* 23: 394–402.
Connolly JAD (2005) Computation of phase equilibria by linear programming: A tool for geodynamic modeling and its application to subduction zone decarbonation. *Earth and Planetary Science Letters* 236: 524–541.
Connolly JAD (2009) The geodynamic equation of state: What and how. *G-cubed* 10. Q10014.
Craig TJ, Kelemen PB, Hacker BR, and Copley A (2020) Reconciling geophysical and petrological estimates of the thermal structure of southern Tibet. *G-cubed* 21. e2019GC008837.
Cruz-Uribe AM, Marschall HR, Gaetani GA, and Le Roux V (2018) Generation of alkaline magmas in subduction zones by partial melting of mélange diapirs—An experimental study. *Geology* 46: 343–346.
Cui D-D, Guo J-L, Shinevar WJ, Guo L, Xu W-C, Zhang H-F, and Jin Z-M (2023) Geophysical-geochemical modeling of deep crustal compositions: Examples of continental crust in typical tectonic settings and North China Craton. *Journal of Geophysical Research* 128. e2022JB025536.
Currie CA, Beaumont C, and Huismans RS (2007) The fate of subducted sediments: A case for backarc intrusion and underplating. *Geology* 35: 1111–1114.
Czertowicz TA, Scott JM, Waight TE, Palin JM, Van der Meer QHA, Le Roux P, Münker C, and Piazolo S (2016) The Anita Peridotite, New Zealand: ultra-depletion and subtle enrichment in sub-arc mantle. *Journal of Petrology* 57: 717–750.
DeBari SM and Coleman RG (1989) Examination of the deep levels of an island arc: Evidence from the Tonsina ultramafic-mafic assemblage, Tonsina, Alaska. *Journal of Geophysical Research* 94: 4373–4391.
DeBari SM and Sleep NH (1991) High-Mg, low-Al bulk composition of the Talkeetna island arc, Alaska: implications for primary magmas and the nature of arc crust. *Geological Society of America Bulletin* 103: 37–47.
Defant MJ and Drummond MS (1990) Derivation of some modern arc magmas by melting of young subducted lithosphere. *Nature* 347: 662–665.
Dhuime B, Bosch D, Bodinier JL, Garrido CJ, Bruguier O, Hussain SS, and Dawood H (2007) Multistage evolution of the Jijal ultramafic–mafic complex (Kohistan, N Pakistan): implications for building the roots of island arcs. *Earth and Planetary Science Letters* 261: 179–200.
Dhuime B, Bosch D, Garrido CJ, Bodinier JL, Bruguier O, Hussain SS, and Dawood H (2009) Geochemical architecture of the lower-to middle-crustal section of a paleo-island arc (Kohistan Complex, Jijal–Kamila area, northern Pakistan): implications for the evolution of an oceanic subduction zone. *Journal of Petrology* 50: 531–569.
Dhuime B, Wuestefeld A, and Hawkesworth CJ (2015) Emergence of modern continental crust about 3 billion years ago. *Nature Geoscience* 8: 552–555.
Dick HJ, Ozawa K, Meyer PS, Niu Y, Robinson PT, Constantin M, Hebert R, Maeda J, Natland JH, Hirth G, and Mackie S (2002) Primary silicate mineral chemistry of a 1.5-km section of very slow spreading lower ocean crust: ODP hole 735B, Southwest Indian ridge. *Proc. ODP Sci. Res.* 176: 1–60.
Dodson MH (1973) Closure temperature in cooling geochronological and petrological systems. *Contributions to Mineralogy and Petrology* 40: 259–274.
Drummond MS and Defant MJ (1990) A model for trondhjemite-tonalite-dacite genesis and crustal growth via slab melting: Archean to modern comparisons. *Journal of Geophysical Research* 95: 21503–21521.
Ducea MN (2002) Constraints on the bulk composition and root foundering rates of continental arcs: A California arc perspective. *Journal of Geophysical Research* 107.
Ducea M and Chapman AD (2018) Sub-magmatic arc underplating by trench and forearc materials in shallow subduction systems; A geologic perspective and implications. *Earth Science Reviews* 185: 763–779.
Ducea MN and Saleeby JB (1996) Buoyancy sources for a large, unrooted mountain range, the Sierra Nevada, California: evidence from xenolith thermobarometry. *Journal of Geophysical Research* 101: 8229–8244.

Ducea M and Saleeby J (1998a) The age and origin of a thick mafic–ultramafic keel from beneath the Sierra Nevada batholith. *Contributions to Mineralogy and Petrology* 133: 169–185.
Ducea M and Saleeby J (1998b) A case for delamination of the deep batholithic crust beneath the Sierra Nevada, California. *International Geology Review* 40: 78–93.
Ducea MN, Otamendi JE, Bergantz GW, Jianu D, and Petrescu L (2015) The origin and petrologic evolution of the Ordovician Famatinian-Puna arc. *Geological Society of America Memoirs* 212: 125–138.
Ducea MN, Chapman AD, Bowman E, and Balica C (2021a) Arclogites and their role in continental evolution; part 2: relationship to batholiths and volcanoes, density and foundering, remelting and long-term storage in the mantle. *Earth Science Reviews* 214: 103476.
Ducea MN, Chapman AD, Bowman E, and Triantafyllou A (2021b) Arclogites and their role in continental evolution; part 1: Background, locations, petrography, geochemistry, chronology and thermobarometry. *Earth Science Reviews* 214: 103375.
Dwight T, Scott JM, and Schwartz JJ (2019) Emplacement and Paleozoic and Cretaceous recrystallisation of the Broughton Arm peridotite in western Fiordland, New Zealand. *New Zealand Journal of Geology and Geophysics* 62(1): 72–86.
Emo RB, Kamber BS, Downes H, Murphy DT, and Caulfield JT (2021) Evidence for highly refractory, heat producing element-depleted lower continental crust: Some implications for the formation and evolution of the continents. *Chemical Geology* 580: 120389.
England P and Molnar P (1983) The interpretation of inverted metamorphic isograds using simple physical calculations. *Tectonics* 12: 145–157.
Fliedner MM and Klemperer SL (1999) Structure of an island-arc: Wide-angle seismic studies in the eastern Aleutian Islands, Alaska. *Journal of Geophysical Research* 104: 10667–10694.
Fliedner MM, Klemperer SL, and Christensen NI (2000) Three-dimensional seismic model of the Sierra Nevada arc, California, and its implications for crustal and upper mantle composition. *Journal of Geophysical Research* 105: 10899–10921.
Frost BR, Swapp SM, Frost CD, Bagdonas DA, and Chamberlain KR (2018) Neoarchean tectonic history of the Teton Range: Record of accretion against the present-day western margin of the Wyoming Province. *Geosphere* 14: 1008–1030.
Furlong KP and Chapman DS (2013) Heat flow, heat generation, and the thermal state of the lithosphere. *Annual Review of Earth and Planetary Sciences* 41: 385–410.
Furukawa Y (1993) Depth of the decoupling plate interface and thermal structure under arcs. *Journal of Geophysical Research* 98: 20005–20013.
Fyfe WS and McBirney AR (1975) Subduction and the structure of andesitic volcanic belts. *American Journal of Science* 275: 285–297.
Gale A, Dalton CA, Langmuir CH, Su Y, and Schilling J-G (2013) The mean composition of ocean ridge basalts. *G-cubed* 14: 489–518.
Galli A, Le Bayon B, Schmidt MW, Burg JP, and Reusser E (2013) Tectonometamorphic history of the Gruf complex (Central Alps): exhumation of a granulite–migmatite complex with the Bergell pluton. *Swiss Journal of Geosciences* 106: 33–62.
Garbe-Schönberg D, Koepke J, Müller S, Mock D, and Müller T (2022) A reference section through fast-spread lower oceanic crust, Wadi Gideah, Samail Ophiolite (Sultanate of Oman): whole rock geochemistry. *Journal of Geophysical Research* 127. e2021JB022734.
Garrido CJ, Bodinier JL, Burg JP, Zeilinger G, Hussain SS, Dawood H, Chaudhry MN, and Gervilla F (2006) Petrogenesis of mafic garnet granulite in the lower crust of the Kohistan paleo-arc complex (Northern Pakistan): implications for intra-crustal differentiation of island arcs and generation of continental crust. *Journal of Petrology* 47: 1873–1914.
Gaschnig RM, Rudnick RL, McDonough WF, Kaufman AJ, Valley JW, Hu Z, Gao S, and Beck ML (2016) Compositional evolution of the upper continental crust through time, as constrained by ancient glacial diamictites. *Geochimica et Cosmochimica Acta* 186: 316–343.
Geological Society of America (1972) Penrose field conference on ophiolites. *Geotimes* 17: 24–25.
Gerya TV and Meilick FI (2011) Geodynamic regimes of subduction under an active margin: Effects of rheological weakening by fluids and melts. *Journal of Metamorphic Geology* 29: 7–31.
Gerya TV and Yuen DA (2003) Rayleigh-Taylor instabilities from hydration and melting propel 'cold plumes' at subduction zones. *Earth and Planetary Science Letters* 212: 47–62.
Gerya TV, Stöckhert B, and Perchuk AL (2002) Exhumation of high-pressure metamorphic rocks in a subduction channel: A numerical simulation. *Tectonics* 21.
Gerya TV, Perchuk LL, and Burg JP (2007) Transient hot channels: perpetrating and regurgitating ultrahigh-pressure, high temperature crust-mantle associations in collision belts. *Lithos* 103: 236–256.
Gill JB (1974) Role of underthrust oceanic crust in the genesis of a Fijian calc-alkaline suite. *Contributions to Mineralogy and Petrology* 43: 29–45.
Godard M, Awaji S, Hansen H, Hellebrand E, Brunelli D, Johnson K, Yamasaki T, Maeda J, Abratis M, Christie D, and Kato Y (2009) Geochemistry of a long in-situ section of intrusive slow-spread oceanic lithosphere: Results from IODP Site U1309 (Atlantis Massif, 30 N Mid-Atlantic-Ridge). *Earth and Planetary Science Letters* 279: 110–122.
Goes S, Hasterok D, Schutt DL, and Klöcking M (2020) Continental lithospheric temperatures: A review. *Physics of the Earth and Planetary Interiors* 306: 106509.
Gómez-Tuena A, Cavazos-Tovar JG, Parolari M, Straub SM, and Espinasa-Pereña R (2018) Geochronological and geochemical evidence of continental crust 'relamination'in the origin of intermediate arc magmas. *Lithos* 322: 52–66.
Gorczyk W, Gerya TV, Connolly JAD, Yuen DA, and Rudolph M (2006) Large-scale rigid-body rotation in the mantle wedge and its implications for seismic tomography. *G-cubed* 7. https://doi.org/10.1029/2005GC001075.
Gordon SM, Miller RB, and Sauer KB (2017) Incorporation of sedimentary rocks into the deep levels of continental magmatic arcs: Links between the North Cascades arc and surrounding sedimentary terranes. In: Haugerud RA and Kelsey HM (eds.) *The Puget Lowland to East of the Cascade Range: Geologic Excursions in the Pacific Northwest*, vol. 49, p. 101. Geological Society of America.
Green TH (1981) Experimental evidence for the role of acces- sory phases in magma genesis. *Journal of Volcanology and Geothermal Research* 10: 405–422.
Greene A, DeBari SM, Kelemen PB, Blusztajn J, and Clift PD (2006) A detailed geochemical study of island arc crust: the Talkeetna arc section, south-central Alaska. *Journal of Petrology* 47: 1051–1093.
Griffin WL, O'Reilly SY, Ryan CG, Gaul O, and Ionov DA (1998) Secular variation in the composition of subcontinental lithospheric mantle: Geophysical and geodynamic implications. In: Braun J, et al. (eds.) *Structure and Evolution of the Australian Continent, Geodyn. Ser*, Vol. 26, pp. 1–25. Washington DC: American Geophysical Union.
Griffin WL, O'Reilly SY, and Ryan CG (1999) The composition and origin of subcontinental lithospheric mantle. In: Fei Y, Bertka CM, and Mysen BO (eds.) *Mantle Petrology: Field Observations and High-Pressure Experimentation, A Tribute to Francis R. (Joe) Boyd, 6*, ed., pp. 13–45. Spec. Publ. Geochem. Soc.
Grimes CB, John BE, Kelemen PB, Mazdab FK, Wooden JL, Cheadle MJ, Hanghøj K, and Schwarz JJ (2007) Trace element chemistry of zircons from oceanic crust: A method for distinguishing detrital zircon provenance. *Geology* 35: 643–646.
Grove M, Jacobson CE, Barth AP, and Vucic A (2003) *Temporal and spatial trends of Late Cretaceous-early Tertiary underplating of Pelona and related schist beneath southern California and southwestern Arizona*, pp. 381–406. GSA Special Paper 374.
Guo M and Korenaga J (2020) Argon constraints on the early growth of felsic continental crust. *Science Advances* 6: eaaz6234.
Guo M and Korenaga J (2023) The combined Hf and Nd isotope evolution of the depleted mantle requires Hadean continental formation. *Science Advances* 9: eade2711.
Hacker BR (2008) H_2O subduction beyond arcs. *G-cubed* 9. https://doi.org/10.1029/2007GC001707.
Hacker BR and Gerya T (2013) Paradigms, new and old, for ultrahigh-pressure tectonism. *Tectonophysics* 603: 79–88.
Hacker BR, Mehl L, Kelemen PB, Rioux M, Behn MD, and Luffi P (2008) Reconstruction of the Talkeetna intraoceanic arc of Alaska through thermobarometry. *Journal of Geophysical Research* 113. https://doi.org/10.1029/2007jb005208.
Hacker BR, Kelemen PB, and Behn MD (2011) Differentiation of the continental crust by relamination. *Earth and Planetary Science Letters* 307: 501–516.
Hacker BR, Kelemen PB, and Behn MD (2015) Continental lower crust. *Annual Review of Earth and Planetary Sciences* 43: 167–205.
Hamliton W (2003) An alternative earth. *GSA Today* 13: 4–12.
Hanson AE, Gordon SM, Ashley KT, Miller RB, and Langdon-Lassagne E (2022) Multiple sediment incorporation events in a continental magmatic arc: Insight from the metasedimentary rocks of the northern North Cascades, Washington (USA). *Geosphere* 18: 298–326.
Harrison TM (2009) The Hadean crust: evidence from> 4 Ga zircons. *Annual Review of Earth and Planetary Sciences* 37: 479–505.

Hart SR, Blusztajn J, Dick HJB, Meyer PS, and Muehlenbachs K (1999) The fingerprint of seawater circulation in a 500-meter section of ocean crust gabbros. *Geochimica et Cosmochimica Acta* 63: 4059–4080.
Hasterok D and Chapman DS (2011) Heat production and geotherms for the continental lithosphere. *Earth and Planetary Science Letters* 207: 59–70.
Hawkesworth CJ and Kemp AIS (2006) Evolution of the continental crust. *Nature* 443: 811–817.
Hawkesworth CJ, Dhuime B, Pietranik AB, Cawood PA, Kemp AI, and Storey CD (2010) The generation and evolution of the continental crust. *Journal of the Geological Society of London* 167: 229–248.
He Y, Zheng T, Ai Y, Hou G, and Chen QF (2018) Growth of the lower continental crust via the relamination of arc magma. *Tectonophysics* 724: 42–50.
Henrys S, Wech A, Sutherland R, Stern T, Savage M, Sato H, Mochizuki K, Iwasaki T, Okaya D, Seward A, and Tozer B (2013) SAHKE geophysical transect reveals crustal and subduction zone structure at the southern Hikurangi margin, New Zealand. *G-cubed* 14: 2063–2083.
Hermann J, Müntener O, Trommsdorff V, Hansmann W, and Piccardo GB (1997) Fossil crust-to-mantle transition, Val Malenco (Italian Alps). *Journal of Geophysical Research* 102: 20123–20132.
Herzberg CT, Fyfe WS, and Carr MJ (1983) Density constraints on the formation of the continental Moho and crust. *Contributions to Mineralogy and Petrology* 84: 1–5.
Hoffmann JE, Münker C, Næraa T, Rosing MT, Herwartz D, Garbe-Schönberg D, and Svahnberg H (2011) Mechanisms of Archean crust formation inferred from high-precision HFSE systematics in TTGs. *Geochimica et Cosmochimica Acta* 75: 4157–4178.
Hofmann AW (1988) Chemical differentiation of the Earth: The relationship between mantle, continental crust, and oceanic crust. *Earth and Planetary Science Letters* 90: 297–314.
Hofmann AW, Class C, and Goldstein SL (2022) Size and composition of the MORB+ OIB mantle reservoir. *Geochemistry, Geophysics, Geosystems* 23. e2022GC010339.
Holbrook WS, Mooney WD, and Christensen NI (1992) The seismic velocity structure of the deep continental crust. In: Fountain DM, Arculus R, and Kay RW (eds.) *Continental Lower Crust*, pp. 1–42. Amsterdam: Elsevier.
Holbrook SW, Lizarralde D, McGeary S, Bangs N, and Diebold J (1999) Structure and composition of the Aleutian island arc and implications for continental crustal growth. *Geology* 27: 31–34.
Holland JG and Lambert RSJ (1972) Major element composition of shields and the continental crust. *Geochimica et Cosmochimica Acta* 36: 673–683.
Holland T and Powell R (1996) Thermodynamics of order-disorder in minerals. 2. Symmetric formalism applied to solid solutions. *American Mineralogist* 81. 142501437.
Holland TJB and Powell R (1998) An internally consistent thermodynamic data set for phases of petrological interest. *Journal of Metamorphic Geology* 16: 309–343.
Holland T and Powell R (2003) Activity-composition relations for phases in petrological calculations: An asymmetric multicomponent formulation. *Contributions to Mineralogy and Petrology* 145: 492–501.
Holland T, Baker J, and Powell R (1998) Mixing properties and activity-composition relationships of chlorites in the system MgO-FeO-Al_2O_3-SiO_2-H_2O. *European Journal of Mineralogy* 10: 395–406.
Hopkins MD, Harrison TM, and Manning CE (2010) Constraints on Hadean geodynamics from mineral inclusions in> 4 Ga zircons. *Earth and Planetary Science Letters* 298: 367–376.
Huang Y, Chunakov V, Mantovani F, Rudnick RL, and McDonough WF (2013) A reference Earth model for the heat-producing elements and associated geoneutrino flux. *Geochemistry, Geophysics, Geosystems* 14: 2003–2029.
Jacobson CE, Oyarzabal FR, and Haxel GB (1996) Subduction and exhumation of the Pelona-Orocopia-Rand schists, southern California. *Geology* 24: 547–550.
Jagoutz O and Behn MD (2013) Foundering of lower arc crust as an explanation for the origin of the continental Moho. *Nature* 504: 131–134.
Jagoutz O and Kelemen PB (2015) Role of arc processes in the formation of continental crust. *Annual Review of Earth and Planetary Sciences* 43: 363–404.
Jagoutz O and Schmidt MW (2012) The formation and bulk composition of modern juvenile continental crust: The Kohistan arc. *Chemical Geology* 298–299: 79–96.
Jagoutz O and Schmidt MW (2013) The composition of the foundered complement to the continental crust and a re-evaluation of fluxes in arcs. *Earth and Planetary Science Letters* 371–372: 177–190.
Jagoutz OE, Burg JP, Hussain S, Dawood H, Pettke T, Iizuka T, and Maruyama S (2009) Construction of the granitoid crust of an island arc part I: geochronological and geochemical constraints from the plutonic Kohistan (NW Pakistan). *Contributions to Mineralogy and Petrology* 158: 739–755.
Jagoutz O, Müntener O, Schmidt MW, and Burg JP (2011) The roles of flux-and decompression melting and their respective fractionation lines for continental crust formation: Evidence from the Kohistan arc. *Earth and Planetary Science Letters* 303: 25–36.
Jaupart C and Mareschal JC (2003) Constraints on crustal heat production from heat flow data, v.3, Rudnick, R.L., ed. In: Holland HD and Turekian KK (eds.) *Treatise on Geochemistry*, pp. 65–84. Amsterdam: Elsevier.
Jaupart C and Mareschal JC (2014) Constraints on crustal heat production from heat flow data, v.4, Rudnick, R.L., ed. In: Holland HD and Turekian KK (eds.) *Treatise on Geochemistry*, 2nd ed., pp. 53–73. Amsterdam: Elsevier.
Jaupart C, Francheteau J, and Shen XJ (1985) On the thermal structure of the southern Tibetan crust. *Geophysical Journal International* 81: 131–155.
Jaupart C, Mareschal JC, and Iarotsky L (2016) Radiogenic heat production in the continental crust. *Lithos* 262: 398–427.
Jordan TH (1978) Composition and development of the continental tectosphere. *Nature* 274: 544–548.
Jordan TH (1988) Structure and Formation of the Continental Tectosphere. *Journal of Petrology*: 11–37. Special Volume.
Jordan EK, Lieu W, Stern R, Carr M, Feigenson M, and Gill JB (2012) *CentAm & IBM Geochem Database version 1.02*. EarthChem IDEA. https://doi.org/10.1594/IEDA/100053.
Jull M and Kelemen PB (2001) On the conditions for lower crustal convective instability. *Journal of Geophysical Research* 106: 6423–6446.
Kay RW (1978) Aleutian magnesian andesites: melts from subducted Pacific Ocean crust. *Journal of Volcanology and Geothermal Research* 4: 117–132.
Kay RW (1980) Volcanic arc magmas: implications of a melting-mixing model for element recycling in the crust-upper mantle system. *Journal of Geology* 88: 497–522.
Kay RW and Kay SM (1991) Creation and destruction of lower continental crust. *Geologische Rundschau* 80: 259–278.
Kay RW, Sun S-S, and Lee-Hu C-n (1978) Pb and Sr isotopes in volcanic rocks from the Aleutian Islands and Pribilof Islands, Alaska. *Geochimica et Cosmochimica Acta* 42: 263–273.
Kelemen PB (1995) Genesis of high Mg# andesites and the continental crust. *Contributions to Mineralogy and Petrology* 120: 1–19.
Kelemen PB and Behn MD (2016) Formation of lower continental crust by relamination of buoyant arc lavas and plutons. *Nature Geoscience* 9: 197–205.
Kelemen PB and Hacker BR (2016) The South Tibetan Tadpole Zone: Ongoing density sorting at the Moho beneath the Indus-Tsangpo suture zone (and beneath volcanic arcs?). *EGU General Assembly Conference Abstracts*. EPSC2016-9841.
Kelemen PB, Shimizu N, and Dunn T (1993) Relative depletion of niobium in some arc magmas and the continental crust: Partitioning of K, Nb, La and Ce during melt/rock reaction in the upper mantle. *Earth and Planetary Science Letters* 120: 111–134.
Kelemen PB, Hart SR, and Bernstein S (1998) Silica enrichment in the continental upper mantle lithosphere via melt/rock reaction. *Earth and Planetary Science Letters* 164: 387–406.
Kelemen PB, Hanghøj K, and Greene A (2003a) One view of the geochemistry of subduction-related magmatic arcs, with an emphasis on primitive andesite and lower crust. In: Rudnick RL (ed.) *The Crust, Vol. 3, Treatise on Geochemistry, (H.D. Holland and K.K. Turekian, eds.)*, pp. 593–659. Oxford: Elsevier-Pergamon.
Kelemen PB, Rilling JL, Parmentier EM, Mehl L, and Hacker BR (2003b) Thermal structure due to solid-state flow in the mantle wedge beneath arcs. *Geophysical Monograph* 138: 293–311.
Kelemen PB, Yogodzinski GM, and Scholl DW (2003c) Along-strike variation in lavas of the Aleutian island arc: Implications for the genesis of high Mg# andesite and the continental crust, Chapter 11. In: Eiler J (ed.) *Inside the Subduction Factory, AGU Monograph 138*, pp. 293–311. Washington DC: American Geophysical Union.
Kelemen PB, Kikawa E, Miller DJ, and Party SS (2007) Leg 209 summary: Processes in a 20-km-thick conductive boundary layer beneath the Mid-Atlantic Ridge, 14–16 N. *Proceedings of the Ocean Drilling Program: Scientific Results* 209: 1–33.
Kelemen PB, Hanghøj K, and Greene A (2014) One view of the geochemistry of subduction-related magmatic arcs, with an emphasis on primitive andesite and lower crust. In: Rudnick RL (ed.) *The Crust, Vol. 4, Treatise on Geochemistry, 2nd ed. (H.D. Holland and K.K. Turekian, eds.)*, pp. 746–805. Oxford: Elsevier-Pergamon.
Kelley KA and Cottrell E (2012) The influence of magmatic differentiation on the oxidation state of Fe in a basaltic arc magma. *Earth and Planetary Science Letters* 329–330: 109–121.
Kelly RK, Kelemen PB, and Jull M (2003) Buoyancy of the continental upper mantle. *Geochemistry, Geophysics, Geosystems* 42.

Kimbrough DL and Grove M (2007) Evidence for rapid recycling of subduction erosion forearc material into Cordilleran TTG batholiths: Insight from the Peninsular Ranges of southern and Baja California. *EOS. Transactions of the American Geophysical Union* 88: T11B–T0581B.
Kind R, Yuan X, Saul J, Nelson D, Sobolev SV, Mechie J, Zhao W, Kosarev G, Ni J, Achauer U, and Jiang M (2002) Seismic images of crust and upper mantle beneath Tibet: Evidence for Eurasian plate subduction. *Science* 298: 1219–1221.
Klein BZ (2019) *Processes and rates of arc crust growth and differentiation in the Southern Sierra Nevada crustal section*. MIT PhD thesis.
Klein BZ and Behn MD (2021) On the evolution and fate of sediment diapirs in subduction zones. *Geochemistry, Geophysics, Geosystems* 22. e2021GC009873.
Klein BZ, Jagoutz OE, and VanTongeren JA (2016) Are arc lower crustal metasediments derived from above or below? A detrital zircon study in the lower crust of the Sierra Nevada, California. *AGU Fall Meeting Abstracts*: V51B–01.
Korenaga J, Kelemen PB, and Holbrook SW (2002) Methods for resolving the origin of large igneous provinces from crustal seismology. *Journal of Geophysical Research* 107. https://doi.org/10.1029/2001JB001030.
Kotowski AJ, Cisneros M, Behr WM, Stockli DF, Soukis K, Barnes JD, and Ortega-Arroyo D (2022) Subduction, underplating, and return flow recorded in the Cycladic Blueschist Unit exposed on Syros, Greece. *Tectonics* 41. e2020TC006528.
Kress VC and Carmichael ISE (1991) The compressibility of silicate liquids containing Fe2O3 and the effect of composition, temperature, oxygen fugacity and pressure on their redox states. *Contributions to Mineralogy and Petrology* 108: 82–92.
Laske G, Masters G, Ma Z, and Pasyanos M (2012) CRUST1.0: An Updated Global Model of Earth's Crust. *Geophysical Research Abstracts* 14. EGU2012-3743-1.
Laske G, Masters G, Ma Z, and Pasyanos M (2013) Update on CRUST1.0: a 1-degree global model of Earth's crust. *Geophysical Research Abstracts* 15. EGU2013–658.
Laurent O, Martin H, Moyen JF, and Doucelance R (2014) The diversity and evolution of late-Archean granitoids: Evidence for the onset of "modern-style" plate tectonics between 3.0 and 2.5 Ga. *Lithos* 205: 208–235.
Le Pichon X, Fournier M, and Jolivet L (1992) Kinematics, topography, shortening, and extrusion in the India–Eurasia collision. *Tectonics* 11: 1085–1098.
Le Pichon X, Henry P, and Goffe B (1997) Uplift of Tibet: From eclogite to granulites - implications for the Andean Plateau and Variscan belt. *Tectonophysics* 273: 57–76.
Lee CTA and Anderson DL (2015) Continental crust formation at arcs, the arclogite "delamination" cycle, and one origin for fertile melting anomalies in the mantle. *Science Bulletin* 60: 1141–1156.
Lee CTA, Cheng X, and Horodyskyj U (2006) The development and refinement of continental arcs by primary basaltic magmatism, garnet pyroxenite accumulation, basaltic recharge and delamination: insights from the Sierra Nevada. *Contributions to Mineralogy and Petrology* 151: 222–242.
Li Z and Gerya TV (2009) Polyphase formation and exhumation of high- to ultrahighpressure rocks in continental subduction zone; numericalmodeling and application to the Sulu ultrahigh-pressure terrane in eastern China. *Journal of Geophysical Research* 114.
Liao KZ, Morton DM, and Lee CTA (2013) Geochemical diagnostics of metasedimentary dark enclaves: a case study from the Peninsular Ranges Batholith, southern California. *International Geology Review* 55: 1049–1072.
Linn AM, Depaolo DJ, and Ingersoll RV (1992) Nd-Sr isotopic, geochemical, and petrographic stratigraphy and paleotectonic analysis: Mesozoic Great Valley forearc sedimentary rocks of California. *GSA Bulletin* 104: 1264–1279.
Lizarralde D, Holbrook WS, McGeary S, Bangs NL, and Diebold JB (2002) Crustal construction of a volcanic arc, wide-angle seismic results from the western Alaska Peninsula. *Journal of Geophysical Research* 107: EPM-4.
Lucazeau F (2019) Analysis and mapping of an updated terrestrial heat flow data set. *Geochemistry, Geophysics, Geosystems* 20: 4001–4024.
Lysak SV (1992) Heat flow variations in continental rifts. *Tectonophysics* 208: 309–323.
Mareschal JC and Jaupart C (2013) Radiogenic heat production, thermal regime and evolution of continental crust. *Tectonophysics* 609: 524–534.
Marschall HR and Schumacher JC (2012) Arc magmas sourced from mélange diapirs in subduction zones. *Nature Geoscience* 5: 862–867.
Marsh BD (1979) Island arc development: Some observations, experiments, and speculations. *Journal of Geology* 87: 687–713.
Martin H (1986) Effect of steeper Archean geothermal gradient on geochemistry of subduction-zone magmas. *Geology* 14: 753–756.
Matteini M, Mazzuoli R, Omarini R, Cas R, and Maas R (2002) The geochemical variations of the upper cenozoic volcanism along the Calama–Olacapato–El Toro transversal fault system in central Andes (24°S): Petrogenetic and geodynamic implications. *Tectonophysics* 345: 211–227.
Matzel JE, Bowring SA, and Miller RB (2004) Protolith age of the Swakane Gneiss, North Cascades, Washington: Evidence of rapid underthrusting of sediments beneath an arc. *Tectonics* 23.
McDonough WF and Sun S-S (1995) The composition of the Earth. *Chemical Geology* 120: 223–253.
McDonough WF, Šrámek O, and Wipperfurth SA (2020) Radiogenic power and geoneutrino luminosity of the Earth and other terrestrial bodies through time. *Geochemistry, Geophysics, Geosystems* 21. e2019GC008865.
McKenzie D and Priestley K (2008) The influence of lithospheric thickness variations on continental evolution. *Lithos* 102: 1–11.
Miller NC and Behn MD (2012) Timescales for the growth of sediment diapirs in subduction zones. *Geophysical Journal International* 190: 1361–1377.
Miller RB, Paterson SR, Matzel JP, and Snoke AW (2009) Plutonism at different crustal levels: Insights from the∼ 5–40 km (paleodepth) North Cascades crustal section, Washington. Crustal cross sections from the western North American Cordillera and elsewhere: Implications for tectonic and petrologic processes. *GSA Special Paper* 456: 125–149.
Misch P and Rice JM (1975) Miscibility of tremolite and hornblende in progressive Skagit metamorphic suite, North Cascades, Washington. *Journal of Petrology* 16: 1–21.
Miyashiro A (1961) Evolution of metamorphic belts. *Journal of Petrology* 2: 277–311.
Molnar P and England P (1990) Temperatures, heat flux, and frictional stress near major thrust faults. *Journal of Geophysical Research* 95: 4833–4856.
Monsalve G, Sheehan A, Schulte-Pelkum V, Rajaure S, Pandey MR, and Wu F (2006) Seismicity and one-dimensional velocity structure of the Himalayan collision zone: Earthquakes in the crust and upper mantle. *Journal of Geophysical Research* 111. https://doi.org/10.1029/2005JB004062.
Monsalve G, Sheehan A, Rowe C, and Rajaure S (2008) Seismic structure of the crust and the upper mantle beneath the Himalayas: Evidence for eclogitization of lower crustal rocks in the Indian Plate. *Journal of Geophysical Research* 113: B08315.
Morgan P (1982) Heat flow in rift zones. *Continental and Oceanic Rifts* 8: 107–122.
Morris JD and Hart SR (1983) Isotopic and incompatible element constraints on the genesis of island arc volcanic from Cold Bay and Amak Island, Aleutians, and implications for mantle structure. *Geochimica et Cosmochimica Acta* 47: 2015–2030.
Müntener O and Hermann J (1996) The Val Malenco lower crust–upper mantle complex and its field relations (Italian Alps). *Schweizerische Mineralogische und Petrographische Mitteilungen* 76: 475–500.
Müntener O, Kelemen PB, and Grove TL (2001) The role of H_2O during crystallization of primitive arc magmas under uppermost mantle conditions and genesis of igneous pyroxenites: An experimental study. *Contributions to Mineralogy and Petrology* 141: 643–658.
Myers JD, Marsh BD, and Sinha AK (1985) Strontium isotopic and selected trace element variations between two Aleutian volcanic centers (Adak and Atka): implications for the development of arc volcanic plumbing systems. *Contributions to Mineralogy and Petrology* 91: 221–234.
Nabelek J, Hetenyi G, Vergne J, Sapkota S, Kafle B, Mei J, Su H, Chen J, Huang B-S, Mitchell L, Sherstad D, Arsenault M, Baur J, Carpenter S, Donnahue M, Myers D, Tseng TL, Bardell T, VanHoudnos N, Pandey M, Chitrakar G, Rajaure S, Xue G, Wang Y, Zhou S, Liang X, Ye G, Liu CC, Lin J, Wu CL, and Barstow N (2009) Underplating in the Himalaya-Tibet collision zone revealed by the Hi-CLIMB experiment. *Science* 325: 1371–1374.
Nair R and Chacko T (2008) Role of oceanic plateaus in the initiation of subduction and origin of continental crust. *Geology* 36: 583–586.
Natland JH and Dick HJ (1996) Melt migration through high-level gabbroic cumulates of the East Pacific Rise at Hess Deep: the origin of magma lenses and the deep crustal structure of fast-spreading ridges. *Proc. ODP Sci. Res.* 147: 21–58.
Neumann N, Sandiford M, and Foden J (2000) Regional geochemistry and continental heat flow: implications for the origin of the South Australian heat flow anomaly. *Earth and Planetary Science Letters* 183: 107–120.

Newton RC, Charlu TV, and Kleppa OJ (1980) Thermochemistry of the high structural state plagioclases. *Geochimica et Cosmochimica Acta* 44: 933–941.
Nielsen SG and Marschall HR (2017) Geochemical evidence for mélange melting in global arcs. *Science Advances* 3: e1602402.
NOAA National Geophysical Data Center (2009) *ETOPO1 1 Arc-Minute Global Relief Model. NOAA National Centers for Environmental Information*. Accessed March 18, 2023.
Nutman AP, Bennett VC, Friend CR, Polat A, Hoffmann E, and Van Kranendonk M (2021) Fifty years of the Eoarchean and the case for evolving uniformitarianism. *Precambrian Research* 367: 106442.
O'Reilly SY, Griffin WL, Djomani YHP, and Morgan P (2001) Are lithospheres forever? Tracking changes in subcontinental lithospheric mantle through time. *GSA Today* 11: 4–10.
Otamendi JE, Ducea MN, Tibaldi AM, Bergantz GW, de la Rosa JD, and Vujovich GI (2009) Generation of tonalitic and dioritic magmas by coupled partial melting of gabbroic and metasedimentary rocks within the deep crust of the Famatinian magmatic arc, Argentina. *Journal of Petrology* 50: 841–873.
Otamendi JE, Pinotti LP, Basei MAS, and Tibaldi AM (2010) Evaluation of petrogenetic models for intermediate and silicic plutonic rocks from the Sierra de Valle Fértil-La Huerta, Argentina: Petrologic constraints on the origin of igneous rocks in the Ordovician Famatinian-Puna paleoarc. *Journal of South American Earth Sciences* 30(1): 29–45.
Otamendi JE, Ducea MN, and Bergantz GW (2012) Geological, petrological and geochemical evidence for progressive construction of an arc crustal section, Sierra de Valle Fertil, Famatinian Arc, Argentina. *Journal of Petrology* 53: 761–800.
Peacock SM (1987) Creation and preservation of subduction-related inverted metamorphic gradients. *Journal of Geophysical Research* 92: 12763–12781.
Peacock SM (1996) Thermal and petrologic structure of subduction zones. *Geophysical Monograph* 96: 119–133.
Pearson DM, MacLeod DR, Ducea MN, Gehrels GE, and Patchett JP (2017) Sediment underthrusting within a continental magmatic arc: Coast Mountains batholith, British Columbia. *Tectonics* 36: 2022–2043.
Pease G, Gelb A, Lee Y, and Keller B (2023) A Bayesian formulation for estimating the composition of Earth's crust. *Journal of Geophysical Research* 128. e2023JB026353.
Pertermann M, Hirshmann MM, Hametner K, Günther D, and Schmidt MW (2004) Experimental determination of trace element partitioning between garnet and silica-rich liquid during anhydrous partial melting of MORB-like eclogite. *Geochemistry, Geophysics, Geosystems* 5.
Peterson JJ, Fox PJ, and Schreiber E (1974) Newfoundland ophiolites and the geology of the oceanic layer. *Nature* 247: 194–196.
Polat A, Appel PW, and Fryer BJ (2011) An overview of the geochemistry of Eoarchean to Mesoarchean ultramafic to mafic volcanic rocks, SW Greenland: implications for mantle depletion and petrogenetic processes at subduction zones in the early Earth. *Gondwana Research* 20: 255–283.
Pollack HN and Chapman DS (1977) Onthe regional variation of heat flow, geotherms, and lithospheric thickness. *Tectonophysics* 38: 279–296.
Pollack HN, Hurter SJ, and Johnson JR (1993) Heat flow from the Earth's Interior: Analysis of the global data set. *Reviews of Geophysics* 31: 267–280.
Puetz SJ, Condie KC, Pisarevsky S, Davaille A, Schwarz CJ, and Ganade CE (2017) Quantifying the evolution of the continental and oceanic crust. *Earth Science Reviews* 164: 63–83.
Qin SK, Zhang ZM, Palin RM, Ding HX, Dong X, and Tian ZL (2022) Tectonic burial of sedimentary rocks drives the building of juvenile crust of magmatic arc. *GSA Bulletin* 134: 3064–3078.
Quick JE, Sinigoi S, and Mayer A (1995) Emplacement of mantle peridotite in the lower continental crust, Ivrea-Verbano zone, northwest Italy. *Geology* 23: 739–742.
Raitt RW (1963) The crustal rocks. In: Hill MN (ed.) *The Sea*, pp. 85–102. New York: John Wiley.
Rapp RP, Shimizu N, Norman MD, and Applegate GS (1999) Reaction between slab-derived melts and peridotite in the mantle wedge: experimental constraints at 3.8 GPa. *Chemical Geology* 160: 335–356.
Rapp RP, Shimizu N, and Norman MD (2003) Growth of early continental crust by partial melting of eclogite. *Nature* 425: 605–609.
Reid MR, Hart SR, Padovani ER, and Wandless GA (1989) Contribution of metapelitic sediments to the composition, heat production, and seismic velocity of the lower crust of southern New Mexico, U.S.A. *Earth and Planetary Science Letters* 95: 367–381.
Rosas JC and Korenaga J (2018) Rapid crustal growth and efficient crustal recycling in the early Earth: Implications for Hadean and Archean geodynamics. *Earth and Planetary Science Letters* 494: 42–49.
Rothstein DA and Manning CE (2003) Geothermal gradients in continental magmatic arcs: Constraints from the eastern Peninsular Ranges batholith. *GSA Special Paper 374*. pp. 337–354. México: Baja California.
Rudnick RL (1992) Xenoliths: Samples of the lower continental crust. In: Fountain DM, Arculus RJ, and Kay RW (eds.) *The Lower Continental Crust*, pp. 269–316. Amsterdam: Elsevier.
Rudnick RL (1995) Making continental crust. *Nature* 378: 571–577.
Rudnick RL and Fountain DM (1995) Nature and composition of the continental crust: A lower crustal perspective. *Reviews of Geophysics* 33: 267–309.
Rudnick RL and Gao S (2003) Composition of the continental crust. In: Rudnick RL (ed.) *The Crust, Vol. 3, Treatise on Geochemistry (H.D. Holland and K.K. Turekian, eds.)*, pp. 1–64. Oxford: Elsevier-Pergamon.
Rudnick RL and Gao S (2014) Composition of the continental crust. In: Rudnick RL (ed.) *The Crust, Vol. 4, Treatise on Geochemistry, 2nd edition (H.D. Holland and K.K. Turekian, eds.)*, pp. 1–51. Oxford: Elsevier-Pergamon.
Rudnick RL and Presper T (1990) Geochemistry of intermediate to high-pressure granulites. In: Vielzeuf D and Vidal P (eds.) *Granulites and Crustal Evolution*, pp. 523–550. Amsterdam: Kluwer.
Rudnick RL, McDonough WF, and O'Connell RJ (1998) Thermal structure, thickness and composition of continental lithosphere. *Chemical Geology* 145: 395–411.
Ryerson FJ and Watson EB (1987) Rutile saturation in magmas: implications for TiNbTa depletion in island-arc basalts. *Earth and Planetary Science Letters* 86: 225–239.
Saleeby JB (1990) Progress in tectonic and petrogenetic studies in an exposed cross-section of young (~ 100 Ma) continental crust, southern Sierra Nevada, California. In: *NATO Advanced Study Institute on Exposed Cross-Sections of the Continental Crust*, pp. 137–158. Springer: Dordrecht. Springer Netherlands.
Saleeby JB, Sams DB, and Kistler RW (1987) U/Pb zircon, strontium, and oxygen isotopic and geochronological study of the southernmost Sierra Nevada batholith, California. *Journal of Geophysical Research* 92: 10443–10466.
Saleeby J, Ducea M, and Clemens-Knott D (2003) *Production and loss of high-density batholithic root, Southern Sierra Nevada*. California. *Tectonics* 22.
Sammon LG and McDonough WF (2021) A geochemical review of amphibolite, granulite and eclogite facies lithologies: Perspectives on the deep continental crust. *Journal of Geophysical Research* 126. 2021JB022791.
Sammon LG, McDonough WF, and Mooney WD (2022) Compositional attributes of the deep continental crust inferred from geochemical and geophysical data. *Journal of Geophysical Research* 127. e2022JB024041.
Santa Cruz CRC, Zellmer GF, Stirling CH, Straub SM, Brenna M, Reid MR, Németh K, and Barr D (2023) Transcrustal and source processes affecting the chemical characteristics of magmas in a hyperactive volcanic zone. *Geochimica et Cosmochimica Acta* 352: 88–106.
Sauer KB, Gordon SM, Miller RB, Vervoort JD, and Fisher CM (2017) Transfer of metasupracrustal rocks to midcrustal depths in the North Cascades continental magmatic arc, Skagit Gneiss Complex, Washington. *Tectonics* 36: 3254–3276.
Sauer KB, Gordon SM, Miller RB, Vervoort JD, and Fisher CM (2018) Provenance and metamorphism of the Swakane Gneiss: Implications for incorporation of sediment into the deep levels of the North Cascades continental magmatic arc, Washington. *Lithosphere* 10: 460–477.
Saunders AD, Tarney J, and Weaver SD (1980) Transverse geochemical variations across the Antarctic Peninsula: im- plications for the genesis of calc-alkaline magmas. *Earth and Planetary Science Letters* 46: 344–360.
Schiano P, Clocchiatti R, Shimizu N, Maury RC, Jochum KP, and Hofmann AW (1995) Hydrous, silica-rich melts in the sub-arc mantle and their relationship with erupted arc lavas. *Nature* 377: 595–600.
Scholl DW (2021) Seismic imaging evidence that forearc underplating built the accretionary rock record of coastal North and South America. *Geological Magazine* 158: 104–117.
Schubert G and Sandwell D (1989) Crustal volumes of the continents and of oceanic and continental submarine plateaus. *Earth and Planetary Science Letters* 92: 234–246.
Schulte-Pelkum V, Monsalve G, Sheehan A, Pandey MR, Sapkota S, Bilham R, and Wu F (2005) Imaging the Indian subcontinent beneath the Himalaya. *Nature* 435: 1222–1225.
Sclater JG, Jaupart C, and Galson D (1980) The heat flow through oceanic and continental crust and the heat loss from the Earth. *Reviews of Geophysics* 18: 269–311.
Scott JM (2020) An updated catalogue of New Zealand's mantle peridotite and serpentinite. *New Zealand Journal of Geology and Geophysics* 63: 428–449.

Shi D, Wu Z, Klemperer SL, Zhao W, Xue G, and Su H (2015) Receiver function imaging of crustal suture, steep subduction, and mantle wedge in the eastern India-Tibet continental collision zone. *Earth and Planetary Science Letters* 414: 6–15.
Shillington DJ, Van Avendonk HJA, Holbrook WS, Kelemen PB, and Hornbach MJ (2004) Composition and structure of the central Aleutian island arc from arc-parallel wide-angle seismic data. *Geochemistry, Geophysics, Geosystems* 5.
Shillington DJ, Van Avendonk HJ, Behn MD, Kelemen PB, and Jagoutz O (2013) Constraints on the composition of the Aleutian arc lower crust from Vp/Vs. *Geophysical Research Letters* 40: 2579–2584.
Sotiriou P, Polat A, Windley BF, and Kusky T (2022) Temporal variations in the incompatible trace element systematics of Archean volcanic rocks: Implications for tectonic processes in the early Earth. *Precambrian Research* 368: 106487.
Stein CA (1995) Heat flow of the Earth. In: Ahrens TJ (ed.) *Global Earth Physics. A Handbook of Physical constants. AGU Reference Shelf 1*, pp. 144–158. Washington DC: American Geophysical Union.
Stein M and Goldstein SL (1996) From plume head to continental lithosphere in the Arabian–Nubian shield. *Nature* 382: 773–778.
Sui S, Shen W, Mahan K, and Schulte-Pelkum V (2022) Constraining the crustal composition of the continental U.S. using seismic observables. *GSA Bulletin*.
Swapp SM, Frost CD, Frost BR, and Fitz-Gerald DB (2018) 2.7 Ga high-pressure granulites of the Teton Range: Record of Neoarchean continent collision and exhumation. *Geosphere* 14: 1031–1050.
Tang M, Rudnick RL, McDonough WF, Gaschnig RM, and Huang Y (2015) Europium anomalies constrain the mass of recycled lower continental crust. *Geology*. in press.
Tang M, Chen K, and Rudnick RL (2016) Archean upper crust transition from mafic to felsic marks the onset of plate tectonics. *Science* 351: 372–375.
Tatsumi Y, Hamilton DL, and Nesbitt RW (1986) Chemical characteristics of fluid phase released from a subducted lithosphere and origin of arc magmas: Evidence from high-pressure experiments and natural rocks. *Journal of Volcanology and Geothermal Research* 29: 293–309.
Tatsumoto M (1969) Lead isotopes in volcanic rocks and possible ocean-floor thrusting beneath island arcs. *Earth and Planetary Science Letters* 6: 369–376.
Tewksbury-Christle CM, Behr WM, and Helper MA (2021) Tracking deep sediment underplating in a fossil subduction margin: Implications for interface rheology and mass and volatile recycling. *Geochemistry, Geophysics, Geosystems* 22. e2020GC009463.
Tilhac R, Ceuleneer G, Griffin WL, O'Reilly SY, Pearson NJ, Benoit M, Henry H, Girardeau J, and Gregoire M (2016) Primitive arc magmatism and delamination: petrology and geochemistry of pyroxenites from the Cabo Ortegal complex, Spain. *Journal of Petrology* 57: 1921–1954.
Todd VR (2015) *Geologic Map of the Julian 7.5'Quadrangle, San Diego County, California. US Geol. Surv. Open File Report*.
Todd VR (2016) *Geologic Map of the Morena Reservoir 7.5-Minute Quadrangle*. San Diego County, California (No. 95-50), US Geological Survey.
Tozer B, Stern TA, Lamb SL, and Henrys SA (2017) Crust and upper-mantle structure of Wanganui Basin and southern Hikurangi margin, North Island, New Zealand as revealed by active source seismic data. *Geophysical Journal International* 211: 718–740.
Turkina OM (2023) Variations in trace element and isotope composition of Neoarchean mafic granulites of the southwest Siberian Craton: a consequence of various mantle sources or crustal contamination. *Petrology* 31: 204–222.
VanTongeren JA, Kelemen PB, Garrido CJ, Godard M, Hanghoj K, Braun M, and Pearce JA (2021) The composition of the lower oceanic crust in the Wadi Khafifah section of the southern Samail (Oman) ophiolite. *Journal of Geophysical Research* 126. e2021JB021986.
Vitorello I and Pollack HN (1980) On the variation of continental heat flow with age and the thermal evolution of the continents. *Journal of Geophysical Research* 85: 983–995.
Waldbaum DR and Thompson JB (1968) Mixing Properties Of Sanidine Crystalline Solutions 2. Calculations Based On Volume Data. *American Mineralogist* 53: 2000–2017.
Walker BA Jr, Bergantz GW, Otamendi JE, Ducea MN, and Cristofolini EA (2015) 2015. A MASH zone revealed: the mafic complex of the Sierra Valle Fértil. *Journal of Petrology* 56(9): 1863–1896.
Wang K, Cai K, Sun M, Wang X, Xia XP, Zhang B, and Wan B (2022) Diapir melting of subducted mélange generating alkaline arc magmatism and its implications for material recycling at subduction zone settings. *Geophysical Research Letters* 49. e2021GL097693.
Wanless VD, Perfit MR, Ridley WI, and Klein E (2010) Dacite petrogenesis on mid-ocean ridges: Evidence for oceanic crustal melting and assimilation. *Journal of Petrology* 51: 2377–2410.
Warren CJ, Beaumont C, and Jamieson RA (2008) Modelling tectonic styles and ultrahigh pressure (UHP) rock exhumation during the transition from oceanic subduction to continental collision. *Earth and Planetary Science Letters* 267: 129–145.
Wei CJ and Powell R (2003) Phase relations in high-pressure metapelites in the system KFMASH (K_2O-FeO-MgO-Al_2O_3-SiO_2-H_2O) with application to natural rocks. *Contributions to Mineralogy and Petrology* 145: 301–315.
White RV, Tarney J, Kerr AC, Saunders AD, Kempton PD, Pringle MS, and Klaver GT (1999) Modification of an oceanic plateau, Aruba, Dutch Caribbean: Implications for the generation of continental crust. *Lithos* 46: 43–68.
White RW, Powell R, Holland TJB, and Worley BA (2000) The effect of TiO_2 and Fe_2O_3 on metapelitic assemblages at greenschist and amphibolitefacies conditions: mineral equilibria calculations in the system K_2O-FeO-MgO-Al_2O_3-SiO_2-H_2O-TiO_2-Fe_2O_3. *Journal of Metamorphic Geology* 18: 497–511.
White RW, Powell R, and Phillips GN (2003) A mineral equilibria study of the hydrothermal alteration in mafic greenschist facies rocks at Kalgoorlie, Western Australia. *Journal of Metamorphic Geology* 21: 455–468.
Whitney DL (1992) High-pressure metamorphism in the Western Cordillera of North America: An example from the Skagit Gneiss, North Cascades. *Journal of Metamorphic Geology* 10: 71–85.
Wittlinger G, Farra V, Hetényi G, Vergne J, and Nábělek J (2009) Seismic velocities in Southern Tibet lower crust: a receiver function approach for eclogite detection. *Geophysical Journal International* 177: 1037–1049.
Xiao M, Yao YJ, Cai Y, Qiu HN, Xu YG, Xu X, Jiang YD, Li YB, Xia XP, and Yu YJ (2019) Evidence of Early Cretaceous lower arc crust delamination and its role in the opening of the South China Sea. *Gondwana Research* 76: 123–145.
Yan H, Long X, Li J, Wang Q, Zhao B, Shu C, Gou L, and Zuo R (2019) Arc andesitic rocks derived from partial melts of mélange diapir in subduction zones: Evidence from whole-rock geochemistry and Sr-Nd-Mo isotopes of the Paleogene Linzizong volcanic succession in southern Tibet. *Journal of Geophysical Research* 124: 456–475.
Yin A, Manning CE, Lovera O, Menold CA, Chen X, and Gehrels GE (2007) Early Paleozoic tectonic and thermomechanical evolution of ultrahigh-pressure (UHP)metamorphic rocks in the northern Tibetan Plateau, northwest China. *International Geology Review* 49: 681–716.
Yogodzinski GM, Volynets ON, Koloskov AV, Seliverstov NI, and Matvenkov VV (1994) Magnesian andesites and the subduction component in a strongly calc-alkaline series at Piip Volcano, Far Western Aleutians. *Journal of Petrology* 35: 163–204.
Yogodzinski GM, Kay RW, Volynets ON, Koloskov AV, and Kay SM (1995) Magnesian andesite in the western Aleutian Komandorsky region: Implications for slab melting and processes in the mantle wedge. *Geological Society of America Bulletin* 107: 505–519.
Zandt G, Gilbert H, Owens TJ, Ducea M, Saleeby J, and Jones CH (2004) Active foundering of a continental arc root beneath the southern Sierra Nevada in California. *Nature* 431 (7004): 41–46.
Zartman RE and Reed JC Jr (1998) *Zircon geochronology of the Webb Canyon gneiss and the Mount Owen quartz monzonite, Teton Range, Wyoming: Significance to dating late Archean metamorphism in the Wyoming Craton*. The Mountain Geologist.
Zhao W, Mechie J, Brown LD, Guo J, Haines S, Hearn T, Klemperer SL, Ma YS, Meissner R, Nelson KD, Ni JF, Pananont P, Rapine R, Ross A, and Saul J (2001) Crustal structure of central Tibet as derived from project INDEPTH wide-angle seismic data. *Geophysical Journal International* 145: 486–498.
Zhu G, Gerya TV, Yuen DA, Honda S, Yoshida T, and Connolly JAD (2009) Three-dimensional dynamics of hydrous thermal–chemical plumes in oceanic subduction zones. *Geochemistry, Geophysics, Geosystems* 10.